Technische Universität München
TUM Campus Straubing für Biotechnologie und Nachhaltigkeit

Advancing knowledge and prediction of physical clogging to enhance the long-term infiltration capacity of Managed Aquifer Recharge sites in response to accelerating water demand and scarcity

Maria Chiara Lippera

Vollständiger Abdruck der vom TUM Campus Straubing für Biotechnologie und Nachhaltigkeit der Technischen Universität München zur Erlangung einer

Doktorin der Naturwissenschaften (Dr. rer. nat)

genehmigten Dissertation.

Vorsitz: Prof. Dr. Nicolas Plumeré

Prüfende der Dissertation:

1. Prof. Dr. Thomas Vienken
2. Priv. Doz. Dr. Gabriele Chiogna

Die Dissertation wurde am 24.08.2023 bei der Technischen Universität München eingereicht und durch den TUM Campus Straubing für Biotechnologie und Nachhaltigkeit am 22.12.2023 angenommen.

Acknowledgements

I would like to express my sincere gratitude to Prof. Dr. Thomas Vienken and Dr. Ulrike Werban for their guidance, support, and mentorship during my doctoral journey. Their commitment to excellence, depth of knowledge, and dedication have shaped my research journey. Their feedbacks, encouragement, and constructive criticism have contributed to developing my research skills and academic growth. I extend my gratitude to Prof. Dr. Thomas Vienken for giving me the opportunity to join the prestigious academic environment of the Technische Universität München (TUM) and for supporting my doctoral qualification at the Graduate Centre TUM Campus Straubing (GCS).

I thank the Head of Department Prof. Dr. Peter Dietrich and the entire Department of Monitoring and Exploration Technologies at UFZ where I have been employed. The technicians are a fundamental part of the department with their support and assistance in equipment maintenance and technical troubleshooting. My particular gratitude goes to Paul Remmler and Manuel Kreck. I also thank the master's student Hermann Grün for his valuable work.

I am deeply grateful for having been part of the Marie Skłodowska-Curie Innovative Training Network. This has been a springboard to an excellent professional career. Being part of the consortium and the MAR community has been an insightful experience. Many thanks to the PIs and the MARSoluT Project Management team: Christoph Schüth, Annette Wefer-Roehl and Karl Ernst Roehl. Within the consortium, it really felt as being part of a big family, especially with the other Early Stage Researchers (ESRs), with whom we shared productive workshops, attended conferences together, had endless engaging discussions, and of course, many funny moments. Our support for each other has been precious and I hope we will always remain in touch, regardless of where our professional lives will take us.

Also a special thank to Rebecca, my comrade within the project and the office. We shared so much in this life adventure, from the very start at our arrival in Germany, to now the finalization of all our efforts, and she has been a real example of grit and perseverance. This journey would also not have been the same without the support of other strong women in our department: Carmen, Sophie and Nele. I thank all the 'older' PhD students I have met over the years and who have given me some words of motivation, although I have seen many of them leaving.

Thanks very much to all my new friends in Leipzig, who brought me joy and some evenings of distractions. My first WG constellation will always remain one of my best memories. I also have the deepest gratitude to my boyfriend Fabian, who supported me in every moment, from the long walks during the pandemic to the evenings talking about the research project. I also thank his family for their vivid interest and support.

To conclude, I am immensely grateful to my family. Although I miss them constantly, they always stand by me and help me overcome difficult times. I dedicate this work to my mother Lucia, who has been a constant inspiration to me as both a woman and an engineer. She gave me strength in the most difficult moments and always supported me in pursuing an excellent academic career, even though she gave up a brilliant career herself for the sake of the family. I share these achievements with her.

Table of Contents

Summary

Managed Aquifer Recharge (MAR) is a viable solution for the sustainable use of water resources and has been proposed as an adaptation strategy to climate change. This technique secures groundwater supplies during periods of high demand by reallocating and storing surface water during wet periods. It also preserves groundwater resources while counteracting the effects of variations in hydrogeological regimes and groundwater over-exploitation. Advancing this technology requires improving the operational efficiency of MAR sites and minimising the risk of failure. One longstanding challenge in MAR applications is clogging, predominantly caused by physical processes. During operations, fine sediments and particles accumulate in the sediment matrix, reducing the infiltration capacity of the facility. The site's functionality is compromised, and remediation techniques can significantly increase operation and maintenance (O&M) costs. In extreme cases, the site is abandoned. MAR research lacks predictive tools based on a systematic understanding of clogging mechanisms, which could be essential to prevent site failure.

This research aims to assess the risk of physical clogging in MAR planning, minimising operative costs and ensuring long-lasting efficiency. To achieve this, a numerical model for physical clogging processes was developed to be combined with site characterisation techniques. Firstly, physical clogging models from different fields of applied engineering were reviewed, and their transferability to MAR applications was addressed. Then, after identifying the main processes and key parameters, a conceptual framework for modelling clogging was established.

A major gap identified in the modelling of physical clogging was the vertical distribution of intrusive fines in the sediment matrix during water recharge. For this purpose, data sets of clogging profiles from the literature were reviewed and complemented with soil column experiments. The soil column experiments were designed to cover a wider range of fines and sandy porous media reflecting MAR conditions. A linear relationship was found between the relative mass of deposited particles at the water-sediment interface and a clogging predictor, representative of the primary porous media’s and intruding particles’ characteristics. The relationship is valid for internal clogging conditions, and a mathematical solution defines the deposition decay rate over depth. For the experiments under superficial clogging conditions, a retention limit was formulated, after which the external cake starts to form. The quantification of the vertical distribution of the intrusive fines allowed the simulation of the evolution in the soil hydraulic properties during infiltration. The results of the developed physical clogging model were tested on the column outflow throughout the experiment.

The findings were validated in field conditions, accounting for the site-specific features affecting the formation of clogging in the field and testing routines for site characterisation. Site characterisation was carried out at the Suvereto infiltration basin (Italy) via a shallow electromagnetic induction survey, soil sampling and infiltrometer tests. The laboratory and data analysis revealed the importance of incorporating spatial features to explain the remobilisation of fines within the basin. The parameters collected in the field could adequately explain the observed physical clogging, and the projected evolution in infiltration capacity was consistent with the values recorded for the whole basin.

The developed methodology can be applied to multiple sites from field characterisation data, which is a significant advantage over existing approaches. Assessing the risk of physical clogging assists the decision-making in developing design and management strategies for cost-efficient maintenance. Enhancing recharge rates at MAR sites is a valuable contribution to overcoming accelerating water demand and scarcity.

Zusammenfassung

Managed Aquifer Recharge (MAR), auch als künstliche Grundwasseranreicherung bezeichnet, ist eine Technik die sich zur nachhaltigen Bewirtschaftung von Grundwasserressourcen eignet und als mögliche Anpassungsstrategie an den Klimawandel gilt. Diese Technik sichert die Grundwasserversorgung in Zeiten hoher Nachfrage indem Oberflächenwasser während feuchten, niederschlagsreichen Perioden umverteilt und in Grundwasserleitern gespeichert wird. Dadurch kann sowohl Schwankungen im hydrogeologischen System als auch der Übernutzung von Grundwasserressourcen entgegengewirkt werden. Dies trägt zur Schonung von Grundwasserreserven bei. Zur weiteren Entwicklung und Etablierung der MAR-Technologie ist eine Verbesserung der Effizienz und der Betriebssicherheit von MAR-Standorten erforderlich. Eine seit langem bestehende Herausforderung bei MAR-Anwendungen ist die primär durch physikalische Prozesse bedingte Kolmation, im Folgenden als Clogging bezeichnet. Im Laufe der Zeit kommt es zur Ansammlung von feinen Sedimenten und Partikeln in der Sedimentmatrix und somit zur Verringerung der Versickerungskapazität der Anlage. Dies beeinträchtigt die Funktionalität des Standorts und macht Revitalisierungsverfahren notwendig, welche die Betriebs- und Wartungskosten erheblich erhöhen. In extremen Fällen kann dies zur Aufgabe des Standorts führen. Prognoseinstrumente, welche ein systematisches Verständnis der Clogging-Prozesse ermöglichen fehlen bislang in der MAR-Forschung.

Ziel dieser Forschungsarbeit ist es, das Risiko des physischen Cloggings bereits bei der Planung von MAR-Anlagen bewerten zu können, um somit die Betriebs- und Wartungskosten zu minimieren und eine dauerhafte Effizienz zu gewährleisten. Dazu wurde ein numerisches Modell für physisches Clogging-Prozesse entwickelt, das in Verbindung mit Techniken zur Standortcharakterisierung eingesetzt werden kann. Zunächst wurden Modelle für physisches Clogging aus verschiedenen Bereichen der angewandten Technik auf ihre Übertragbarkeit auf MAR-Anwendungen hin untersucht. Nach Identifizierung der wesentlichen Prozesse und Schlüsselparameter wurde ein konzeptioneller Rahmen für die Modellierung von Clogging-Prozessen erstellt.

Eine wichtige Lücke bei der Modellierung des physischen Cloggings ist die vertikale Verteilung der intrusiven Feinstoffe in der Sedimentmatrix während der Wasseranreicherung. Daher wurden Datensätze von Clogging-Profilen aus der Literatur herangezogen und mit Bodensäulenexperimenten ergänzt. Die Bodensäulenexperimente wurden so konzipiert, dass sie ein breiteres Spektrum an feinkörnigen und sandigen porösen Medien abdecken, die den MAR-Bedingungen entsprechen. Es wurde gezeigt, dass eine lineare Beziehung zwischen der relativen Masse der abgelagerten Partikel an der Wasser-Sediment-Grenzfläche und einem Clogging-Prädiktor besteht, der die Eigenschaften des primären porösen Mediums und der

eindringenden Partikel repräsentiert. Diese Beziehung gilt für interne Clogging-Bedingungen, und eine mathematische Lösung definiert die Ablagerungsabnahme über die Tiefe. Aus den Experimenten unter oberflächlichen Clogging-Bedingungen wurde eine Rückhaltegrenze formuliert, nach der sich der äußere “Cake“ zu bilden beginnt. Ausgehend von der Quantifizierung der vertikalen Verteilung der intrusiven Feinstoffe wurde die Entwicklung der hydraulischen Eigenschaften mithilfe des entwickelten physischen Clogging-Modells simuliert und während des gesamten Säulenversuchs über den Abfluss getestet.

Die so gewonnenen Ergebnisse wurden anschließend im Feldmaßstab validiert, um Feldfaktoren am Standort und Testroutinen zur Standortcharakterisierung zu integrieren. Die Standortcharakterisierung wurde im Infiltrationsbecken von Suvereto (Italien) mittels elektromagnetischen Induktionsmessungen, Bodenprobenahmen und Infiltrometertests durchgeführt. Die Labor- und Datenanalyse zeigte, wie wichtig die Einbeziehung räumlicher Merkmale ist, um die Remobilisierung von Feinstoffen innerhalb des Beckens zu erklären. Die im Feld erhobenen Parameter können das beobachtete physische Clogging angemessen erklären und die prognostizierte Entwicklung der Infiltrationsraten stimmt mit den gemessenen Werten für das gesamte Becken überein.

Die entwickelte Methodik kann auf der Grundlage von Feldcharakterisierungsdaten auf andere Standorte übertragen werden, was einen erheblichen Vorteil bei der Bewertung des Clogging-Risikos darstellt. Dies unterstützt den Entscheidungsprozess bereits in der Planungsphase bei der Bewertung von Gestaltungs- und Bewirtschaftungsstrategien zur Verringerung von Clogging an MAR-Standorten und trägt somit zur Bewältigung des zunehmenden Wasserbedarfs und der Wasserknappheit bei.

List of Publications

The listed first-authorship original research papers have been accepted and published in international, English language, peer-reviewed journals during the time of the qualification programme at the Graduate Centre TUM Campus Straubing:

- Lippera, M.C., Werban, U. and Vienken, T. *Improving clogging predictions at managed aquifer recharge sites: a quantitative assessment on the vertical distribution of intrusive fines*. Hydrogeol J 31, 71–86 (2023). https://doi.org/10.1007/s10040-022-02581-7

- Lippera, M.C., Werban, U., Rossetto R., and Vienken, T. *Understanding and predicting physical clogging at managed aquifer recharge systems: A field-based modeling approach*. Advances in Water Resources, 177, 104462 (2023). https://doi.org/10.1016/j.advwatres.2023.104462

- Lippera, M.C., Werban, U. and Vienken, T. *Application of physical clogging models to managed aquifer recharge: a review of modelling approaches from applied engineering fields*. Acque Sotterranee - Italian Journal of Groundwater (Accepted).

List of Figures

List of Tables

List of Abbreviations

AOC	Assimilable Organic Carbon content
ASR	Aquifer Storage and Recovery
ASTM	American Society for Testing and Materials
ASTR	Aquifer Storage Transfer and Recovery
BAU	Business as Usual
BDOC	Biodegradable Organic Carbon
CK	Chisel-Knives
CMD	Electromagnetic Conductivity Meter
Cr	Chromium
DGPS	Differential Global Positioning System
Eca	Apparent Electrical Conductivity
EMI	Electromagnetic Induction
EPS	Extracellular Polymeric Substances
ERT	Electrical Resistivity Tomography
Fe	Iron
GDE	Groundwater Dependent Ecosystems
GIS	Geographic Information System
GRACE	Gravity Recovery and Climate Experiment
GRIPP	Groundwater Solutions Initiative for Policy and Practice
GSD	Grain Size Distribution
IAH	International Association of Hydrogeologists
IGRAC	International Groundwater Resources Assessment Centre
K	Hydraulic conductivity
LOI	Loss-on-Ignition
MAR	Managed Aquifer Recharge

MFI	Modified Fouling Index
Mg	Manganese
NTU	Nephelometric Turbidity Units
OM	Organic matter
PFI	Parallel filter index
PSD	Particles size distribution
RMSE	Root-mean-square error
SAT	Soil Aquifer Treatment
SCADA	Supervisory Control and Data Acquisition
SDG	Sustainable Development Goals
SIR	Regional Hydrological Service
SP	Suspended pParticles
TDO	Total Dissolved Oxygen
TDS	Total Dissolved Solids
tTEM	Towed Transient Electromagnetic
TOC	Total Organic Carbon
TSS	Total Suspended Solids
UNESCO	United Nations Educational, Scientific and Cultural Organization
WWAP	World Water Assessment Programme

1 Introduction

1.1 Sustainability of water resources

The security of our global freshwater resources is at risk due to the rising demand of growing populations and global economies. Among 186 countries worldwide with a total population of 7.78 billion, approximately 8% face severe water scarcity, while around 72% are experiencing some degree of water insecurity (MacAlister 2023). Freshwater resources are more vulnerable given the adverse effect of climate change, altering the hydrological cycle and making rainfall patterns more unpredictable, leading to an increase in the frequency and intensity of both floods and droughts. The World Meteorological Organization (2022) declared in their report "*State of Global Water Resources"* that significant regions across the world registered decreased streamflows compared to the average of the 30-year hydrological base period, indicating a dryer-than-normal state. Additionally, terrestrial water storage in 2021 was categorised as below average during this period. Under prolonged droughts, surface water resources and water storages are more vulnerable than aquifers (Scanlon et al. 2023). Because of limited surface water availability in the next decades, groundwater will have a central role in ensuring the resilience of the global population to current and future water crises. Groundwater makes up approximately 99% of all available liquid freshwater on the planet. This natural resource is frequently undervalued despite its vital importance, leading to improper management and overexploitation (United Nations 2022).

The Sustainable Development Goals (SDGs) of the 2030 Development Agenda aims to protect water resources with the goal SDG 6 - "Ensure availability and sustainable management of water and sanitation for all". More specifically, target 6.6 contains a direct reference to groundwater resources: "By 2020, protect and restore water-related ecosystems, including mountains, forests, wetlands, rivers, aquifers and lakes". Also, SDG 12 - "Ensure sustainable consumption and production patterns" and SDG 13 - "Take urgent action to combat climate change and its impacts" have interlinkages to groundwater resources in resolving their targets. Despite there are at least 53 targets in the 2030 Development Agenda that have interlinkages with the use of groundwater and its management, the outlined SDGs generally did not acknowledge the important role that groundwater currently plays and will continue to play in achieving sustainable development (Guppy et al. 2018). The United Nations General Assembly has declared the period between 2018-2028 as the Water Action Decade for Sustainable Development, intending to speed up efforts to address water security challenges in conjunction with the 2030 Agenda for Sustainable Development.

This recognition of the vast potential of groundwater resources and the need to manage it sustainably has been addressed by the *UN Water World Water Day 2022 Campaign* with IGRAC, the International Groundwater Resources Assessment Centre. In the same year, the

UNESCO's World Water Assessment Programme (WWAP) prepared the *UN World Water Development Report 2022 'Groundwater: Making the invisible visible'*.

The report affirms that approximately 50% of the worldwide urban population depends on groundwater sources for water supply. This is the case especially for developing economies, due to insufficient piped water supply in peri-urban settlements. The number of private wells used for urban self-supply has increased in recent years. Moreover, of all the global groundwater withdrawals, almost 70% goes to irrigation, watering 38% of the world's land, around 22% is for domestic use, and 9% is served for industrial processes (United Nations 2022). Besides the above-listed provisioning services for human water-use purposes, groundwater resources provide regulatory and supporting services. The supporting services are vital for groundwater-dependent ecosystems (GDE), which are impacted by anthropogenic water consumption and climate change (Kløve et al. 2014). In global food security projections, the anticipated global demand for food by 2050 is expected to increase by 35% to 56%, relative to 2010, with a population at risk of hunger that could reach +30%, accounting for climate change effects (van Dijk et al. 2021). To satisfy the anticipated global demand for water and agriculture by 2050, it will be crucial to regulate groundwater abstractions in a sustainable way. Groundwater regulation and top-down governance are difficult to implement due to the conception of groundwater resources being related to land ownership, and thus being treated as a private resource (United Nations 2022).

Groundwater depletion is a reality worldwide, and this is the case when more water is abstracted from aquifers than is naturally recharged through the hydrological cycle (Wada et al. 2010). Over the years, global datasets, global hydrogeological models and satellite data have been employed to address the non-renewability of the groundwater resource (Döll et al. 2014; Gleeson et al. 2012). Using satellite data for global water-resource assessments, such as the Gravity Recovery and Climate Experiment (GRACE) satellite mission, revealed a depletion trend in groundwater storage that could be related to regions with intensified agriculture or population pressures (Richey et al. 2015).

Surface water and groundwater should be managed jointly to increase the resiliency of water-resource systems and ensure the sustainability of water resources in the future (Scanlon et al. 2023). The World Bank's 2023 report "What the Future Has in Store : A New Paradigm for Water Storage - Overview for Policy Makers" calls for more effective, efficient, and sustainable storage methods. This can be achieved by implementing integrated water resources management principles and combining natural and built storage as a cohesive system, optimising the current infrastructure and managing risks through diversification.

To shift the paradigm from conventional surface water storage systems, one groundwater-based human strategy to adapt to climate change and increase freshwater availability is Managed aquifer recharge (MAR).

1.2 Managed Aquifer Recharge

MAR is defined as the intentional recharge of water to aquifers for subsequent recovery or environmental benefit (NRMMC et al. 2009). Differently from the term "artificial recharge", the management process assures adequate protection of human health and the environment. In MAR the quantity and quality of groundwater resources are managed effectively. Water quality is vital in developing the potential of this technology (Hartog and Stuyfzand 2017). Worldwide, the MAR implementation has accelerated at a rate of 5% per year since the mid-1960s, combined with a decline in new large dams constructions (Dillon et al. 2018; Institute 2018). Compared to dams, MAR techniques offer the advantage of lower capital costs, reduce evaporation losses, problems with algae or mosquitoes, and can be located in areas with high water demands (Dillon et al. 2022). Further natural treatment is provided to water resources through mechanical filtering, sorption and biodegradation in the vadose zone (Sprenger et al. 2017). Combined groundwater and surface water storage are expected to increase the flexibility in the sustainable use of water resources at relatively low economic cost and environmental impact. (Vanderzalm et al. 2022).

Besides securing groundwater supply during high demand and reallocating the exceeding surface water in wet periods, MAR techniques address the ecological, societal and economic impacts of declining groundwater levels (Zheng et al. 2021). In depleted coastal aquifers, saltwater intrusion can be controlled by creating a hydraulic barrier maintaining the seaward gradient in the aquifer system (El-Rawy et al. 2019). MAR can repressurise aquifers that have undergone significant and extensive drawdowns, contrasting aquifer-system compaction and land subsidence phenomena (Ting et al. 2020). Moreover, the water quality of deteriorated aquifers can be improved and groundwater-dependent ecosystems can benefit from the augmentation of fresh water in aquifers with controlled water quality (Dillon 2005).

MAR techniques are relatively low-cost infrastructures, but since they rely on natural heterogeneous systems, they require aquifer characterisation to be effectively implemented (Maliva 2015). The scale and technical complexity are highly dependent on the local conditions and the source of water selected for recharge, which can be surface water from rivers, storm-water, treated wastewater or desalinated seawater (Casanova et al. 2016). MAR technologies can be divided into five major classes, namely: Spreading methods, in channel modification, wells and shaft recharge, induced bank filtration and rainwater harvesting (Zhang et al. 2020).

Spreading methods are the simplest and most commonly applied MAR technique, including infiltration ponds and soil aquifer treatment (SAT), the infiltration and percolation of treated wastewater through sub-surface soil passage (Sprenger et al. 2017). In channel modification, a dam is constructed and the riverbed or channel bed is scarified to enhance water recharge (Standen et al. 2020). In deep aquifers, wells and shaft recharge techniques are indicated as aquifer storage and recovery (ASR) and aquifer storage transfer and recovery (ASTR)(Pyne 2005). In induced bank filtration, a well pumps water induce infiltration from the surface water body to the aquifer (Rossetto et al. 2020). Finally, rainwater harvesting methods are implemented in urban areas to collect and return water to the hydrological cycle (Fig.1).

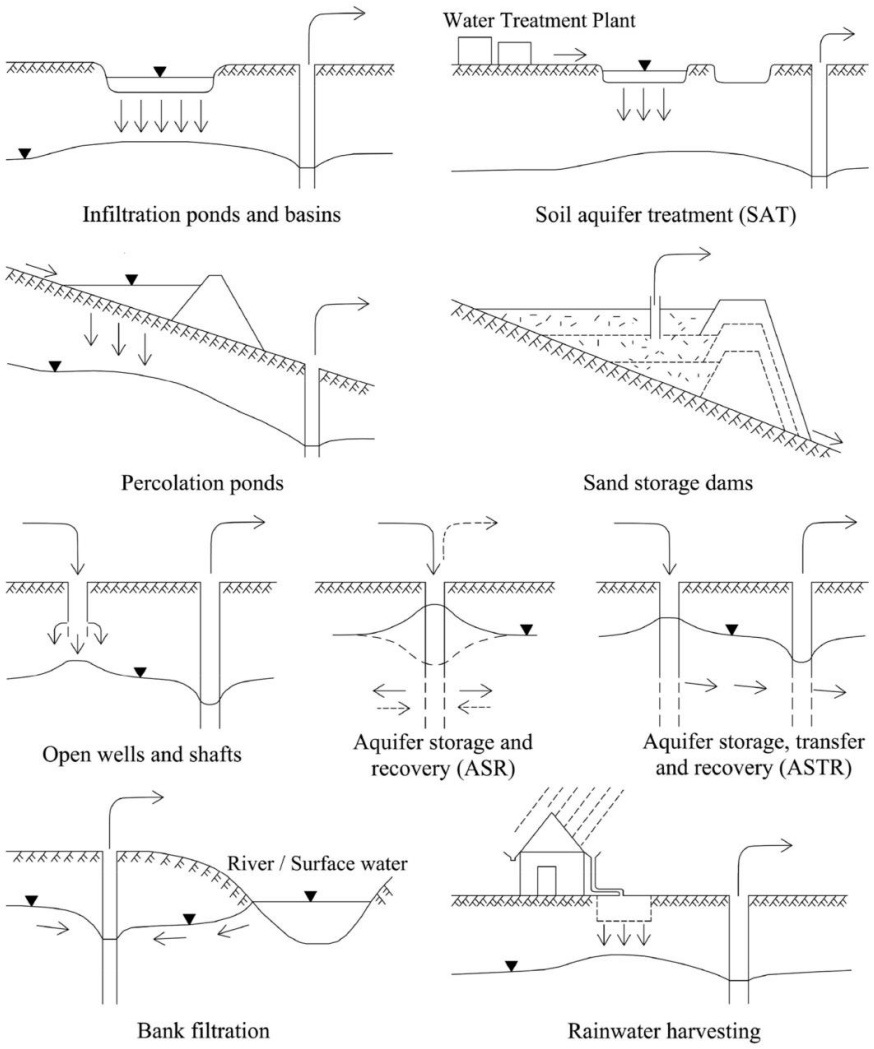

Figure 1: Main classes of MAR technology from Zhang et al. (2020).

Due to the illustrated advantages compared to traditional water storage and treatment methods, MAR technology is expected to increase worldwide and be applied in multiple contexts. Still, challenges and problems need to be solved to accelerate the growth and expansion of this technique. One of the long-lasting issues is clogging mechanisms and its prevention.

1.3 Clogging processes

Clogging is defined by Bouwer (2002) as the "bane of all artificial recharge systems". This process generally occurs through the accumulation of fine sediments and other particles in the infiltrating surface, affecting the infiltration capacity of the site. Because of clogging, the performance of the MAR system can be compromised, resulting in the failure of MAR operations. Cleaning cycles and maintenance operations are required to restore the system's functioning. Sprenger et al. (2017) documented the number of MAR site abandonment in Europe because of the loss of performance and increased costs. Although clogging and maintenance strategies are of vital concern in MAR practices, these have not been reported in detail in the available MAR literature (Sprenger et al. 2017).

Clogging mechanisms can be related to four main types of clogging: physical, biological, chemical and mechanical. Physical clogging originates from the intrusion and deposition of organic and inorganic suspended solids. Suspended solids are transported during water recharge and intrude, altering the permeability of the porous media and eventually building up, forming an external cake (Bouwer 2002). Especially if the water source is floodwater, eroded suspended solids, such as clay and silt particles, are a concern and turbidity levels need to be monitored. To minimise physical clogging is vital to reduce the concentration of suspended solids in the recharge water (Martin 2013a).

When algae growth and microorganisms' biomass accumulate, it is defined as biological clogging. Microorganism form biofilms, mainly responsible for clogging the pores, which comprise microbial cells and extracellular polymeric substances (EPS) embedded in a surface (Baveye et al. 1998; Camprovin et al. 2017). The density of the biofilm formation is related to the substrate concentration, while the bacteria growth depends upon nutrients, such as nitrogen and phosphorus, and organic carbon content in the recharge water (Kim et al. 2010). Both aerobic and anaerobic bacteria can grow on wells equipment, such as pumps, tubes and in the aquifer itself, and the flow rate of injection can control the formation rate of biofilms (Martin 2013a).

Chemical clogging is caused by the formation of insoluble precipitates, predominantly calcium carbonate, iron oxides and iron hydroxides. Minerals can be naturally found dissolved in groundwater and surface water. Carbonates and sulphides precipitation is associated with variations in pressure temperature or pH during recharge and mixing. The presence of oxygen can accelerate iron precipitation. When oxygenated water is recharged, carbon dioxide and hydrogen sulphide is released (Custodio et al. 1982; Pérez Paricio 2001). Iron or manganese oxides and hydroxises precipitation can be facilitated through the action of bacteria, making it not always possible to discern biological from chemical clogging (Majkić-Dursun et al. 2015; Martin 2013a; Pavelic et al. 2007).

Finally, mechanical clogging indicates the trapping of air in the vadose zone and consequent reduction in infiltration capacity. Dissolved air is realised when going out of solution from the infiltrating water because of a drop in water pressure or temperature (Bouwer 2002). Microorganisms can contribute to the production of biogenic gases, and both entrapped air and biogenic gases can occupy 7–20% of the entire pore space (Beckwith and Baird 2001; Heilweil and Marston 2013). Several studies in MAR literature indicate that physical clogging is the predominant process, followed by mechanical, biological and chemical processes (Dillon et al. 1994; Pavelic et al. 2011; Rinck-Pfeiffer et al. 2000).

Figure 2: Types of clogging (physical, biological and chemical) at MAR sites, from Escalante (2013) and Willis-Jones and Brandes de Roos (2013).

In recharge wells, the source of recharge water should go through ultra-filtration, such as membrane and ultra-violet treatment, in order to prevent clogging. Still, velocity-induced clogging can occur when the critical interstitial velocity is exceeded and the clays, naturally present in the aquifer, become mobile. The fines migrate in the direction of the flow until they are trapped in a narrower pore throat, reducing the injection capacity (Bennion et al. 1998). Recharge wells can be redeveloped and rehabilitated from clogging with conventional techniques, such as frequent and periodic “backwashing”, air jetting or acidising treatments (Pavelic et al. 2007). A detailed list of clogging remediation methods in recharge wells is reported in Martin (2013b).

In MAR basins, the downward movement and retention of fine-grained sediments, originating from the soil formation itself or transported by the infiltrating water over MAR operations, can significantly impact the drainage properties (Beganskas and Fisher 2017; Hutchinson et al. 2013; Racz et al. 2012). Pilot tests are usually constructed to test the performance of the MAR system given the site-specific conditions, and schedules for wetting and drying periods are developed by trial and error (Bouwer 2002). In order to reduce clogging impacts, low and constant recharge rates with frequent rehabilitation are recommended by constructing multiple infiltration basins, ensuring continuous recharge (Jeong et al. 2018). Regular drying and periodic cleaning of the basin need to be included in the definition of the MAR site hydraulic loading rates, considering the “down” time (Bouwer 2002).

Cleaning operations usually occur at the end of the drying period, after the clogging layer is left drying, decomposing and cracking. The mechanical removal of the superficial clogged material should be done with scrapers, graders, or manually with rakes. Disking or plowing are common practices to temporarily rehabilitate the soil, although fines and other clogging material keep accumulating within the soil (Bouwer 2002). The standard rehabilitation, could be ineffective when the formation of the damage is internal rather than only superficial. As reported in the Standard Guidelines for Managed Aquifer Recharge (American Society of Civil Engineers 2020), the periodical removal of native clogged sediments and the deepening of the facility is not sustainable and could permanently compromise the MAR site. On the other side, operations such as the periodical importation of new permeable sediment or washing to separate the clogged material from the coarser matrix are highly expensive. In most severe cases, the accumulation of fines in the facility controls the useful site lifespan.

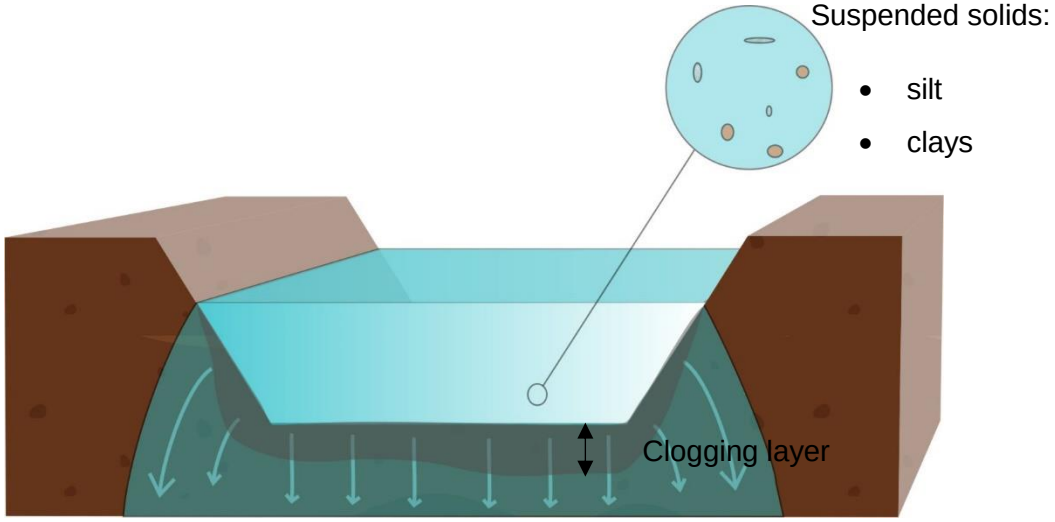

Figure 3: Scheme of fines intrusion in MAR spreading methods during water recharge

1.4 Water Standards

Clogging processes are highly interdependent and are commonly experienced directly on the site during MAR operations. As mentioned in the previous section, clogging can be controlled by pre-treatment of the recharge water and rehabilitation techniques. The use of these techniques always depends on the recharge system type and hydrogeological setting, for which an appropriate MAR scheme and site selection is preferable for successful operations (Jeong et al. 2018).

Water quality standards to prevent clogging in MAR design are the total suspended solids (TSS), total dissolved solids (TDS) and turbidity level for smaller particles, expressed in Nephelometric Turbidity Units (NTU). Total Organic Carbon (TOC) and Total Phosphorous (P) control biological clogging, while Iron (Fe), Manganese (Mg), Chromium (Cr) are standards for chemical clogging. Total Dissolved Oxygen (TDO) is associated with mechanical clogging and

chemical clogging (Fernandez Escalante et al. 2020). These water-quality parameters to prevent clogging in MAR sites vary considerably among water quality standards in different countries, especially regarding TOC and TSS. For example, TSS has to be < 5 mg/l in Florida, while in Mexico, recharge water can have a concentration of 150 mg/l (Fernandez Escalante et al. 2020).

Three more specific parameters to predict the clogging potential for wells injection are reported in MAR literature (Bouwer 2002). The Modified Fouling Index (MFI) is performed through a 0.45 µm Millipore filter test to determine the water's tendency to clog the membrane (Schippers and Verdouw 1980). This indicator of clogging potential is equal to the line describing the slope of the inverse of the flow rate versus the amount of water passing through the membrane at a constant pressure in standardised conditions (Pyne 1995). The Assimilable Organic Carbon content (AOC) measures microbial growth potential and is expressed as the fraction of organic carbon that microorganisms can assimilate in an acetate solution producing the same bacterial growth. (Van Der Kooij et al. 1982). Biodegradable Organic Carbon (BDOC) is preferable for higher organic carbon concentrations and is easier to determine; the water is passed through batch tests with soil slurries, and degradation in organic carbon is annotated (Bouwer 2002).

Attempts to determine the clogging rate in porous media have been done through Parallel filter index (PFI) (Hijnen et al. 2020). The recharge water is injected in sand columns filled with the aquifer material or composed of sand with the same hydraulic conductivity. The head losses are then measured for a constant filtration rate higher than the infiltration rates in the aquifer formation, acting as an early warning system. These parameters are useful to compare relative clogging potential for various sources of recharge water, but they cannot entirely predict clogging since declines in injection rates also depend on the variations in water quality and the hydraulic characteristics of the aquifer (Bouwer 2002). The characteristics of the native soils and their heterogeneity also have a major impact (Barry et al. 2017).

Using the MFI clogging indicator, Buik and Willemsen (2002) derived a relationship to predict the rate of physical clogging in recharge wells. The clogging rate depends on the infiltration rate on the borehole wall, suspended solids and aquifer characteristics, determined over the median diameter of the sandy aquifer. The work was based on Olsthoorn (1982) relating the MFI to the permeability of the formed “external cake”, and the available relations between the MFI values and the pore sizes of the membranes. Maliva (2020) reports that the relationship for the clogging rate in recharge wells cannot only work for the clogging rate between back-flushing events, and it cannot predict when clogging will occur. On this regard, the understanding of deposition mechanisms is vital to determine the formation of clogging, also in surface spreading methods.

1.5 Deposition mechanisms

In particle filtration theory, distinct deposition mechanisms are presented. Filter or "external" cake forms when the suspended particles have larger grain size than the porous media grain size, thus the particles accumulate on the surface of the granular material. This process is also defined as surface clogging. The "internal" filter cake forms when smaller suspended particles, enter the interstitial space of the bed and deposit according to the mechanism of straining or size exclusion, leading to the formation of the internal clogging. When two or more particles enter the pore space at once, they form a particle bridge and the blocking of the pore throat is reported as "bridging" (Kanti Sen and Khilar 2006). Physical-chemical forces control the transport and govern the physical-chemical filtration mechanism for colloidal and a range of intermediate particles, with a diameter size <1 µm (Herzig, Leclerc et al. 1970). For this particle size ranges, the Brownian motion controls the collision mechanism, and electrostatic interaction and London-van-der-Waals forces regulate the attachment mechanism (McDowell-Boyer et al. 1986; Zamani and Maini 2009).

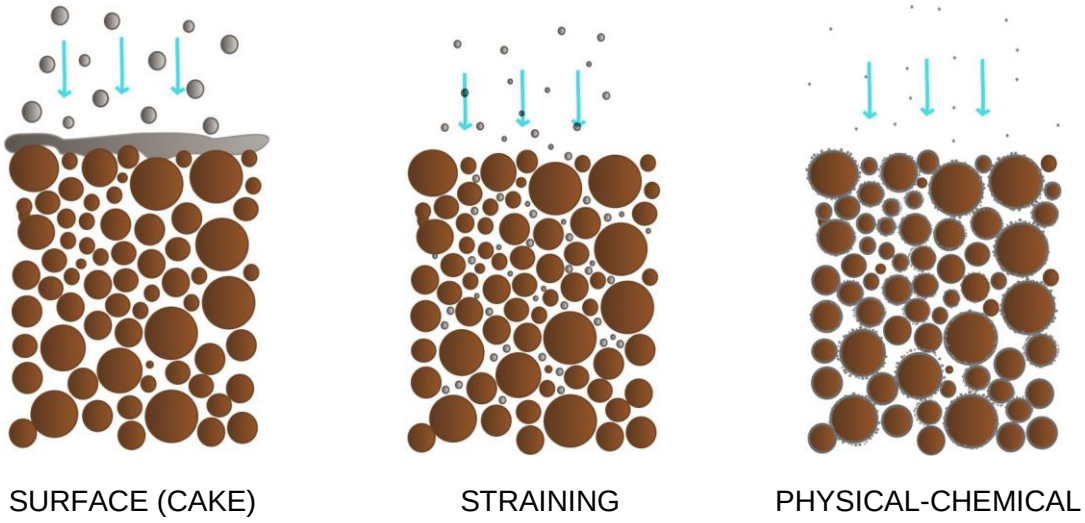

Figure 4: The three main filtration mechanism, adapted from McDowell-Boyer et al. (1986)

Differently from larger suspended particles, the very small diameter size of colloidals, determines not only the predominance of surface forces over the deposition process, but also the slower sedimentation rate, in relation to the square of their particle size. Colloidal particles remain dispersed longer, whereas suspended particles settle rather rapidly by sedimentation under normal gravity (Elimelech et al. 1998).

Besides the challenges in the quantification of the physical and chemical interactions taking place at the single particle on a collector, microscopic modelling goes beyond the purpose of this research. The focus has been on permeability reductions triggered by fine-grained suspended particles (>1 µm), in the clay and silt range. Over this range of suspended particles the volumetric forces, namely gravity and hydrodynamics forces, control the interstitial

movement of particles in the porous media. The particles' entrapment follows geometric considerations based on the ratio of the size of fines to the size of the pore constrictions of the porous media. Several clogging analyses appoint the ratio of the diameters as the critical parameter controlling the diverse deposition mechanisms, namely blocking, bridging or surface deposition, and piping (Gruesbeck and Collins 1982; Herzig et al. 1970; Muecke 1979).

Depending on the native sediment, the nature of fines and their internal rearrangement, the formation of superficial or internal clogging is triggered, determining not only the depth but also the rate at which it occurs.

1.6 Clogging risk assessment

The water standards defined in the previous sections indicate the threshold limits for clogging formation but are not specific to the site's characteristics. Currently, comprehensive models of clogging in porous media have not been developed, and existing models for clogging only address specific observations from a single experimental set-up (Du et al. 2018a; Xie et al. 2020). The comprehensive numerical code CLOG for simulating clogging processes in MAR sites requires further calibration of the kinetic parameters for application (Pérez Paricio 2001). The effect of clogging on the infiltration dynamic has been incorporated in numerical simulations in HYDRUS and MODFLOW through time-variable scaling factors acting on parameters for hydraulic conductivity (Glass et al. 2020; Majumdar et al. 2008). Laboratory experiments or observations of water levels are still necessary to calibrate these models and replicate the overall behaviour.

According to Zhang et al. (2020), one of the primary challenges facing research on Managed Aquifer Recharge (MAR) is the absence of systematic and comprehensive studies on the clogging mechanisms. Standardised methods should be established to assess and predict clogging and develop more effective, easy-to-apply prevention and rehabilitation measures.

Although the current research in MAR has progressed in detecting on-going clogging and its management, there is still a need to develop modelling tools to predict potential reductions in MAR infiltration capacity and incorporate risks for cost-effective design (Dillon et al. 2018; Maliva 2020). Conventional and advanced site characterisation methods should be developed to integrate data into models and explore different design and operational options, allowing local solutions to meet performance objectives before construction begins, e.g., determining optimal infiltration and recovery schedules (Ringleb et al., 2016).

Assessing the risk of clogging at a MAR site could minimise clogging and ensure successful MAR performance, avoiding considerable economic expenditures in the later remediation of the site. Through site characterisation and modelling tools, a range of design and management options could be evaluated during the planning phase of the site. Costs of operation and

maintenance could be reduced, ensuring long-lasting sustained recharge rates. Developing strategies for cost-efficient maintenance at the specific site can assist the decision-making process during the MAR planning phase or undergoing operations.

1.7 Research questions and objectives

The following research questions have been defined at the start of the research process to assess the risk of physical clogging at MAR sites:

- How can clogging behaviour or the susceptibility of MAR infrastructures be assessed, ideally prior to the operation phase of the MAR site?
- Which design and operation options would effectively reduce the risk of clogging?
- Which maintenance operations would be the most cost-efficient?

To answer the posed questions, the objectives of the work have been:

- To identify and understand the main mechanisms that cause the reduction in the infiltration rates and include them within a modelling scheme;
- To develop methods for site characterisation to assess the risk of clogging at the specific site;
- To compare the costs and benefits of different alternatives in reducing the potential damages of clogging.

In order to answer the first research question, physical clogging phenomena have to be investigated at the temporal and spatial dimensions. The quantification of the time for the MAR facility to be clogged and the depth at which fines accumulate, would provide estimates on the frequency of cleaning operations and the depth of sediments to be treated. The risk assessment can determine the expected lifespan of the MAR infrastructure and the costs of proper maintenance. Predictions on the state variable of a system are made through observations and modelling.

First, a review of existing clogging models in literature was performed, and the relevant mechanisms gained from these studies were collected under a conceptual framework for modelling clogging (Accepted Paper). The datasets of the clogging profiles were then collected from the literature and integrated with column experiments to parametrise the resulting model on the basis of the system's physical characteristics (Publication I). Once the predictions proved valid from the laboratory experiments, they were tested in field conditions, accounting for the site-specific features affecting the spatial formation of clogging at the site (Publication II).

Through the setting up of the model and parameterisation from site characterisation techniques, quantitative estimations can be performed to determine the frequency of cleaning

operations, the lifespan of the MAR site and the costs required for maintenance. A schematisation of the research steps undertaken and relative publications is illustrated in Fig. 5.

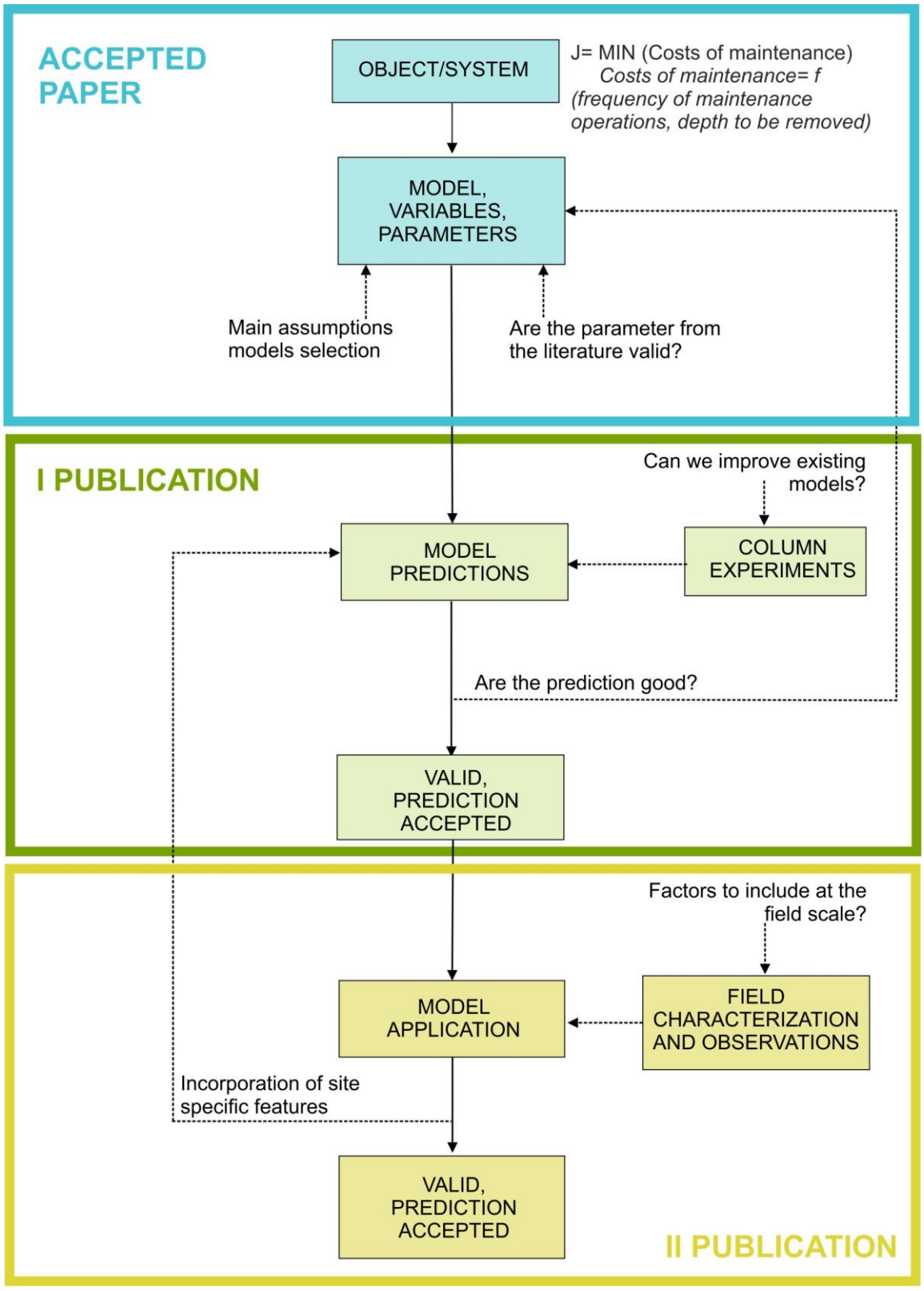

Figure 5: Scheme for model development, adapted from Dym (2004).

2 Material and Methods

2.1 Literature Review

A literature review was performed in the initial phase of the research process. The literature review aimed to critically assess the studies developing models for physical clogging processes. Experimental and observational studies restricted to cause-effect relationships were excluded from the literature review. For the review, the scientific databases of Scopus (https://www.scopus.com) and Web of Science (https://www.webofscience.com) were consulted, and results from Google Scholar (https://scholar.google.com) were integrated. The research included academic papers, theses and conference proceedings.

First, the papers were classified based on the engineering field of application. The main fields of application identified for physical clogging modelling were the following ones:

- Managed Aquifer recharge application
- Petroleum engineering application (deep bed filtration)
- Subsurface-flow treatment wetlands
- Geotechnical engineering application

Within each field of application, the authors' studies were first collected and summarised, excluding redundant studies. The selected studies were compared and contrasted, highlighting the authors' subsequent work, and developing theories and relationships were emphasised.

Mathematical formulations developed in the studies were highlighted. The strengths and weaknesses of each developed model for physical clogging were discussed, highlighting the validity of existing parameters in the literature and the dependence of parameters on column experiment calibration.

In order to organise the studies and allow for comparison, each study in the literature review defined the respective scope of application, the model category, fines of interest and hydraulic operating conditions.

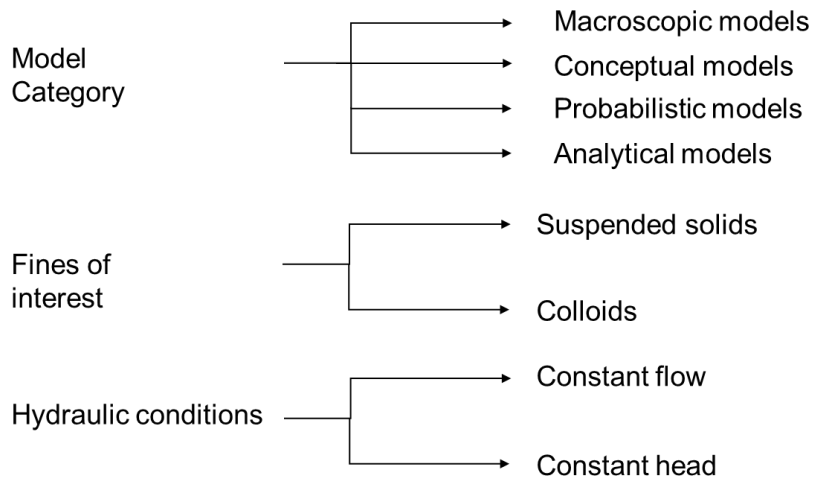

Figure 6: Classification of the numerical models within the literature reivew.

2.2 Process-based framework

A process-based framework for modelling physical clogging was created from the main processes underlined in the studies. The mathematical formulation collected within each study was divided into three tables: (i) particles' distribution in porous media (ii) changes in porosity ϕ (iii) changes in permeability *k.*

For each equation, parameters were reported, with emphasis on available parameters from the literature. The organisation in tables of the main mathematical formulations to model physical clogging allowed to observe the choices of the authors to describe the same process under a conceptual framework. These mathematical formulations have been tested afterwards with data from the literature and then from own performed experiments. The coefficient of determination R^2 assessed how well the models replicated the decrease in soil permeability from volumes of retained particles.

In order to develop a model for physical clogging, the state variables of the system were defined:

- Retained volume of particles in the porous media *σ(z,t)*
- Permeability *k(z,t)*

From the literature review, it followed that the parameters involved in the physical clogging mechanisms are:

Table 1: Conditions and responsible parameters for physical clogging

	Water quality conditions	**Geometric conditions**	**Hydraulic conditions**	**Hydro-geochemical conditions**
Parameters	• Initial particle concentration in the influent C_0	• Particle size distribution *PSD* • Grain size (→ pore space) distribution of the medium *GSD*	•Pore flow velocity *u* • Initial hydraulic conductivity K_0	• Ionic strength of water *IS* (for clays)

The main gap from the literature review in physical clogging modelling was the expected depth at which particles deposit, thus the internal distribution of particles within the porous media. The literature review revealed that a geometric component plays a role in the entrapment of particles, and the hydraulic component, for constant flow conditions, is responsible for the remobilisation of particles and, thus, the "wash-out" effect.

It was chosen to focus on developing the model for physical clogging for the one-dimensional flow in surface spreading methods. The possibility to reverse the flow direction, known as back-washing, is a common technique in the remediation of clogging in injection wells. Thus, It was decided to develop the model for physical clogging starting from the case of vertical flow in constant head conditions.

2.3 Dataset review from literature

The infiltration process in MAR sites involves the deposition and wash-out of particles, with a first phase where fine particles intrude at a specific depth. For fine-grained sediments, the capture of fines into the porous media and relative depth is mainly related to the particles size distribution (PSD) of the suspension and the pore space of the soil, which can be attributed to the soil's grain sizes distribution (GSD). During the infiltration process, as more fines accumulate, clogging starts to occur, resulting in a decrease in infiltration rates. This process, in turn, accumulates additional fines that deposit over the formed layer.

We attempted to cover a gap in the literature from the water-quality indicators for physical clogging to the sophisticated models at the pore scale, which are not feasible for a rapid and cost-effective assessment of physical clogging risk at managed aquifer recharge sites. With the objective of closing the gap from the literature review, datasets of clogging profiles were collected from column experiment studies, which reflected MAR conditions.

Clogging profiles were parametrised as exponential decay functions, similar to the work of Huston and Fox (2015) in river ecology. The exponential decay function, describing the vertical

profile of infiltrated fines in gravel beds, is theoretically derived from the mass conservation of fine sediments for a finite volume in the work of Cui et al. (2008).

$$\frac{\partial F}{\partial t} + \frac{\partial q}{\partial z} = 0 \tag{1}$$

$$\frac{\partial q}{\partial z} = -\beta q \tag{2}$$

With F the fraction of fine sediments to the total soil volume, q the fine sediment flux per unit area, and β the trapping coefficient.

In the Wooster et al. (2008) study, semi-empirical relations from experimental runs were derived to fit the vertical profile knowing the grain size distribution for the gravel bed and infiltrating fines. From the observations of the clogging profiles in Huston and Fox (2015), two main assumptions followed: first, the maximum sediment intrusive depth Z_c is reached at the very early stage of the clogging process as a function of the pore water velocity distribution for the clean substrate; secondly, the clogging profile along depth follows an exponential decay. Observing the maximum fraction of fines deposit at the water-sediment interface, reaching the close 0% in correspondence of the maximum clogging depth Z_c, the clogging profile is described in terms of the fine sediment fraction as:

$$\frac{f}{f_s} = e^{-\beta z} \tag{3}$$

With f_s the maximum expected fine sediment fraction at the water-sediment interface and β the coefficient for the exponential decay with depth. In Huston and Fox (2015), f_s is estimated from the information of the gravel and fine porosity.

Since the studies mentioned above were performed for sediment transport in hydraulically turbulent open channel flow, we tested whether the main assumptions for the clogging profiles in Huston and Fox (2015) were holding for vertical infiltration of particles in laminar flow conditions, similar to water recharge in surface spreading methods.

We collected retention profile datasets, in internal clogging conditions, from the studies of Alem et al. (2014), Ahfir et al. (2017) and Tippelt (2015). The experiments were performed in soil columns with a porous media in the grain size range of coarse medium sand, in the 0.25–1 mm range. Experiments conducted on gravel substrates, such as those conducted by Gibson et al. (2009) and Tang et al. (2020) were not considered. Similarly, the silt profiles in chromatography columns from Du et al. (2018b) were excluded from the analysis due to the different experimental setups. In the selected studies, a low concentration of fine particles in suspension was let infiltrate in the sand column, and after a certain infiltrated volume, deposited particles were wet-sieved.

In Alem et al. (2014) and Ahfir et al. (2017) the deposited particles are expressed in terms of volumetric retention (cm3/cm3) and mass retention (g/g) to the porous media, while in Tippelt (2015) the total deposited mass is expressed for the sieved section. To compare the datasets from the selected studies, the proportion of deposited mass relative to the total mass of infiltrated particles was calculated for each section. At the central point of each section, an average value was computed by dividing the relative mass% over the section length and assigning the relative mass of deposited clay to a specific depth.

After data processing, the clogging profiles in terms of relative mass on total infiltrating mass were fitted to exponential decay functions in MATLAB R2019a. The objective was to derive the parameters for the relative mass of deposited particles at the surface ($f_{z=0}$) and the decay rate of deposition (α). The coefficient of determination R^2 was employed to test whether the exponential decay explained the particle deposition variation over depth.

The parameters $f_{z=0}$ and α were then related to the clogging predictors from the experimental setting, such as the diameter sizes d_{50} (inflow particles), D_{50} (porous media). The information on the geometric conditions was restricted in part of the databases to the median diameter, which is in line with the static chosen by Bradford et al. (2003) to describe straining effects. Predictors from experimental hydraulic conditions, such as the initial hydraulic conductivity of the porous media and flow velocity, were also tested. Data on the hydro-geochemistry conditions of the experiments could not be compared since part of the studies were conducted with deionised water. The number of datasets available for the analysis was restricted by the accessibility of retention profiles in the relevant literature. Typically, filtration studies do not provide this information since particles concentrations are measured automatically at the effluent. The absence of retention profile data in the literature presents a limitation in comprehending the processes of straining and deposition within porous media (Alem et al. 2013).

2.4 Laboratory experiments

Due to the limited dataset of retention profiles in literature, column experiments were conducted to extend the datasets to sands with different granulometry, reflecting MAR conditions, and observe the intrusion and deposition of silt particles.

Silt particles were prepared for the suspension from a silty soil collected at the Bad Lauchstädt site. The soil was pre-sieved, dried and tested for organic matter removal. At the Soil Lab at the Department of Soil System Science UFZ Halle, mechanical sieve shakers separated the silt fraction <63 µm from the residual soil. The particle size distributions and statistics were performed first by sedimentation methods (Sedigraph) at the Faculty of Physic and Earth Sciences in Leipzig. Laser diffraction analyses (Cilas Particle Size 920) were later performed

at the Institute of Geosciences and Geography in Halle. The two methods are based on different physical principles and assumptions, and even though laser diffraction underestimates the plate-like clay particles, sedimentation analysis 'overestimate' these particles due to the lower apparent density and inaccurate application of Stokes' Law (Buurman et al. 2001). There is no correct or incorrect method to apply for particles size analysis, as long as the results from the two methods are kept separated. Since the other studies in the dataset employ laser diffraction analysis for the particles size distribution, this method was preferred for comparison. Under laser diffraction, the silt particles had a median diameter of d_{50} = 31.01 (±0.20) µm.

Column experiments were set up reproducing surface spreading methods in MAR systems. The design of the soil column experiment replicated constant head conditions through the installation of the upper and lower reservoir, outflow and valves adjustments. The column had a diameter of 4.8 cm and a height of 50 cm, with a constant head of 20 cm above the sand surface, resulting in a hydraulic gradient of 1.44 cm/cm. A precision balance scale (KERN PCB) was programmed to record the variations in the outflow from the soil column. The data were recorded with a USB to RS232 serial port, and the time series of water mass was processed into flow velocity (cm/s).

Turbidity values (NTU) for the column effluent were measured using a turbidimeter (HACH 2100P). Water samples were collected before the start of the suspension's infiltration and during the experiment's run to verify the mass balance of the transported particles in the porous media. A calibration was conducted before to correlate the known a priori suspended particles (SP) concentrations (mg/l) with the measured (NTU) values of the created suspension.

At the end of the experiment, samples were taken at the column sections and at the porous media surface, dried, weighed, and annotated after wet-sieving and drying. To achieve this, techniques for soil samples collection without disrupting the column were first tested. Soil samples were retrieved from the column at 7 sections. Multiple methods to sieve and measure the silt fraction from the sand grains were examined to reduce the errors. Preliminary soil column experiments were run to assess the reproducibility of results from the running of the sand column, checking the hydraulic behaviour, and the procedure for the soil sample analysis.

Finally, the experiments were run with sands in the grain sizes range of 0.1-0.4 mm, 0.2-0.7 mm, 0.4-0.8 mm, and 0.5-1 mm. The sand was compacted according to the bulk density specified in the sand technical sheet, and the resulting porosity was calculated with the bulk density method for the sand particle density of 2.65 $\mathrm{g/cm^3}$, always specified in the technical sheet. The concentration of the suspension was 1 g/L of silt. The column was first saturated from the bottom with a peristaltic pump to prevent air trapping. After reaching stable outflow

conditions, the suspension infiltrated up to 14 litres. The experiments complemented the dataset from the literature and provided new insights into the surface deposition process, namely, the formation of the external cake.

In internal clogging conditions, a linear relationship was established for the proportion of fines present at the water-sediment interface, and the geometric ratio d_{50}/D_{50}. While the process of fines accumulation at the surface is formulated mathematically through a retention limit at the surface, in accordance to the observations and suspension-porous media properties. The parametrisation of the clogging profiles, starting from the geometric predictor, and limit for particles' superficial accumulation and external cake formation, is integrated into the model for physical clogging.

The following normalised form of the Kozeny-Carman equation from Alem et al. (2013) was validated for the outflow at the soil column:

$$\frac{k(z,t)}{k_0} = \frac{\phi(z,t)^3}{\phi_0^3}\frac{(1+\phi_0)^2}{(1+\phi(z,t))^2}\frac{S_0^2}{S(z,t)^2}\left(\frac{T_0}{T(z,t)}\right)^2 \tag{4}$$

with ϕ the porosity, *S* the specific surface area per unit volume of particles (1/cm) and the tortuosity T=$\phi^{-\mathrm{m}}$, with formation factor (Archie, 1942) m=1.3 for a sandy medium.

The specific surface area accounts for the additionally deposited particles:

$$S = \frac{1}{1-\phi}\left[(1-\phi_0)S_0 + (1-\phi_d)\frac{\sigma}{\rho_p}S_p\right] \tag{5}$$

with S_0 and ϕ_0 specific surface and porosity from clean bed, S_p and ϕ_d specific surface and porosity of the deposited particles (Boller and Kavanaugh, 1995).

The formulation from Herzig et al. (1970) is employed to replicate the decrease in porosity of the porous media:

$$\phi(z,\mathrm{t}) = \phi_0 - \beta\sigma(z,t) \tag{6}$$

with β the inverse of the compaction factor of retained particles $\beta = 1/(1-\phi_d)$. The porosity of the retained fines ϕ_d is derived from the average densities of deposited particles (Alem et al. 2013; Boller and Kavanaugh 1995):

$$\phi_d = 1 - \frac{\rho_d}{\rho_p} = 1 - [\frac{\rho_w}{\rho_p} + \left(1 - \frac{\rho_w}{\rho_p}\right)\frac{1}{a}N^{1-b} \tag{7}$$

With ρ_d the average deposit density, ρ_p the soil particles density, ρ_w the water density, *N* the number of particles in a deposit site, and *a* and *b* are constants taken as *a* = 1, *b* = 1.3.

Based on the expected clogging profiles, from the quantification of the vertical distribution of fines, the expected decrease in porosity, and increase in the specific surface area and tortuosity of the porous media are computed for every cm-depth, and the total decrease of the effective permeability is computed through the harmonic mean:

$$\frac{k_{\mathrm{tot}}(t)}{k_0} = \frac{L}{\sum_{\mathrm{z=0}}^{\mathrm{L}} \frac{l}{k(z,t)/k_0}} \tag{8}$$

In the case of surface clogging, the equation for the effective permeability is adapted to include the forming layer of the external cake (Lippera et al. 2023a):

$$\frac{k_{\mathrm{tot}}(t)}{k_0} = \frac{L + L_{\mathrm{cake}}(t)}{\sum_{\mathrm{z=0}}^{\mathrm{L}} \frac{l}{\frac{k(z,t)}{k_0}} + \frac{L_{\mathrm{cake}}(t)}{\frac{k_{\mathrm{cake}}}{k_{\mathrm{z=0,limit}}}}} \tag{9}$$

with $L_{\mathrm{cake}}(t)$ the thickness of the external cake , $k_{\mathrm{z=0,limit}}$ the permeability of the porous media at the surface when $M_{\mathrm{z=0,limit}}$ is met, and k_{cake} the permeability of the fines depositing superficially.

The variation in total hydraulic conductivity is then evaluated with the R^2 coefficient from the outflow rate of the column, using the Darcy equation:

$$K = \frac{Q}{\frac{\Delta H}{L} A} \tag{10}$$

With ΔH the difference in hydraulic heads in the experimental set up, and *L* and *A* also design parameters of the experimental set-up.

2.5 Field validation

In October 2021, a field campaign was conducted at the managed aquifer recharge (MAR) site in Suvereto, Italy, in collaboration with the Scuola Superiore Sant'Anna. The objective of the field work was the implementation of the clogging risk assessment to the field scale. More specifically, part of the study objectives were detecting hydraulic and physical properties at the MAR site and testing routines for parametrisation of the developed clogging model. The MAR site in Suvereto was well-suited for this purpose, given the availability of monitoring time series from the supervisory control and data acquisition (SCADA) system.

The field-work consisted in the shallow characterisation of soil horizontal heterogeneities, at the effective penetration depths of 0.25 m, 0.5 m, and 0.9 m, through an Electromagnetic Induction (EMI) survey, performed with the CMD Mini Explorer (GF Instruments, Brno, CZ) electromagnetic conductivity meter operated in horizontal dipole orientation. Apparent Electrical Conductivity (ECa) in milliSiemens per meter (mS/m), is a depth-weighted average of the soil electrical conductivity to a specific depth. The mapping of this physical variable is

employed in geophysical methods to describe near-surface ground values (Popp et al. 2012). This key parameter can distinguish variations in soil texture, clay content, volumetric water content and salinity (Doolittle and Brevik 2014). Coordinates and elevation values were recorded continuously with the DGPS (Leica TPS1200+, Leica Geosystems, Heerbrugg, CH) at 0.2 s frequency.

After identification of the sampling locations, double-ring infiltrometer tests were conducted to measure the local infiltration rates (Eijkelkamp Soil & Water, Giesbeek, NL ; ASTM D33 85-03 standard test method). At the exact locations, soil samples were collected to characterise the sediment matrix and fines content at five different depths, at depth intervals of 0-1 cm, 1-3 cm, 3-8 cm, 8-13 cm, and 18-23 cm.

The EMI maps were interpreted by interpolating the data via Ordinary Kriging in SAGA GIS software. The resulting variograms were fitted with a power model. The data from the infiltrometer test were interpreted with the Philip (1957) model to derive the asymptotic value of the hydraulic conductivity near saturation. The laboratory work was conducted at the Institute of Geosciences and Geography in Halle, using the laser diffraction machine (Cilas Particle Size 920), to determine the particle distribution of the fine material in the soil samples in the fraction 0.7- 63 µm. The intrusive fines were characterised by the particles' size distribution of the collected surface crust and the observed variation in fines content in the soil samples. Organic matter (OM) content in samples was also measured through the weight Loss-on-Ignition (LOI) test. The results from collecting multiple data from the MAR site provided insight into the spatial distribution of clogging inside the basin.

During the secondment in Pisa at BioLabs of the Scuola Superiore Sant'Anna, historical data of infiltration capacity at the basin were analysed from the recordings of the level logger at 1.70 m depth at the centre of the basin, and records of the pump activation times, always having a recording frequency of 15 min. Recorded historical data of turbidity (NTU) at the intake of the Suvereto basin were also analysed. Data of levels (m) in the river Cornia at Ponte per Montione and rainfall data (mm) from the Regional Hydrological Service (SIR) were analysed to understand the dynamics of suspended solids load associated with flooding events. Total suspended solids (TSS) analysis was conducted at the BioLabs for the recharged water of the site. It was not possible to perform a correlation between total suspended solids (TSS) and recorded turbidity (NTU) values due to the clean water conditions <1 mg/L. During the research stay, the dry conditions over the months of February and March 2022 did not allow for water sampling following a flooding event. Since the Suvereto site does not pump water inside the basin when the turbidity threshold is over 100 NTU, and from the historical time series the NTU values are relatively low and stable, the input of external fines from flooding events was excluded from the clogging analysis for the Suvereto site.

Without the recharge water being the primary source of incoming fines, the work provided insights into how field factors intervene in the spatial distribution of clogging at the site. This is a significant progress from clogging models, which have only been validated in soil column experiments. Moreover, the quantitative assessment of the distribution of intrusive fines was validated with the observations of the clogging profiles from the collected soil samples. The evolution in the infiltration capacity of the site was then simulated and compared with the infiltration rates for the whole pond computed from the recorded water levels and pumps activations time series at the Suvereto basin for the recharge seasons 2019-2020 and 2020-2021.

2.6 Scenario analysis

The model for physical clogging was developed and validated from column experiments, and its application was tested in field conditions. The advantage of the method developed is that it can be used for planning, for which scenario analyses were carried out. During the planning phase of a site, clogging prevention measures can be either through planning or management decisions. These planning or management decisions and their feasibility depend on the physical, normative, and technical constraints specific to the site. Thus every design alternative has to be simulated according to the specific site characteristics, and part of the design alternatives should be excluded a priori when not feasible.

Design alternatives that can be evaluated for a MAR site were restricted to the following:

- Not doing anything
- Regular maintenance with ploughing up to *X* cm
- Excavation and sand replacement of *Y* cm
- Construction of the sedimentation pond
- Water pre-treatment
- Source control through monitoring

Each alternative should be evaluated based on the costs of realisation, maintenance, and expected total recharged volume over a number of years.

Besides the scenarios where the input of fines arrives to the site, and no maintenance is done, other scenarios, including cleaning operations, can be simulated under the following modelling steps developed during the research work. The cleaning operations, such as ploughing, are computed by assuming perfect mixing of the sediment matrix in the upper *X* cm. For the external input of fines arriving at the site per unit area, the mass percentage of particles associated with a diameter interval *j*, the diameter class of the particles size distribution, is computed:

$$M_{input}^{j}(t) = \frac{M_{tot}(t)}{A_{basin}} P^{j}(t) \tag{11}$$

$P^{j}(t)$ is the percentage of particles in the diameter class *j*. The mass of sediments already present in the matrix for the class *j* and the new mass in input for the class *j* are the following:

$$M_{mixed}^{j}(t) = L(1-n)\rho_{sed} P^{j}(t) + M_{input}^{j}(t) \tag{12}$$

ρ_{sed} is the solid density of the sediment matrix, *L* is the length of interest of *X* cm, and $M_{mixed}^{j}(t)$ is the new soil mass for the diameter class *j* in the sediment matrix per unit area of the basin. The new mixed particles size distribution for the sediment matrix in the upper *X* cm can thus be calculated:

$$P^{j}(t+1) = \frac{M_{mixed}^{j}(t)}{\sum_{j=1}^{N} M_{mixed}^{j}(t)} \tag{13}$$

and the evolution over time of the grain size distribution of the sediment matrix leads to a higher fines percentage and a decrease in percentages of coarser sediments, making the soil more vulnerable to clogging.

Design alternatives for sand replacement are simulated by considering the physical properties of the specific sand for the length of *Y* cm. The layer of the native sediment below *Y* cm likely would still be restricting the flow of the recharge water into the deeper layers. However, sand with the designed granulometry can capture the fines over its length and still provide sustained drainage avoiding superficial clogging.

Scenarios for constructing a sedimentation pond have been tested by considering design variables, such as the length of the sedimentation pond and the height of its outlet. The formula from Fair and Geyer (1954) is employed to compute the trapped fraction of target sediments:

$$R = 1 - \left[1 + \frac{1}{n} \frac{V_p}{(Q/Af)}\right] - n \tag{14}$$

with V_p the settling velocity of target sediments with diameter (m), computed through the Stoke's law, n = 1/(1 − λ) the turbulence parameter, with λ the hydraulic efficiency coefficient, given the basin configuration. The sedimentation pond's effectiveness in trapping fines load is estimated and the potential of the sedimentation basin in mitigating clogging issues at the MAR site is evaluated.

In order to showcase applications of the developed model for physical clogging, the Loria infiltration site was object of the simulations. The Loria infiltration basin is situated in the northern region of Italy's upper Venetian Plain. Its geographic location falls within the catchment region of the Brenta River, around 15 km north of Cittadella in the Padua Province.

The flood-water from the Lugana stream is the primary source of recharge water, and is directed into the pond at irregular intervals via an adjustable inlet. Operated by the “Consorzio di Bonifica Brenta”, the basin has a total capacity of 40,000 m³. The groundwater table is located at a depth of roughly 40 m. For more informations, see P.A.T.I. (2013), Fontana et al. (2014) and Tippelt (2015).

A site characterisation was performed in this infiltration site in 2015 during the MARSOL project, by the Monitoring and Exploration Technology Department of the Helmholtz Centre for Environmental Research – UFZ. The data from the collected soil samples were used in the first publication (Lippera et al. 2023a) to showcase the applicability of the results. The electromagnetic profile measurements such as EM38DD and EM31, along with gamma-ray spectrometric measurements, are used to identify zones to assign the physical properties from the soil samples. Thus, the expected variation in the infiltration rates at the sampled location, is related to the variation in total infiltration capacity of the basin. Zones with “low”, “medium” and “high” vulnerability to clogging are classified.

Four major flooding events are assumed to recharge the Loria site over the year (MARSOL D7.1 2016). It is considered for each flooding event a 3 hrs peak discharge and 8 hrs flood recession. The Loria basin can reduce the river maximum thirty-year flow from 10 m^3/s to 5.5m^3/s (P.A.T.I. 2013). Thus a discharge rate of 4.5 m^3/s is considered to enter the Loria basin. During a flooding event, the site is filled with water and a spillway controls the water level and prevent it from exceeding the site's capacity. Once the flooding has passed, the bottom outlet is opened as a safety measure. Therefore, the computed recharge volumes pertain to a reference 11-hour duration of the flooding event. From the soil parameters and site information, the expected decline in hydraulic properties and the corresponding total recharged volumes over the years were computed at the Loria basin and compared for different maintenance and design scenarios. Given the characteristics of the Loria site, the design scenarios were modelled, to evaluate the potential volume of recharged water over 12 years.

3 Results

The publications are sorted according to the performed research workflow.

3.1 Accepted Paper

Lippera, M.C., Werban, U. and Vienken, T. *Application of physical clogging models to managed aquifer recharge: a review of modelling approaches from applied engineering fields*. Acque Sotterranee - Italian Journal of Groundwater (Accepted).

This manuscript condenses the findings of the literature review performed during the first research period. This work was vital to understand the existing numerical models for physical clogging in literature, their limitations, and the gaps to close for MAR sites' application. The literature review provided the foundation for the succeeding research stages.

Studies were collected from the MAR literature and other engineering fields dealing with water infiltration in natural heterogeneous systems. The studies were first organised, highlighting the respective scope of application, the hydraulic conditions and the range of fines of interest. This classification allows for a first orientation in numerical models for clogging assessment. The studies' modelling approaches were categorised based on the main assumptions and the conceptualisation of the soil volume. A description of these modelling approaches is essential to understand the advances in each path of study and where the main opportunities and limitations lie.

From the selected studies, the mathematical equations for the main physical clogging processes were systematically organised in tables for comparison. Particle transport and deposition, reduction in porosity and subsequent reduction in hydraulic conductivity are the main modelled processes common to the studies. Standard formulations and alternative choices undertaken by the studies are discussed in the manuscript. This comparison enables to transfer the knowledge in replicating the variations in hydraulic properties associated with physical clogging. The predictive capabilities of the physical clogging models are discussed, examining the extent to which they rely on parameters that require calibration based on specific experimental configurations. The ultimate goal is to provide recommendations to predict clogging phenomena in MAR applications, particularly for surface spreading methods, and establish a process-based workflow that can be combined with site characterization technologies.

Researchers, engineers, and MAR practitioners can consult this literature review also to comprehend limitations and recommendations in the practical application of the existing numerical models for physical clogging.

The author of this thesis conducted the literature review and addressed the opportunities and limitations of the analysed studies. She conducted the systematic review by categorizing mathematical models and organizing mathematical equations in tables. She outlined the conceptual model for physical clogging processes and developed the concept for the publication. She wrote the manuscript, created the graphs and illustrations, and was responsible for the publication review process.

3.2 Publication I

Lippera, M.C., Werban, U. and Vienken, T. Improving clogging predictions at managed aquifer recharge sites: a quantitative assessment on the vertical distribution of intrusive fines. Hydrogeol J 31, 71–86 (2023). https://doi.org/10.1007/s10040-022-02581-7

This publication addresses the gap identified from the literature review: determining the intrusion and deposition depth of external fines in porous media during MAR operations.

Eight experimental datasets were reviewed from multiple soil-column studies in the literature. Specifically, the available profiles of deposited fines were used for the analysis. The experiments needed to reflect MAR conditions for surface spreading methods, from the grain size range of the porous media to the fines particle concentrations and water flow. Due to the limited number of datasets, four additional column experiments were performed, extending the analysis to surface deposition processes for silt particles. In the performed column experiments, 1 g/L of silt suspension, with particles' median diameter d_{50}=31.01 (±0.20) µm, was infiltrated in quartz sands in the grain-size ranges of 0.5–1.0, 0.4–0.8, 0.2–0.7, and 0.1–0.4 mm. The 50 cm long column had a constant head of 20 cm above the porous media and a total hydraulic gradient of 1.44 cm/cm. Turbidity values and outflow rates at the column were monitored during infiltration. At the end of the experiment, soil samples were taken at the column sections to determine the retention profile of deposited particles.

The data analysis involved defining the collected datasets in relative masses of deposited fines to the total infiltrated mass and parametrizing the vertical profiles as exponential decay functions over depth. A linear relationship was established between the relative mass of fines at the water-sediment interface and the geometric ratio d_{50}/D_{50} of the experimental setup. A mathematical solution is then used to define the decay rate of fines deposition over depth. This coefficient determines the expected depth of clogging and the clogging vertical profile. Additionally, in the experiments characterised by superficial clogging, a retention limit at the surface is formulated to determine the mass limit of infiltrating particles after which the external cake starts forming. Finally, the use of the Kozeny-Carman equation is validated in computing reductions in soil permeability using the observed outflow rates from the column experiments.

In surface clogging, a parameter representative of the hydraulic conductivity of the filter cake is introduced to compute the effective hydraulic conductivity perpendicular to the flow.

The findings are then applied to a MAR case study to showcase the quantification of clogging effects starting from available soil samples' data. This work enables the assessment of clogging vulnerability during the planning phase of MAR schemes. The application of the developed model could assist in determining cost-effective strategies for MAR operations and maintenance and contribute to the scheme's overall efficiency.

The author of this thesis actively participated in the development and conceptual design of the research project, from the design of the experiments to the data analysis. She collected the datasets from the literature and evaluated them. She performed the experiments by setting up the instrumentation, running the experiments, and collecting the data and samples. She performed the data analysis and evaluated and interpreted the observations using the developed model for physical clogging. She visualised the results and drew the study's conclusion. She applied the findings to a MAR case study, wrote the manuscript and was responsible for the publication review process.

3.3 Publication II

Lippera, M.C., Werban, U., Rossetto R., and Vienken, T. Understanding and predicting physical clogging at managed aquifer recharge systems: A field-based modeling approach. Advances in Water Resources, 177, 104462 (2023). https://doi.org/10.1016/j.advwatres.2023.104462

This publication investigates the application of the developed physical clogging model to MAR field conditions at tests site characterization routines. The fieldwork is carried on at the operative MAR site in Suvereto, Italy. This MAR site was selected due to its extensive monitoring network, which allows for the control of MAR operations and monitoring of recharge cycles.

The recharge system comprises a two-stage infiltration basin that diverts water from the Cornia River during high-flow periods. Through a supervisory control and data acquisition (SCADA) system, water is pumped when the thresholds comply with the water quality and the river's minimum environmental flow. The water is first conveyed to a sedimentation pond and then flows to the adjacent infiltration pond for infiltration.

Field characterization was conducted in October 2021 during the dry season. First, shallow electromagnetic induction surveys (EMI) were performed to map the sediments' heterogeneities spatially. The hydraulic and physical properties of the sediments were

measured at point locations by performing double-ring infiltrometer test and computing the hydraulic conductivity near saturation. At the same locations, soil samples were collected at discrete depths to analyse the grain size distribution and organic matter (OM). Following the laboratory analysis from the field characterization, clogging patterns were observed, although the recharge water presents a low content of TSS. The spatial features of the basin are integrated into the model for physical clogging to explain the remobilization of fines inside the basin.

This work aims to verify that the parameters collected in the field sufficiently explain observed physical clogging, to reproduce site characterization and modelling routines in other MAR schemes. For this reason, a module for soil erosion was incorporated to compute the input of remobilized fines material from the slopes, given the topography of the basin and the soil texture information. It was then assumed that the mass of remobilised fine material is evenly distributed across the bottom of the basin, with slope <3%, in agreement with the observations. For the locations presenting physical clogging, thus having increasing fines content at the more superficial layers, the model for the vertical retention of fines was validated with an RMSE of 2.53% and 12.53%. The potential original infiltration rates were calculated from the measured value of the infiltrometer test and the exceeding fines content, and compared with the ones at the not-clogged locations. Finally, the overall model is set-up to predict the evolution in infiltration rates at the whole pond. From the erosion and fines mobilization processes, the evolution in the hydraulic properties at the basin bottom is computed, and thus the evolution in the whole basin infiltration rates is updated. These values are compared with the reduction in the median infiltration rate over the past two recharge seasons and show to be in agreement.

The findings of this study demonstrated that by incorporating the site-specific features, routines for site characterization and physical clogging model can be transferred to multiple MAR schemes. This allows MAR practitioners to apply the developed methodology to assess the risk of physical clogging at multiple sites.

The author of this thesis actively participated in the development and conceptual design of the research project. She organised the routines for the site characterization and conducted the field measurements and sampling. She performed the laboratory analysis and evaluated and interpreted the field datasets. She set up the model for physical clogging for the site and compared it to recorded historical data. She visualised the results and drew the study's conclusion. She wrote the manuscript and was responsible for the publication review process.

4 Discussion

The physical clogging Risk Assessment numerical model provides a rapid and cost-effective method of identifying areas at risk of clogging and estimating the time until infiltration rates are significantly reduced. The development of the numerical tool answered the research question to assess the susceptibility of MAR infrastructures prior to their operation phase. The selection and development of the model, with parameters that can be determined from site characterization, ensures this method to be transferable to multiple sites, taking into account the sediment heterogeneities and variability in water quality of the recharged water.

4.1 General model discussion

The first objective of the research work was to identify and understand the main mechanisms that cause the reduction in the infiltration rates and include them within a modelling scheme. The development of the numerical tool has been limited to a range of sediments and intrusive fines applicable to MAR surface spreading methods. The interdependence of physical clogging processes with other biological or chemical mechanisms has not been incorporated into the model, although concomitant mechanisms can influence the formation of clogging.

Physical clogging is generally recognized as the principal type of clogging on the field. However, it can be challenging to distinguish between single clogging mechanisms, making it necessary to evaluate the formation of clogging as a whole, as reported in Rinck-Pfeiffer et al. (2000). Bacteria and algae formation in spreading methods can contribute to the physical clogging of the pores (Bouwer 2002). Moreover, the concentration of suspended particles in the infiltration surface provides a good substrate for biofilm formation. As the suspended particles settle on the porous media, they can provide a surface for the microorganisms to attach and begin to form the biofilm (Martin 2013a; Pyne 2005). Thus, the formation of physical clogging can enhance the adhesion of microorganisms to the surface and the production of the biofilm, the matrix of EPS. The biofilm formation itself would be affected by the clogging state, since at a high recharge rate, biological clogging accumulates rapidly, but it can be easily eliminated with a high shear force. On the other hand, when the recharge rate is low, clogging may be delayed until biofilms grow, and the resulting biofilm would be strong enough to resist from being detached (Kim et al. 2010). Models for algae or microorganism growth could thus be integrated into a more comprehensive clogging risk assessment incorporating the effect of physical clogging on biological clogging formation and vice-versa. Otherwise, biological clogging indicators such as AOC and BDOC, defined in Sec. 1.4, could be integrated to report a higher risk of clogging at the site.

Chemical clogging could also interfere with the formation of physical clogging (Pérez Paricio 2001). When fresh water is recharged into a brackish aquifer system, and there is a low

concentration of positively charged ions to form bonds between the clay platelets, such as calcium, magnesium, and potassium, the clay particles become less stable and can begin to mobilize and expand due to substitution with water molecules (Bennion et al. 1998; Martin 2013a). Since clay swelling and dispersion are a particular case of physical clogging, site characterization techniques should be adopted to detect the presence of swelling clays, such as smectites. The effect of self-filtration of dispersed particles could be incorporated into the clogging model by determining the content and the particles size distribution of potentially dispersed clays due to changes in the ionic strength, and following changes in soil structure due to clay dispersion and swelling. This is the case especially for aquifers with fresh water injection, when the change in water composition is sudden. Clays deflocculation can be reduced when there is a gradual transition from freshwater to groundwater, and the addition of Ca+ or Mg++ into the recharge water lowers the risk of particles mobilization and swelling (Martin 2013a). Also, when mixing fresh water and groundwater, the potential for geochemical reactions can be assessed through PHREEQC (Parkhurst and Appelo 1999). The saturation index of the iron hydroxide Fe(OH)3 and of calcite (CaCO3) can be computed under varying redox conditions to examine the potential for chemical clogging (Dillon et al. 2010; Page et al. 2014). In the model for physical clogging, considerations of the potential for the concomitant effect of geochemical clogging can be incorporated. At the Suvereto site (Sec. 2.5), precipitated carbonates were found in the surface crust, which might have contributed to the retention of fines at the surface.

The effect on the compressible clogging material, such as the accumulated organic solids, loose clay and mucky layers, can contribute to the retention of fines at the surface of the porous media (Bouwer 2002). Hutchinson et al. (2013) report that an increase in the ponding depth might lead to an overburden pressure and consolidation of the upper layer. This reduction in porosity, due to consolidation from the increase in intergranular pressure, could be integrated into the model for physical clogging.

Other types of clogging could be integrated as modules into the numerical tool for physical clogging risk assessment, with the perspective of deriving a comprehensive model for clogging. One example is the developed model by Pérez Paricio (2001) for MAR sites, including transport and deposition of suspended solids, bacterial growth, mineral precipitation, gas binding and compaction of the upper layer. The model in question did not find its application due to the high uncertainty related to the parameters, especially the kinetic terms, making it not possible to derive reliable predictions on clogging development unless conducting first pilot tests and interpreting observations with CLOG (Pérez-Paricio and Carrera 2000). Thus, the developed physical clogging Risk Assessment numerical tool, could be extended to

include modules of other clogging mechanisms and interrelated processes, always preserving its characteristic to be parametrised from site characterization data.

4.2 Validity of the model

The research focused on physical clogging in surface-spreading methods, which is complicated to prevent and rehabilitate. For injection wells, periodic backwashing can still prolong the operational life of wells as a preventive measure (Martin 2013b). The application of the numerical model is restricted to surface spreading methods, such as infiltration basins and infiltration trenches, making it of high interest for practitioners dealing with recharge water with a high TSS load, which could be the case for flood-water recharge when no pre-treatment is possible. Even when the TSS load is low in infiltration basins, the external input of intrusive fines can be generated from erosion processes, as seen in Lippera et al. (2023b). The validity range of the model is conditioned by the hydraulic conditions and the range of fines-porous media given the reviewed datasets and performed column experiments.

The developed numerical tool for physical clogging has been parametrized under vertical and laminar flow conditions. Given the constant head column setup, the model was not tested for different flow velocities to understand the role of hydrodynamic forces on the transport and deposition of suspended solids, as done in Alem et al. (2013). Within the tested constant head conditions, the geometric predictor, through the median diameter of the porous media, might still play a role in restricting the flow at the pores, thus contributing indirectly to the hydrodynamic effect (Lippera et al. 2023a). These assumptions valid for surface spreading methods, should not be extended to clay colloid transport in injection wells, given the different hydraulic operating conditions and the physical and chemical forces contributing to the movement and attachment mechanisms. Several MAR studies have investigated physical clogging in relation to water flow velocities under constant flow conditions and geochemistry (Mays and Martin 2013; Torkzaban et al. 2015; Ye et al. 2019). The description of these processes with advection-dispersion equations has been applied to MAR in recharge wells with pre-treated water and clogging by clay colloids (Mays and Martin 2013; Pyne 1995). The relationship found in Lippera et al. (2023a) for the vertical distribution of fines might not hold for high flow velocities and increased pressure for recharge wells application.

Regarding the geometrical conditions, the range of investigated fines in this research has been clay and silt particles (0.98 – 62.5 µm), intruding into sandy porous media (250 – 1000 µm). Thus, the range of validity for this analysis is within a geometric ratio d_{50}/D_{50} of 0.001 to 0.25 within these types of sediments. Previous studies in the literature have derived qualitative rules for clogging based on the sole geometric ratios. The design criteria in granular filters (Terzaghi et al. 1967), based on the diameter sizes of the filter and base soil (Table 3), ensure drainage and prevent fines migration from the base soil (Das 2010). Army (1971) and Sherard et al.

(1984) revisited and developed further these filter design criteria (Table 3). Although broadly used in geotechnical applications, these approaches have been criticised for their too conservative nature and restricted functioning range to uniformly graded and well-graded soil (Honjo and Veneziano 1989; Indraratna et al. 2008). In Gibson et al. (2009), filter criteria thresholds are used to delineate bridging ($D_{15}\ /d_{85} < 10.6$) and unimpeded static percolation ($D_{15}\ /d_{85} > 14.5$) in the vertical distribution of interstitial deposits across a gravel bed. In Yousif et al. (2017), the reduction in permeability is found to be proportional to $D_{15}^2/(C_u d_{85})$.

Sakthivadivel (1969) studied particles straining based on the ratio of the media diameter to the suspended particle diameter d_m/d_p. However, McDowell-Boyer et al. (1986) reports that for broad grain size distributions within the range $d_m/d_p < 10$ and $d_m/d_p > 20$, smaller particles might be filtered by the action of the larger particles retained near the surface, in a combination of surface and straining filtration.

Empirical ratios of the size of fines to the size of the pore constrictions from Khilar and Fogler (1998) are also reported in Table 3 for comparison. Plugging behaviour due to blocking, bridging or surface deposition, and piping are categorised based on previous clogging analysis (Gruesbeck and Collins 1982; Herzig et al. 1970; Muecke 1979). However, the range 0.1-0.01 for piping or multiparticle blocking is conditioned by other factors, such as the concentration of fines and the flow rate.

Table 2: Empirical ratios in clogging literature

	Method	**Paper**	**Equation**
1	Empirical filter criteria, (a)Terzaghi and Peak(1967), (b)U.S. Army (1971), (c) Sherard et al. (1984)	Indraratna et al., (1997), Gibson et al. (2009), Yousif et al., (2017)	• $\frac{D_{15}}{d_{85}} < 4$ (a) $\frac{D_{15}}{d_{15}} < 4$ $C_u < 2$ uniform sand • $\frac{D_{15}}{d_{85}} < 5$ $C_u < 6$ sand (b) • $\frac{D_{15}}{d_{85}} < 5$ Sandy silts and clays (c) $\frac{D_{15}}{d_{85}} < 9$ Fine silts and clays
2	Ratio size of media to the suspended particle from straining filtration results, Sakthivadivel (1969) column experiments	McDowell-Boyer, Hunt et al. (1986)	• $\frac{d_m}{d_p} < 10$ external cake formation • $10 < \frac{d_m}{d_p} < 20$ retained particles occupy 30% of the pore volume • $\frac{d_m}{d_p} > 20$ retained particles occupy 2-5% of the pore volume • $\frac{d_m}{d_p} < 10\ and\ \frac{d_m}{d_p} > 20$ surface and straining filtration

3	Ratio size of suspended particles on size of pore constriction, from Herzig et al.; 1970 Gruesbeck and Collins, 1982, Muecke, 1979.	Khilar and Fogler (1988)	• $\frac{d_p}{d_0}$ >= 1 Plugging due to blocking or size exclusion • $0.1 < \frac{d_p}{d_0} < 0.6$ Plugging due to bridging and multi-particle blocking • $0.04 < \frac{d_p}{d_0} < 0.10$ Plugging due to surface deposition, bridging and multi-particle blocking • $0.01 < \frac{d_p}{d_0} < 0.04$ Surface deposition. Multi-particle blocking may or may not occur • Less than 0.01 Piping

The findings from Lippera et al. (2023a), agree with the qualitative categorisation for clogging behaviour. The results comply with the threshold of d_{50}/D_{50}=0.005 for initial straining of particles (Bradford et al. 2003; Zaidi et al. 2020) and with d_{50}/D_{50}=0.05 for significant straining (Bradford et al. 2002; Sakthivadivel 1969). Compared to the studies in Table 3, which considered the ratio of the size of the suspended particles to the pore diameter of the porous media, adopting $d_p = d_{50}$ and the average pore diameter (µm) as $d_0 = 0.235D_{50}$ valid for sands (G.Mahmoodlu et al. 2016), the found relationship for the clogging profile is consistent with the thresholds for the formation of the external cake for $\frac{d_p}{d_0} > 1$, the occurrence of multiparticle blocking between 0.1 to 0.01, and piping below 0.01 (Gruesbeck and Collins 1982; Herzig et al. 1970; Muecke 1979).

Huston and Fox (2015) propose adjusting the geometric ratio $\frac{d_{ss}}{d_{fs}}$ with a secondary parameter, the geometric standard deviation of the matrix sediment (σ_m), to account for the possible filling of the macropores by the smaller particles within the substrate mixture itself. In the model parametrization in Lippera et al. (2023a), the datasets from the selected studies did not comprise the complete porous media grain size distribution. However, since all the reviewed studies and performed column experiments used artificial quartz sand, the grain size distributions of the porous media are likely uniformly-graded. In the occurrence of a gap-graded soil, the assessment of the risk of clogging due to self-filtration, could be carried out by separating the grain-size curve into two parts and defining the geometric ratio between the coarser fraction and the finer one, similarly to the internal stability criterion in Lowe (1988). Two separated curves with d_{50} and $d_{50,\mathrm{crust}}$ are considered for the intrusive fines showing bimodal distribution in Lippera et al. (2023b). Depending on the grain size distribution of the sampled sediment and the particle size distribution of the intrusive particles, multimodal size distributions should be considered when defining the empirical ratio in gap-graded soils.

4.3 Site characterization for physical clogging risk assessment

The second objective of the work was to develop methods for site characterization to assess the risk of clogging at the specific site. The research fulfilled the objective by defining the clogging parameters and guidelines for site characterization (MARSoluT deliverable), as summarised in Table 3. The definition of parameters, collection procedure and post-analysis, are necessary to implement the developed model for physical clogging and assess the risk.

Table 3: Physical clogging parameters for risk assessment defined in the research project.

Parameter	Procedure	Post-analysis
Hydraulic conductivity (K) of native sediments (m/s)	Infiltrometer tests	Near-saturated K for infiltrometer tests
Grain Size Distribution	Soil sampling	Laser diffraction for fine fraction
Porosity	Undisturbed core sampling	Drying of the sample and dry bulk density calculation.
Particle's Concentration (mg/L)	Water Sampling	Total suspended solids (TSS) analysis
Turbidity (NTU)	Turbidimeter measurements	Correlation with TSS values
Permeability ($\boldsymbol{k_f}$) of fines material (m/s)	Sampling of fine material	Laboratory measurement

At the start of the site characterization, the detection of the sediments' heterogeneities can support the selection of point locations for parameters' collection. In Lippera et al. (2023b), Electromagnetic Induction (EMI) surveys were tested in horizontal dipole orientation to map the variability of soil properties affecting clogging development. The shallow characterisation can identify zones of impendence in the vertical infiltration, while electrical resistivity tomography (ERT) cross-sections or towed transient electromagnetic (tTEM) systems are employed in MAR to characterize the morphology of the aquifer and determine preferential lateral infiltration pathways (Perzan et al. 2023; Sendrós et al. 2020).

Geophysical methods have also been developed in MAR monitoring to detect variations in infiltration pathways by time-lapse electrical resistivity tomography (De Carlo et al. 2020; Nenna et al. 2014; Ulusoy et al. 2015). The spatial and temporal variations in infiltration rates due to clogging have been observed in MAR basins through thermal loggers and fiber-optic distributed temperature sensing (Becker et al. 2013; Mawer et al. 2016; Medina et al. 2020; Racz et al. 2012). The mentioned geophysical methods can be employed in future applications for clogging monitoring following the risk assessment. Also, instantaneous profile

measurement systems of water content have been developed to accurately monitor reductions in infiltration capacity in the field during MAR (Barquero et al. 2019).

The hydraulic conductivity of sediments is an important parameter to determine on-site. During field clogging investigation, Zaidi et al. (2020) also determined the infiltration rates at point locations via double-ring infiltrometer tests. In Ganot et al. (2017), single-ring infiltrometers tests and wetting-front propagation methods are used for point measurements of infiltration rates. Bouwer (1986) states that the double-ring infiltrometer test can be effective in the presence of an obstructing layer on the surface. The leakage effect along the cylinder's inner wall is minimised. However, Rice et al. (2014) proved that the single-ring infiltrometer test with the divergence correction method is more accurate than the double-ring infiltrometer test when designing a MAR site.

In further applications, the MFI clogging indicator (Buik and Willemsen 2002), introduced in Sec. 1.4, could also be integrated within the site parameters for the developed methodology. This MAR indicator has been related to the concentration of suspended solids and the intrinsic permeability of the filter cake in Olsthoorn (1982). Thus, field measurements to determine the intrusive fines parameters could be reduced by substituting them with MFI measurements. This aggregated parameter could contribute to further standardisation of the developed method to assess the risk of clogging at MAR sites.

4.4 Application of the model

The third and last objective of the research work was to compare the costs and benefits of different alternatives in reducing the potential damages of clogging. The developed numerical tool answers the need to compare design and management measures that could reduce the risk of clogging. Some measures that Dillon et al. (2022) recommend include selecting an appropriate aquifer, scheme design (e.g. sedimentation pond construction), using source control, and selectively recharging by monitoring or pre-treating the recharge water. Additionally, management actions, such as implementing drying and cleaning cycles for the basin, can be part of the operation scheme. Remediation techniques may include mechanical removal of the surface crust or scraping the basin's surface, deeper tillage using tools such as Chisel-Knives (CK) Cultivators and plows (Negev et al. 2020).

Effective planning and operational activities can be outlined through the proposed quantitative approach to estimate the risk of clogging. Simulation of clogging for different planning and management scenarios can ensure a stable infiltration capacity of the site over the long term under controlled costs. Ringleb et al. (2016) state the importance of using modelling approaches to evaluate various design and management options for optimal local solutions.

The set of scenarios can be ranked based on prospected costs and infiltration performance, to find the most effective design and operation option.

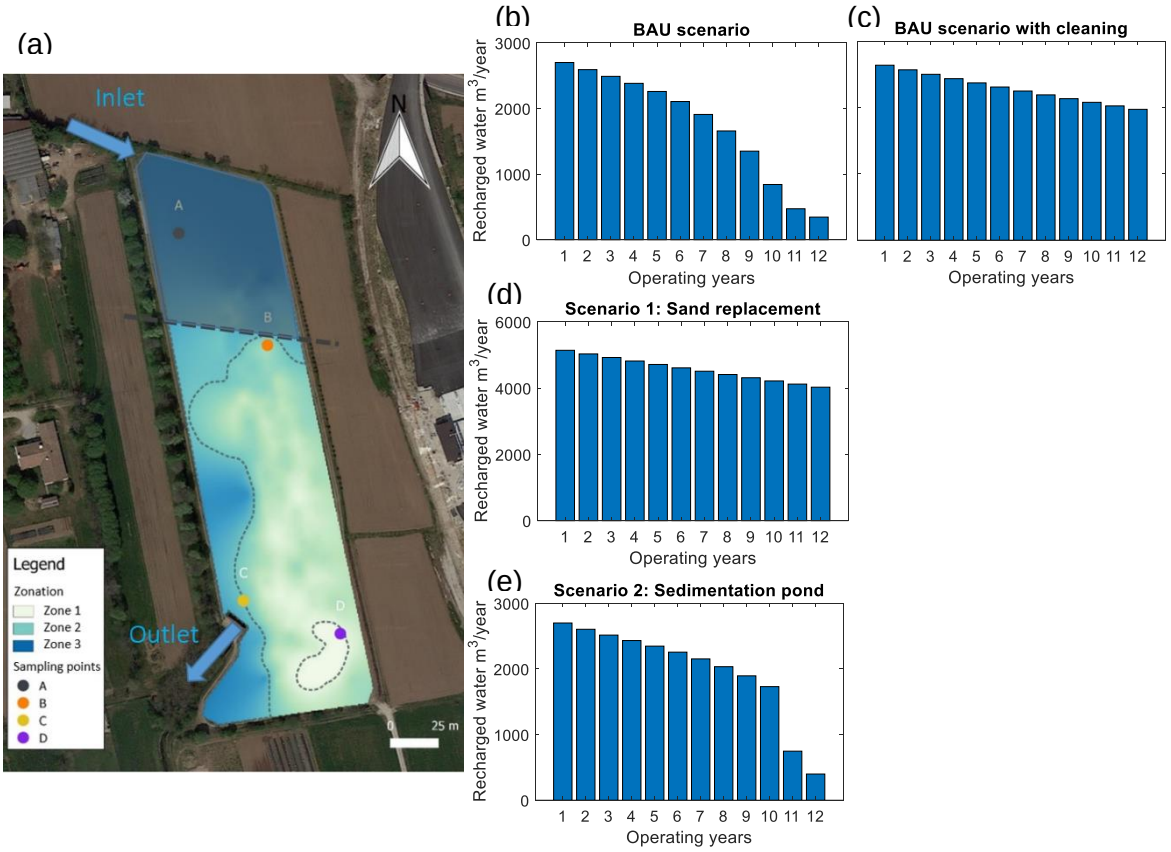

Figure 7: Design and management scenarios for the Loria basin, Italy. a) is the map of the Loria site and the subdivision of zone with Low (zone 1) vulnerability to clogging, Medium (zone 2) vulnerability, and High (zone 3) vulnerability. The grey area indicate the space to construct a sedimentation pond. The simulated recharged volumes over the years are shown for the no-maintenance and ploughing scenario (b)(c) and the design scenarios (d) (e).

The application of the risk-based modelling approach to the Loria basin is here extended, to discuss the design and operation scenarios, illustrated in Fig.6. From the simulations, it emerges that following the cleaning operations of the basin after each flooding events, the total recharged volumes would be $2.9 \times 10^4\ m^3$ over 12 years, compared to $2.1 \times 10^4\ m^3$ with the business as usual (BAU) scenario, which corresponds to not-doing anything. Assuming perfect mixing of the soil in the upper 15 cm following each flooding event, would down the formation of a thin and superficial impendent clogging layer. Although the increase in fines percentages and the decrease in coarser sediments at the sediment matrix, might lead to the necessity in the long run to remediate the deeper portion of soil. For the design options to excavate 50 cm of native soil with artificial quartz sand in the grain sizes range of 04-0.8 mm, the total water recharge over 12 years would be $5.8 \times 10^4\ m^3$. The volume of recharged water is considerably higher compared to the other scenarios. This is mainly explained by the removal of the clogged soil and the higher permeability of the sand, although the native soil under the excavated depth would still restrict the infiltration rates. The effectiveness of the construction of a sedimentation

pond in trapping fines load and thus reducing clogging of the MAR site is modelled with considerations on the feasible design variables, such as the length of the pond and high of the outlet. For the Loria basin, the design of a sedimentation pond, indicated with the *grey area* in Fig. 7.a, in the already-clogged northern area with a length of 85 *m*, would result in a low trapping efficiency due to the high discharge rate during the flooding event and limited space. The total recharged volume over the 12 years would be $2.4 \times 10^4\ m^3$, presenting not a great advantage over the BAU scenario.

The simulation of scenarios that act on the quality of the water, such as the design option to use pre-treated water or selectively recharge through monitoring, are not discussed, although the numerical tool would allow us to simulate them. The design option for water pre-treatment would involve costs for the disposition of a treatment plant and a limited transferred volume due to the treatment capacity. In the second case, monitoring costs would be included, and there would be a consequent reduction in infiltrated volume due to the check on the water quality threshold, cutting-off the flood peak.

Within each design and operation scenario, the recharged volumes per year should be compared with the expected capital, operating and maintenance costs.

4.5 Costs and benefit analysis

Design and operation options can be evaluated in terms of achieved recharged water volumes through the numerical tool for physical clogging. However, comparing the costs and benefits requires a broad discussion. The UNESCO-IAH-GRIPP 2021 "*Managing Aquifer Recharge: A Showcase for Resilience and Sustainability*" (Zheng et al. 2021), has reported 28 MAR schemes worldwide and defined a standard method for costs and benefits analysis of MAR schemes.

The costs associated with MAR are determined using a method called "levelised costs of water recharged" proposed by Ross and Hasnain (2018). This method calculates the constant level of revenue required each year to recover all the expenses incurred during the project's lifespan, including capital, operating and maintenance costs, divided by the annual volume of water recharged and/or recovered. (Zheng et al. 2021). A summary of investment and operating costs for an infiltration basin MAR scheme, is reported in Maréchal et al. (2020). However, determining the benefits of MAR for unit of water volume recharged is challenging, because of the absence of a market price for stored water. For this reason, the benefits of a MAR site are evaluated including the "avoided costs" of a new water treatment plant or other treatment alternatives (Ahmed et al. 2021; Artimo et al. 2021). In case the groundwater use is allocated to agriculture, the benefits can also be estimated from the gross value of additional agricultural

production (Escalante and Sauto 2021) or the unit value of agricultural production (Powers et al. 2021; Ross 2021).

Although costs and financial data are scarcily reported for MAR infrastractures (Ross and Hasnain 2018), within the above defined standard methodology for costs and benefits analysis, costs for clogging reduction strategies should be compared. In Maréchal et al. (2020), the costs for the basin maintenance (€/year) are defined in dependence of the years between two dragging processes and the sand height to be dragged (m). The sand dragging and sand price (€/m^3) are included in the equation, jointly with the infiltration basin surface area (m^2). The developed numerical model assist the estimation of these maintenance costs, providing the frequency of the necessary cleaning operations, given the time at which the site reaches a low threshold in infiltration rates. The costs of soil cleaning are based on the specific tillage technology (e.g. shallow ploughing or deep cultivation), for which prices are available in $/ha. The developed numerical tool, assists in determining the right equipment necessary for the cleaning operations, given the estimated clogging depth and, thus, the portion of the soil to be treated.

When comparing design options to reduce clogging to their maintenance costs, the life span of the MAR site and the discount rate should be included in the costs and benefit analysis to outweigh the higher initial investments. The initial costs associated with the MAR site design vary greatly depending on the location and available resources, costs for water pre-treatment, sedimentation pond construction or monitoring instrumentation to control the water quality. The benefits of each measure can be associated with the evolution in recharged volume over the years, as shown in Fig. 7. The outcomes of the developed numerical tool can be integrated into cost and benefit analysis during the design phase of the MAR site. This procedure can assist MAR operators in optimal decision-making over different alternatives, determining the most cost-efficient measure to reduce the risk of clogging while guaranteeing recharged volumes.

5 Conclusion

The presented dissertation combines a comprehensive approach of site characterisation techniques and numerical modelling to evaluate and reduce the risk of physical clogging at managed aquifer recharge (MAR) sites. The hydrogeological characteristics of the potential MAR site are crucial factors that affect the feasibility of the planned infrastructure. Therefore, it is vital to thoroughly assess whether the proposed site location is susceptible to physical clogging, considering the sediments' physical and hydraulic properties and the recharged water's quality.

The developed numerical tool for clogging risk assessment stands out from previous studies, given the novelty in the model parameterization from site characterization data. The performed research does not claim to fully describe local phenomena that might be influenced by concomitant chemical and biological processes, but rather to provide the MAR industry with a cost-effective method to assess the risk of physical clogging, that moves on from qualitative considerations of water quality parameters or from the construction of long column experiments that do not represent sediments heterogeneities or spatial features on the field. The developed numerical tool has the advantage that it can be implemented from standard techniques used for site characterization, and it provides quantitative estimations of the depth of clogging and the decline in infiltration rates over MAR operations. By assessing the risk of physical clogging, the decision-making process is orientated towards optimal decisions in MAR construction, such as selecting the most suitable site or design of the MAR scheme. Various design and management alternatives to reduce the risk of clogging can be simulated and compared with the respective costs. Reducing the risk of physical clogging can ensure the sustainability of infiltration rates and the longevity of the infrastructure, resulting in more efficient and cost-effective MAR operations.

This research work contributes scientifically to understanding processes in physical clogging and predicting its risks, and it contributes economically to avoiding unexpected costs to MAR investors, advancing the implementation of MAR sites in Europe. Analysis of trends in groundwater levels indicates potential challenges to the long-term sustainability of groundwater resources in Europe over the forthcoming decades. As a response, the adoption and execution of comprehensive groundwater management plans are deemed essential. MAR techniques will play an important role in water resources management as an alternative water storage system in counteracting the impacts of climate change and groundwater depletion. This research contributes to promoting MAR techniques as a key strategy for water scarcity while preserving groundwater sustainability.

6 References

Ahfir ND, Hammadi A, Alem A, Wang H, Le Bras G, and Ouahbi T. (2017). Porous media grain size distribution and hydrodynamic forces effects on transport and deposition of suspended particles. *J Environ Sci (China), 53*, 161-172. doi:https://doi.org/10.1016/j.jes.2016.01.032

Ahmed KM, Sultana S, Chowdhury T, Islam R, Delwaruzzaman M, Alam SM-u, Tuinhof A, Ravenscroft P, Onabolu B, and Akhter N. (2021). Case Study 1: A resilient drinking

water supply using aquifer storage recovery for coastal communities in Batiaghata, Khulna, Bangladesh. *Managing aquifer recharge: A Showcase for Resilience and Sustainability*, 89.

Alem A, Ahfir N-D, Elkawafi A, and Wang H. (2014). Hydraulic Operating Conditions and Particle Concentration Effects on Physical Clogging of a Porous Medium. *Transport in Porous Media, 106*(2), 303-321. doi:https://doi.org/10.1007/s11242-014-0402-8

Alem A, Elkawafi A, Ahfir N-D, and Wang H. (2013). Filtration of kaolinite particles in a saturated porous medium: hydrodynamic effects. *Hydrogeology Journal, 21*(3), 573-586. doi:https://doi.org/10.1007/s10040-012-0948-x

American Society of Civil Engineers. (2020). *Standard Guidelines for Managed Aquifer Recharge* (Vol. 69-19): ASCE/EWRI

Army U. (1971). Dewatering and groundwater control for deep excavations. *TM 5-818-5, NAVFAC P-418, AFM 88-5*.

Artimo A, Puurunen O, and Saraperä S. (2021). Case Study 2: Managed Aquifer Recharge for drinking water supply, Turku Region, Southwestern Finland. *Managing aquifer recharge: A Showcase for Resilience and Sustainability*, 97.

Barquero F, Fichtner T, and Stefan C. (2019). Methods of In Situ Assessment of Infiltration Rate Reduction in Groundwater Recharge Basins. *Water, 11*(4). doi:https://doi.org/10.3390/w11040784

Barry KE, Vanderzalm JL, Miotlinski K, and Dillon PJ. (2017). Assessing the Impact of Recycled Water Quality and Clogging on Infiltration Rates at A Pioneering Soil Aquifer Treatment (SAT) Site in Alice Springs, Northern Territory (NT), Australia. *Water, 9*(3), 179. Retrieved from https://www.mdpi.com/2073-4441/9/3/179

Baveye P, Vandevivere P, Hoyle BL, DeLeo PC, and de Lozada DS. (1998). Environmental Impact and Mechanisms of the Biological Clogging of Saturated Soils and Aquifer Materials. *Critical Reviews in Environmental Science and Technology, 28*(2), 123-191. doi:https://doi.org/10.1080/10643389891254197

Becker MW, Bauer B, and Hutchinson A. (2013). Measuring artificial recharge with fiber optic distributed temperature sensing. *Groundwater, 51*(5), 670-678.

Beckwith CW, and Baird AJ. (2001). Effect of biogenic gas bubbles on water flow through poorly decomposed blanket peat. *Water Resources Research, 37*(3), 551-558.

Beganskas S, and Fisher AT. (2017). Coupling distributed stormwater collection and managed aquifer recharge: Field application and implications. *Journal of Environmental Management, 200*, 366-379.

Bennion DB, Bennion DW, Thomas FB, and Bietz RF. (1998). Injection Water Quality-A Key Factor to Successful Waterflooding. *37*(6). doi:https://doi.org/10.2118/98-06-06

Bouwer H. (1986). Intake Rate: Cylinder Infiltrometer. In *Methods of Soil Analysis* (pp. 825-844).

Bouwer H. (2002). Artificial recharge of groundwater: hydrogeology and engineering. *Hydrogeology Journal, 10*(1), 121-142. doi:https://doi.org/10.1007/s10040-001-0182-4

Bradford SA, Simunek J, Bettahar M, Van Genuchten MT, and Yates SR. (2003). Modeling colloid attachment, straining, and exclusion in saturated porous media. *Environmental science & technology, 37*(10), 2242. doi:https://doi.org/10.1021/es025899u

Bradford SA, Yates SR, Bettahar M, and Simunek J. (2002). Physical factors affecting the transport and fate of colloids in saturated porous media. *Water Resources Research, 38*(12), 63-1-63-12.

Buik N, and Willemsen A. (2002). Clogging rate of recharge wells in porous media. In PJD (Ed.) (Ed.), *Management of Aquifer Recharge for Sustainability* (pp. 195-198): CRC Press.

Buurman P, Pape T, Reijneveld J, De Jong F, and Van Gelder E. (2001). Laser-diffraction and pipette-method grain sizing of Dutch sediments: correlations for fine fractions of marine, fluvial, and loess samples. *Netherlands Journal of Geosciences, 80*(2), 49-57.

Camprovin P, Hernández M, Fernández S, Martín-Alonso J, Galofré B, and Mesa J. (2017). Evaluation of Clogging during Sand-Filtered Surface Water Injection for Aquifer Storage and Recovery (ASR): Pilot Experiment in the Llobregat Delta (Barcelona, Spain). *Water, 9*(4), 263. Retrieved from https://www.mdpi.com/2073-4441/9/4/263

Casanova J, Devau N, and Pettenati M. (2016). Managed Aquifer Recharge: An Overview of Issues and Options. In AJ Jakeman, O Barreteau, RJ Hunt, J-D Rinaudo, & A Ross (Eds.), *Integrated Groundwater Management: Concepts, Approaches and Challenges* (pp. 413-434). Cham: Springer International Publishing.

Cui Y, Wooster JK, Baker PF, Dusterhoff SR, Sklar LS, and Dietrich WE. (2008). Theory of fine sediment infiltration into immobile gravel bed. *Journal of Hydraulic Engineering, 134*(10), 1421-1429.

Custodio E, Isamat J, and Miralles J. (1982). Twenty-five years of groundwater recharge in Barcelone (Spain).

Das BM. (2010). *Geotechnical engineering handbook*: J. Ross publishing.

De Carlo L, Caputo MC, Masciale R, Vurro M, and Portoghese I. (2020). Monitoring the drainage efficiency of infiltration trenches in fractured and karstified limestone via time-lapse hydrogeophysical approach. *Water, 12*(7), 2009.

Dillon P. (2005). Future management of aquifer recharge. *Hydrogeology Journal, 13*(1), 313-316. doi:https://doi.org/10.1007/s10040-004-0413-6

Dillon P, Alley W, Zheng Y, Vanderzalm J, Ward J, Megdal S, Hipke W, Thomas P, Tuthill D, and Carlson R. (2022). *Managed Aquifer Recharge: Overview and Governance*.

Dillon P, Pavelic P, Page D, Miotlinski K, Levett K, Barry K, Taylor R, Wakelin S, Vanderzalm J, and Molloy R. (2010). Developing aquifer storage and recovery (ASR) opportunities in Melbourne—Rossdale ASR demonstration project final report. *WfHC Report to Smart Water Fund, June*.

Dillon P, Stuyfzand P, Grischek T, Lluria M, Pyne RDG, Jain RC, Bear J, Schwarz J, Wang W, Fernandez E, Stefan C, Pettenati M, van der Gun J, Sprenger C, Massmann G, Scanlon BR, Xanke J, Jokela P, Zheng Y, Rossetto R, Shamrukh M, Pavelic P, Murray E, Ross A, Bonilla Valverde JP, Palma Nava A, Ansems N, Posavec K, Ha K, Martin R, and Sapiano M. (2018). Sixty years of global progress in managed aquifer recharge. *Hydrogeology Journal, 27*(1), 1-30. doi:https://doi.org/10.1007/s10040-018-1841-z

Dillon PJ, Hickinbotham MR, and Pavelic P. (1994). Review of international experience in injecting water into aquifers for storage and reuse. In *Water Down Under 94: Groundwater Papers; Preprints of Papers: Groundwater Papers; Preprints of Papers* (pp. 13-14, 16-19): Institution of Engineers, Australia Barton, ACT.

Döll P, Müller Schmied H, Schuh C, Portmann FT, and Eicker A. (2014). Global-scale assessment of groundwater depletion and related groundwater abstractions: Combining hydrological modeling with information from well observations and GRACE satellites. *Water Resources Research, 50*(7), 5698-5720. doi:https://doi.org/10.1002/2014WR015595

Doolittle JA, and Brevik EC. (2014). The use of electromagnetic induction techniques in soils studies. *Geoderma, 223*, 33-45.

Du X, Ye X, and Zhang X. (2018a). Clogging of saturated porous media by silt-sized suspended solids under varying physical conditions during managed aquifer recharge. *Hydrological Processes, 32*(14), 2254-2262. doi:https://doi.org/10.1002/hyp.13162

Du X, Ye X, and Zhang X. (2018b). Clogging of saturated porous media by silt-sized suspended solids under varying physical conditions during managed aquifer recharge. *Hydrological Processes, 32*(14), 2254-2262.

Dym C. (2004). *Principles of Mathematical Modeling*.

El-Rawy M, Al-Maktoumi A, Zekri S, Abdalla O, and Al-Abri R. (2019). Hydrological and economic feasibility of mitigating a stressed coastal aquifer using managed aquifer recharge: a case study of Jamma aquifer, Oman. *Journal of Arid Land, 11*(1), 148-159. doi:https://doi.org/10.1007/s40333-019-0093-7

Elimelech M, Gregory J, and Jia X. (1998). *Particle deposition and aggregation: measurement, modelling and simulation*. Butterworth-Heinemann, Oxford: Colloid and Surface Engineering Series.

Escalante E. (2013). Practical Criteria in the Design and Maintenance of MAR Facilities in Order to Minimise Clogging Impacts Obtained from Two Different Operative Sites in Spain. In (pp. 119-154).

Escalante EF, and Sauto JSS. (2021). Case Study 7: El Carracillo Managed Aquifer Recharge System for rural development in Castilla y León, Spain. *Managing aquifer recharge: A Showcase for Resilience and Sustainability*, 139.

Fair G, and Geyer J. (1954). *Water Supply and Waste Disposal*. New York: John Wiley and Sons.

Fernandez Escalante E, Henao Casas JD, Vidal Medeiros AM, and San Sebastiàn Sauto J. (2020). Regulations and guidelines on water quality requirements for Managed Aquifer Recharge. International comparison. *Acque Sotterranee - Italian Journal of Groundwater, 9*(2). doi:https://doi.org/10.7343/as-2020-462

Fontana A, Mozzi P, and Marchetti M. (2014). Alluvial fans and megafans along the southern side of the Alps. *Sedimentary Geology, 301*, 150-171.

G.Mahmoodlu M, Raoof A, Sweijen T, and Van Genuchten M. (2016). Effects of Sand Compaction and Mixing on Pore Structure and the Unsaturated Soil Hydraulic Properties. *Vadose Zone Journal, 15*. doi:https://doi.org/10.2136/vzj2015.10.0136

Ganot Y, Holtzman R, Weisbrod N, Nitzan I, Katz Y, and Kurtzman D. (2017). Monitoring and modeling infiltration–recharge dynamics of managed aquifer recharge with desalinated

seawater. *Hydrol. Earth Syst. Sci., 21*(9), 4479-4493. doi:https://doi.org/10.5194/hess-21-4479-2017

Gibson S, Abraham D, Heath R, and Schoellhamer D. (2009). Vertical gradational variability of fines deposited in a gravel framework. *Sedimentology, 56*(3), 661-676. doi:https://doi.org/10.1111/j.1365-3091.2008.00991.x

Glass J, Šimůnek J, and Stefan C. (2020). Scaling factors in HYDRUS to simulate a reduction in hydraulic conductivity during infiltration from recharge wells and infiltration basins. *Vadose Zone Journal, 19*(1), e20027.

Gleeson T, Wada Y, Bierkens MFP, and van Beek LPH. (2012). Water balance of global aquifers revealed by groundwater footprint. *Nature, 488*(7410), 197-200. doi:https://doi.org/10.1038/nature11295

Gruesbeck C, and Collins R. (1982). Entrainment and deposition of fine particles in porous media. *Society of Petroleum Engineers Journal, 22*(06), 847-856.

Guppy L, Uyttendaele P, Villholth KG, and Smakhtin VU. (2018). *Groundwater and sustainable development goals: Analysis of interlinkages*.

Hartog N, and Stuyfzand PJ. (2017). Water Quality Considerations on the Rise as the Use of Managed Aquifer Recharge Systems Widens. *Water, 9*(10), 808. Retrieved from https://www.mdpi.com/2073-4441/9/10/808

Heilweil VM, and Marston T. (2013). Evaluation of potential gas clogging associated with managed aquifer recharge from a spreading basin, Southwestern Utah, USA. *Clogging Issues Associated with Managed Aquifer Recharge Methods*.

Herzig JP, Leclerc DM, and Goff PL. (1970). Flow of Suspensions through Porous Media—Application to Deep Filtration. *Industrial & Engineering Chemistry, 62*(5), 8-35. doi:https://doi.org/10.1021/ie50725a003

Hijnen W, Bunnik J, Schippers J, Straatman R, and Folmer H. (2020). Determining the clogging potential of water used for artificial recharge in deep sandy aquifers. In *Artificial recharge of groundwater* (pp. 437-440): CRC Press.

Honjo Y, and Veneziano D. (1989). Improved Filter Criterion for Cohesionless Soils. *Journal of Geotechnical Engineering, 115*(1), 75-94. doi:doi: https://doi.org/10.1061/(ASCE)0733-9410(1989)115:1(75)

Huston DL, and Fox JF. (2015). Clogging of Fine Sediment within Gravel Substrates: Dimensional Analysis and Macroanalysis of Experiments in Hydraulic Flumes. *Journal*

of Hydraulic Engineering, 141(8). doi:https://doi.org/10.1061/(asce)hy.1943-7900.0001015

Hutchinson A, Milczarek M, and Banerjee M. (2013). *Clogging phenomena related to surface water recharge facilities* (Vol. IAH Commission on Managing Aquifer Recharge). Australia.

Indraratna B, Trani LDO, and Khabbaz H. (2008). A critical review on granular dam filter behaviour – from particle sizes to constriction-based design criteria. *Geomechanics and Geoengineering, 3*(4), 279-290. doi:https://doi.org/10.1080/17486020802406632

Institute P. (2018). The world's water 2002–2003 data.

Jeong HY, Jun S-C, Cheon J-Y, and Park M. (2018). A review on clogging mechanisms and managements in aquifer storage and recovery (ASR) applications. *Geosciences Journal, 22*(4), 667-679. doi:https://doi.org/10.1007/s12303-017-0073-x

Kanti Sen T, and Khilar KC. (2006). Review on subsurface colloids and colloid-associated contaminant transport in saturated porous media. *Adv Colloid Interface Sci, 119*(2-3), 71-96. doi:https://doi.org/10.1016/j.cis.2005.09.001

Khilar KC, and Fogler HS. (1998). *Migrations of fines in porous media* (Vol. 12): Springer Science & Business Media.

Kim JW, Choi H, and Pachepsky YA. (2010). Biofilm morphology as related to the porous media clogging. *Water Res, 44*(4), 1193-201. doi:https://doi.org/10.1016/j.watres.2009.05.049

Kløve B, Ala-Aho P, Bertrand G, Gurdak JJ, Kupfersberger H, Kværner J, Muotka T, Mykrä H, Preda E, Rossi P, Uvo CB, Velasco E, and Pulido-Velazquez M. (2014). Climate change impacts on groundwater and dependent ecosystems. *Journal of Hydrology, 518*, 250-266. doi:https://doi.org/10.1016/j.jhydrol.2013.06.037

Lippera MC, Werban U, Rossetto R, and Vienken T. (2023b). Understanding and predicting physical clogging at managed aquifer recharge systems: A field-based modeling approach. *Advances in Water Resources, 177*, 104462. doi:https://doi.org/10.1016/j.advwatres.2023.104462

Lippera MC, Werban U, and Vienken T. (2023a). Improving clogging predictions at managed aquifer recharge sites: a quantitative assessment on the vertical distribution of intrusive fines. *Hydrogeology Journal, 31*(1), 71-86. doi:https://doi.org/10.1007/s10040-022-02581-7

Lowe DR. (1988). Suspended-load fallout rate as an independent variable in the analysis of current structures. *Sedimentology, 35*(5), 765-776.

MacAlister C, Baggio, G, Perera, D, Qadir, M, Taing, L, Smakhtin, V. (2023). *Global Water Security 2023 Assessment*. Retrieved from Hamilton, Canada:

Majkić-Dursun B, Petković A, and Dimkić M. (2015). The effect of iron oxidation in the groundwater of the alluvial aquifer of the Velika Morava River, Serbia, on the clogging of water supply wells. *Journal of the Serbian Chemical Society, 80*(7), 947–957-947–957.

Majumdar PK, Sekhar M, Sridharan K, and Mishra GC. (2008). Numerical Simulation of Groundwater Flow with Gradually Increasing Heterogeneity due to Clogging. *Journal of Irrigation and Drainage Engineering, 134*(3), 400-404. doi:doi:10.1061/(ASCE)0733-9437(2008)134:3(400)

Maliva RG. (2015). Managed aquifer recharge: state-of-the-art and opportunities. *Water Supply, 15*(3), 578-588. doi:https://doi.org/10.2166/ws.2015.009

Maliva RG. (2020). Clogging. In RG Maliva (Ed.), *Anthropogenic Aquifer Recharge: WSP Methods in Water Resources Evaluation Series No. 5* (pp. 307-342). Cham: Springer International Publishing.

Maréchal J-C, Bouzit M, Rinaudo J-D, Moiroux F, Desprats J-F, and Caballero Y. (2020). Mapping economic feasibility of managed aquifer recharge. *Water, 12*(3), 680.

Martin R. (2013a). Clogging issues associated with managed aquifer recharge methods. *IAH Commission on Managing Aquifer Recharge, Australia*, 26-33.

Martin R. (2013b). Clogging remediation methods to restore well injection capacity. *Clogging Issues Associated with Managed Aquifer Recharge Methods*, 207-211.

Mawer C, Parsekian A, Pidlisecky A, and Knight R. (2016). Characterizing Heterogeneity in Infiltration Rates During Managed Aquifer Recharge. *Ground Water, 54*(6), 818-829. doi:10.1111/gwat.12423

Mays D, and Martin R. (2013). Clogging in managed aquifer recharge: flow, geochemistry, and clay colloids. *Clogging Issues Associated with Managed Aquifer Recharge Methods*, 14-24.

McDowell-Boyer LM, Hunt JR, and Sitar N. (1986). Particle transport through porous media. *Water Resources Research, 22*(13), 1901-1921. doi:https://doi.org/10.1029/WR022i013p01901

Medina R, Pham C, Plumlee MH, Hutchinson A, Becker MW, and O'Connell PJ. (2020). Distributed temperature sensing to measure infiltration rates across a groundwater recharge basin. *Groundwater, 58*(6), 913-923.

Muecke TW. (1979). Formation fines and factors controlling their movement in porous media. *Journal of petroleum technology, 31*(02), 144-150.

Negev I, Shechter T, Shtrasler L, Rozenbach H, and Livne A. (2020). The effect of soil tillage equipment on the recharge capacity of infiltration ponds. *Water, 12*(2), 541.

Nenna V, Pidlisecky A, and Knight R. (2014). Monitoring managed aquifer recharge with electrical resistivity probes. *Interpretation, 2*(4), T155-T166.

NRMMC, EPHC, and NHMRC. (2009). Australian Guidelines for water recycling, managing health and environmental risks, vol 2C: managed aquifer recharge. *Natural Resource Management Ministerial Council, Environment Protection and Heritage Council National Health and Medical Research Council*.

Olsthoorn T. (1982). *The clogging of recharge wells, main subjects*: Keuringsinstituut voor Waterleiding Artikelen, KIWA, nv.

P.A.T.I. (2013). Relazione geologica ed idrogeologica PATI Loria e Castello di Godego http://www.prc.loria.geonweb.com/documents/elaborati_QC/Relazione%20geologica%20ed%20idrogeologica.pdf.

Page D, Vanderzalm J, Miotliński K, Barry K, Dillon P, Lawrie K, and Brodie RS. (2014). Determining treatment requirements for turbid river water to avoid clogging of aquifer storage and recovery wells in siliceous alluvium. *Water Research, 66*, 99-110. doi:https://doi.org/10.1016/j.watres.2014.08.018

Parkhurst DL, and Appelo C. (1999). User's guide to PHREEQC (Version 2): A computer program for speciation, batch-reaction, one-dimensional transport, and inverse geochemical calculations. *Water-resources investigations report, 99*(4259), 312.

Pavelic P, Dillon PJ, Barry KE, Vanderzalm JL, Correll RL, and Rinck-Pfeiffer SM. (2007). Water quality effects on clogging rates during reclaimed water ASR in a carbonate aquifer. *Journal of Hydrology, 334*(1-2), 1-16.

Pavelic P, Dillon PJ, Mucha M, Nakai T, Barry KE, and Bestland E. (2011). Laboratory assessment of factors affecting soil clogging of soil aquifer treatment systems. *Water Res, 45*(10), 3153-63. doi:https://doi.org/10.1016/j.watres.2011.03.027

Pérez-Paricio A, and Carrera J. (2000). Validity and sensitivity analysis of a new comprehensive clogging model. *IAHS PUBLICATION*, 47-53.

Pérez Paricio A. (2001). *Integrated modelling of clogging processes in artificial groundwater recharge*: Universidad Politécnica de Cataluña.

Perzan Z, Osterman G, and Maher K. (2023). Controls on flood managed aquifer recharge through a heterogeneous vadose zone: hydrologic modeling at a site characterized with surface geophysics. *Hydrology and Earth System Sciences, 27*(5), 969-990.

Popp S, Altdorff D, and Dietrich P. (2012). Assessment of shallow subsurface characterization with non-invasive geophysical methods at the intermediate hill-slope scale. *Hydrology and Earth System Sciences Discussions, 9*, 2511-2539. doi:10.5194/hessd-9-2511-2012

Powers CA, Flyr B, Winter J, Gibson K, and Brozović N. (2021). Case Study 17: Intentional infiltration using irrigation canals to sustain Central Platte River ecology and irrigation. *Managing aquifer recharge: A Showcase for Resilience and Sustainability*, 233.

Pyne RDG. (1995). *Groundwater recharge and wells: a guide to aquifer storage recovery*. Boca Raton: 1st Edition, CRC press.

Pyne RDG. (2005). *Aquifer storage recovery: a guide to groundwater recharge through wells*: ASR systems.

Racz AJ, Fisher AT, Schmidt CM, Lockwood BS, and Los Huertos M. (2012). Spatial and temporal infiltration dynamics during managed aquifer recharge. *Groundwater, 50*, 562-570. doi:https://doi.org/10.1111/j.1745-6584.2011.00875.x

Rice RC, Milczarek MA, and Keller JK. (2014). *A Critical Review of Single Ring Cylinder Infiltrometers with Lateral Flow Compensation*.

Richey AS, Thomas BF, Lo M-H, Reager JT, Famiglietti JS, Voss K, Swenson S, and Rodell M. (2015). Quantifying renewable groundwater stress with GRACE. *Water Resources Research, 51*(7), 5217-5238. doi:https://doi.org/10.1002/2015WR017349

Rinck-Pfeiffer S, Ragusa S, Sztajnbok P, and Vandevelde T. (2000). Interrelationships between biological, chemical, and physical processes as an analog to clogging in aquifer storage and recovery (ASR) wells. *Water Research, 34*(7), 2110-2118.

Ringleb J, Sallwey J, and Stefan C. (2016). Assessment of Managed Aquifer Recharge through Modeling—A Review. *Water, 8*(12). doi:https://doi.org/10.3390/w8120579

Ross A. (2021). Economic costs and benefits of Managed Aquifer Recharge Case Studies. *Managing aquifer recharge: A Showcase for Resilience and Sustainability*, 73.

Ross A, and Hasnain S. (2018). Factors affecting the cost of managed aquifer recharge (MAR) schemes. *Sustainable Water Resources Management, 4*(2), 179-190. doi:https://doi.org/10.1007/s40899-017-0210-8

Rossetto R, Barbagli A, De Filippis G, Marchina C, Vienken T, and Mazzanti G. (2020). Importance of the Induced Recharge Term in Riverbank Filtration: Hydrodynamics, Hydrochemical, and Numerical Modelling Investigations. *Hydrology, 7*(4), 96. Retrieved from https://www.mdpi.com/2306-5338/7/4/96

Sakthivadivel R. (1969). *Clogging of a granular porous medium by sediment*. Berkeley: Hydraulic Engineering Laboratory, College of Engineering, University of California.

Scanlon BR, Fakhreddine S, Rateb A, de Graaf I, Famiglietti J, Gleeson T, Grafton RQ, Jobbagy E, Kebede S, Kolusu SR, Konikow LF, Long D, Mekonnen M, Schmied HM, Mukherjee A, MacDonald A, Reedy RC, Shamsudduha M, Simmons CT, Sun A, Taylor RG, Villholth KG, Vörösmarty CJ, and Zheng C. (2023). Global water resources and the role of groundwater in a resilient water future. *Nature Reviews Earth & Environment, 4*(2), 87-101. doi:https://doi.org/10.1038/s43017-022-00378-6

Schippers JC, and Verdouw J. (1980). The modified fouling index, a method of determining the fouling characteristics of water. *Desalination, 32*, 137-148. doi:https://doi.org/10.1016/s0011-9164(00)86014-2

Sendrós A, Himi M, Lovera R, Rivero L, Garcia-Artigas R, Urruela A, and Casas A. (2020). Geophysical Characterization of Hydraulic Properties around a Managed Aquifer Recharge System over the Llobregat River Alluvial Aquifer (Barcelona Metropolitan Area). *Water, 12*(12), 3455. Retrieved from https://www.mdpi.com/2073-4441/12/12/3455

Sherard JL, Dunnigan LP, and Talbot JR. (1984). Filters for silts and clays. *Journal of Geotechnical Engineering, 110*(6), 701-718.

Sprenger C, Hartog N, Hernández M, Vilanova E, Grützmacher G, Scheibler F, and Hannappel S. (2017). Inventory of managed aquifer recharge sites in Europe: historical development, current situation and perspectives. *Hydrogeology Journal, 25*(6), 1909-1922. doi:https://doi.org/10.1007/s10040-017-1554-8

Standen K, Costa LR, and Monteiro J-P. (2020). In-channel managed aquifer recharge: a review of current development worldwide and future potential in Europe. *Water, 12*(11), 3099. doi:https://doi.org/10.3390/w12113099

Tang Y, Yao X, Chen Y, Zhou Y, Zhu DZ, Zhang Y, Zhang T, and Peng Y. (2020). Experiment research on physical clogging mechanism in the porous media and its impact on permeability. *Granular Matter, 22*(2). doi:https://doi.org/10.1007/s10035-020-1001-8

Terzaghi K, Peck RB, and Mesri G. (1967). Soil Mechanics in Engineering Practice, John Wiley & Sons. *Inc., New York*.

Ting CS, Chiang KF, Hsieh SH, Tsao CH, Chuang CH, and Fan KT. (2020). Land subsidence and managed aquifer recharge in Pingtung Plain, Taiwan. *Proc. IAHS, 382*, 843-849. doi:https://doi.org/10.5194/piahs-382-843-2020

Tippelt T. (2015). *Investigation of the influence of fine sediment input during flooding events on the long term infiltration capacity of the Loria infiltration basin (Italy).* (Master thesis). Institute of Geophysics and Geology, Leipzig University.

Torkzaban S, Bradford SA, Vanderzalm JL, Patterson BM, Harris B, and Prommer H. (2015). Colloid release and clogging in porous media: Effects of solution ionic strength and flow velocity. *J Contam Hydrol, 181*, 161-71. doi:https://doi.org/10.1016/j.jconhyd.2015.06.005

Ulusoy İ, Dahlin T, and Bergman B. (2015). Time-lapse electrical resistivity tomography of a water infiltration test on Johannishus Esker, Sweden. *Hydrogeology Journal, 23*(3), 551-566.

United Nations. (2022). The United Nations World Water Development Report 2022: Groundwater: Making the Invisible Visible. In: UNESCO Paris, France.

Van Der Kooij D, Visser A, and Hijnen W. (1982). Determining the concentration of easily assimilable organic carbon in drinking water. *Journal-American Water Works Association, 74*(10), 540-545.

van Dijk M, Morley T, Rau ML, and Saghai Y. (2021). A meta-analysis of projected global food demand and population at risk of hunger for the period 2010–2050. *Nature Food, 2*(7), 494-501. doi:https://doi.org/10.1038/s43016-021-00322-9

Vanderzalm J, Page D, Dillon P, Gonzalez D, and Petheram C. (2022). Assessing the costs of Managed Aquifer Recharge options to support agricultural development. *Agricultural Water Management, 263*, 107437. doi:https://doi.org/10.1016/j.agwat.2021.107437

Wada Y, Beek L, van Kempen C, Reckman J, Vasak S, and Bierkens MFP. (2010). Global Depletion of Groundwater Resources. *Geophysical Research Letters, 37*, L20402. doi:10.1029/2010GL044571

Willis-Jones B, and Brandes de Roos I. (2013). Application of large scale managed aquifer recharge in mine water management, Cloudbreak Mine, Western Australia. *Clogging Issues Associated with Managed Aquifer Recharge Methods; Martin, R., Ed*, 156-162.

Wooster JK, Dusterhoff SR, Cui Y, Sklar LS, Dietrich WE, and Malko M. (2008). Sediment supply and relative size distribution effects on fine sediment infiltration into immobile gravels. *Water Resources Research, 44*(3).

World Meteorological Organization. (2022). State of Global Water Resources. *WMO-No. 1308*.

Xie Y, Wang Y, Huo M, Geng Z, and Fan W. (2020). Risk of physical clogging induced by low-density suspended particles during managed aquifer recharge with reclaimed water: Evidences from laboratory experiments and numerical modeling. *Environmental research, 186*, 109527.

Ye X, Cui R, Du X, Ma S, Zhao J, Lu Y, and Wan Y. (2019). Mechanism of suspended kaolinite particle clogging in porous media during managed aquifer recharge. *Groundwater, 57*(5), 764-771.

Yousif OSQ, Karakouzian M, Rahim NOA, and Rashed KA. (2017). Physical Clogging of Uniformly Graded Porous Media Under Constant Flow rates. *Transport in Porous Media, 120*(3), 643-659. doi:10.1007/s11242-017-0946-5

Zaidi M, Ahfir N-D, Alem A, El Mansouri B, Wang H, Taibi S, Duchemin B, and Merzouk A. (2020). Assessment of clogging of managed aquifer recharge in a semi-arid region. *Science of The Total Environment, 730*, 139107.

Zamani A, and Maini B. (2009). Flow of dispersed particles through porous media — Deep bed filtration. *Journal of Petroleum Science and Engineering, 69*(1-2), 71-88. doi:https://doi.org/10.1016/j.petrol.2009.06.016

Zhang H, Xu Y, and Kanyerere T. (2020). A review of the managed aquifer recharge: Historical development, current situation and perspectives. *Physics and Chemistry of the Earth, Parts A/B/C*, 102887.

Zheng Y, Ross A, Villholth KG, and Dillon P, (eds.). (2021). Managing aquifer recharge: a showcase for resilience and sustainability. *UNESCO, Paris. , 10*, 2021.

Appendix

Application of physical clogging models to Managed Aquifer Recharge: a review of modelling approaches from engineering fields

Applicazione dei modelli di clogging fisico agli impianti di ricarica della falda: una revisione degli approcci modellistici da diversi settori ingegneristici

Maria Chiara Lippera[1, 2], Ulrike Werban[2], Thomas Vienken[3, 1]

[1]Technical University of Munich, TUM Campus Straubing for Biotechnology and Sustainability, Straubing, Germany

[2]UFZ - Helmholtz Centre for Environmental Research, Leipzig, Germany

[3]Weihenstephan-Triesdorf University of Applied Sciences, TUM Campus Straubing for Biotechnology and Sustainability, Straubing, Germany

ABSTRACT

Managed aquifer recharge (MAR) sites suffer from the long-lasting problem of clogging. The causes of clogging are physical, biological, chemical and mechanical processes and their complex interaction, with physical clogging being recognised as the predominant process. The intrusion and deposition of particles during water recharge affect the hydraulic properties of the infiltration surface, resulting in a decline in the infiltration capacity of the site over the operating years. Cleaning operations are necessary to restore the original infiltration rates. For this purpose, assessing the risk of clogging can determine the site's vulnerability and improve the scheme’s design. Numerical models are essential to replicate physical clogging processes and predict the decline in infiltration rates. So far, predictive tools for physical clogging assessment have been missing in MAR literature. Hence, the purpose of this study is to analyse and reorganise physical clogging models from applied engineering fields dealing with water infiltration in natural heterogeneous systems. The modelling approaches are illustrated, starting from the main assumptions and conceptualisation of the soil volume and intruding particles. The individual processes are untangled from the multiple studies and reorganised in a systematic comparison of mathematical equations relevant to MAR applications. The numerical models' predictive power is evaluated for transferability, following limitations and recommendations for a process-based model applicable to surface spreading schemes. Finally, perspectives are given for clogging risk assessment at MAR sites from modelling and site characterisation. The predictive tool could assist decision-makers in planning the MAR site by implementing cost-effective strategies to lower the risk of physical clogging.

RIASSUNTO

I siti di ricarica della falda in condizioni controllate (MAR – *Managed Aquifer Recharge*) presentano il persistente problema dei fenomeni di intasamento (*clogging*). Il *clogging* può essere causato da processi di tipo fisico, biologico, chimico e meccanico, con il *clogging* di tipo fisico riconosciuto come il fenomeno predominante. L'intrusione e deposizione di materiale fine durante l'intervento di ricarica compromettono le proprietà idrauliche di infiltrazione del suolo, riducendo la capacità di infiltrazione del sito nel corso degli anni di attività: devono quindi essere previste delle operazioni di manutenzione nel tempo, al fine di ripristinare i tassi di infiltrazione iniziali. Per questi motivi, la valutazione del rischio di *clogging* può agevolare l'identificazione delle vulnerabilità del sito e rendere più efficace la progettazione dell'impianto MAR. I modelli numerici sono essenziali per replicare i processi fisici e simulare la riduzione dei tassi di infiltrazione. Finora, nella letteratura esistente per le tecniche MAR, non si dispone di strumenti previsionali per la valutazione del rischio in questione. Lo scopo di questo studio è quello di analizzare e riorganizzare i modelli numerici per il *clogging* fisico, provenienti da diversi settori dell'ingegneria che si occupano di infiltrazione in sistemi naturali eterogenei. Gli approcci modellistici sono illustrati in questa rassegna della letteratura, partendo dalle ipotesi di base e dall'elaborazione concettuale del volume del suolo e del materiale fine trasportato. I principali processi sono individuati dai molteplici studi e riorganizzati confrontando sistematicamente le equazioni matematiche di rilievo. La capacità predittiva dei modelli numerici è valutata considerandone l'adattabilità ad altri siti, seguono poi limitazioni e raccomandazioni per l'applicazione agli impianti di ricarica. Infine, vengono fornite prospettive per la valutazione del rischio di *clogging* tramite la modellazione e la caratterizzazione del sito. Lo strumento previsionale può essere un sistema di supporto alle decisioni durante la progettazione degli impianti MAR, favorendo strategie economicamente vantaggiose per ridurre il rischio di intasamento fisico.

Keywords

Physical clogging; numerical model; risk assessment; hydraulic conductivity; infiltration; fine sediments

Parole chiave

Intasamento impianto d'infiltrazione; modello numerico; valutazione del rischio; conducibilità idraulica; infiltrazione; sedimenti fini

1. INTRODUCTION

The reduction in recharged volumes due to clogging compromises the functionality of MAR sites (Bouwer, 2002; Dillon et al., 2022; Zhang et al., 2020). Several studies in the MAR literature suggest that physical clogging is the primary process, followed by mechanical, biological and chemical processes (Dillon et al., 1994; Pavelic et al., 2011; Rinck-Pfeiffer et al., 2000). Although the individual clogging mechanisms can occur simultaneously, this study focuses on the physical processes as main contributor to clogging. During water recharge, fine-grained sediments are transported by the source water or can originate from the soil formation itself (Hutchison et al., 2013; Martin, 2013; Racz et al., 2012). The downward movement and retention of particles in soil pores, block the water flow and lead to a pressure drop through the clogged soil (Herzig et al. 1970; Khilar and Fogler 1998). These phenomena impact the drainage properties of the site, which entails a loss in the performance of the infiltration system.

Studies have documented observations of physical clogging directly at MAR schemes (Escalante, 2013; Martin, 2013; Pavelic et al., 2007; Rinck-Pfeiffer et al., 2000). Soil column and field experiments have been undertaken to understand relevant mechanisms in the clogging formation (Du et al., 2018; Duryea, 1996; Fichtner et al., 2019; Mays & Martin, 2013; Pavelic et al., 2011; Sallwey et al., 2019; Zou et al., 2019). The effect of clogging has been integrated into numerical simulation through time-varying parameters calibrated from the field or experimental observations (Glass et al., 2020; Majumdar et al., 2008). The comprehensive numerical code CLOG of Pérez Paricio (2001) simulates the individual clogging processes, however, kinetic parameters require further calibration for application. The modified fouling index (MFI) (Schippers & Verdouw, 1980) has been related to the rate of physical clogging in recharge wells in the work of Buik & Willemsen (2002). Although the predicted clogging rate depends on the infiltration rate on the borehole wall, suspended solids and aquifer characteristics, Maliva (2020) reports that the relationship cannot predict whether or when clogging will occur, and it works only between backflushing events. There have not been progresses in this direction for surface spreading methods. The lack of standardised predictive tools for clogging and adequate water quality monitoring has limited so far the development of more efficient management of MAR sites (Dillon et al., 2018). One main challenge is predicting clogging rates in advance and incorporating risks to derive cost-effective designs for MAR schemes (Maliva, 2020). Up to now, clogging rates have not yet been systematically related to parameters measured at the MAR scheme, to quantify clogging effects in a predictive way, accounting for site conditions and heterogeneities.

Hence, the necessity to extend the research to simulations of physical clogging processes from other engineering applications where water infiltration and drainage properties are vital for the system's functioning. These applications share similar features to MAR systems. In stormwater

treatment, the physical clogging phenomenon can compromise the treatment performance of runoff water (Conley et al., 2020; Kandra et al., 2014; Wang et al., 2012). Similarly to vertical flow treatment wetlands, these sites consist of a filter bed with relatively low O&M costs; therefore, the clogging rate can determine the longevity of the system (Kandra et al. 2014). Cycles of saturation and desaturation regulate the infiltration of wastewater and water runoff, and the prevention of clogging is critical to maintaining hydraulic functioning and pollutant control (Nivala et al., 2012; Pucher & Langergraber, 2019). In geotechnical engineering, physical clogging issues are associated with particle erosion, transport and retention in granular filters due to seepage forces. Filters are applied to base soils, protecting earth-fill dams and preserving their stability from internal erosion. The filtering effectiveness is established by a stability and permeability criterion to prevent soil particles from passing through the filter voids and ensure constant drainage (Terzaghi et al., 1967). In petroleum engineering, infiltration occurs through water injections into the rock reservoir, forcing the oil towards the producing wells. The concomitant migration of particles inside the rock formation causes a reduction in permeability and, consequently, a decline in water injection and oil recovery (Roque et al., 1995). For injection wells, this process is identified by deep bed filtration (Bedrikovetsky et al., 2001; Wennberg & Sharma, 1997). The engineering fields dealing with water infiltration in natural heterogeneous systems are schematised in Fig. 1.

The modelling approaches adopted in engineering applications could be transferred to MAR systems to fill the gaps in physical clogging predictions. Understanding deposition mechanisms and variations in hydraulic properties associated with physical clogging is needed to enhance MAR operations and anticipate potential system failure. This literature review organises the state of the art of physical clogging models to investigate their transferability for potential application to MAR sites. A systematic comparison is necessary to gain an overview of the models and relevant parameters controlling clogging. The predictive power of the models is discussed by examining to which extent they rely on parameters requiring calibration from a specific experimental configuration. The final scope is to provide concrete suggestions on formulas to describe clogging phenomena in MAR applications, especially for surface spreading methods, and derive a process-based workflow to be combined with site characterisation technologies. This work assists in developing a methodology to predict infiltration rates decline at specific MAR sites prior to construction. Incorporating the risk of physical clogging in MAR infrastructures' planning can enhance infiltration rates and limit the operation and maintenance (O&M) costs.

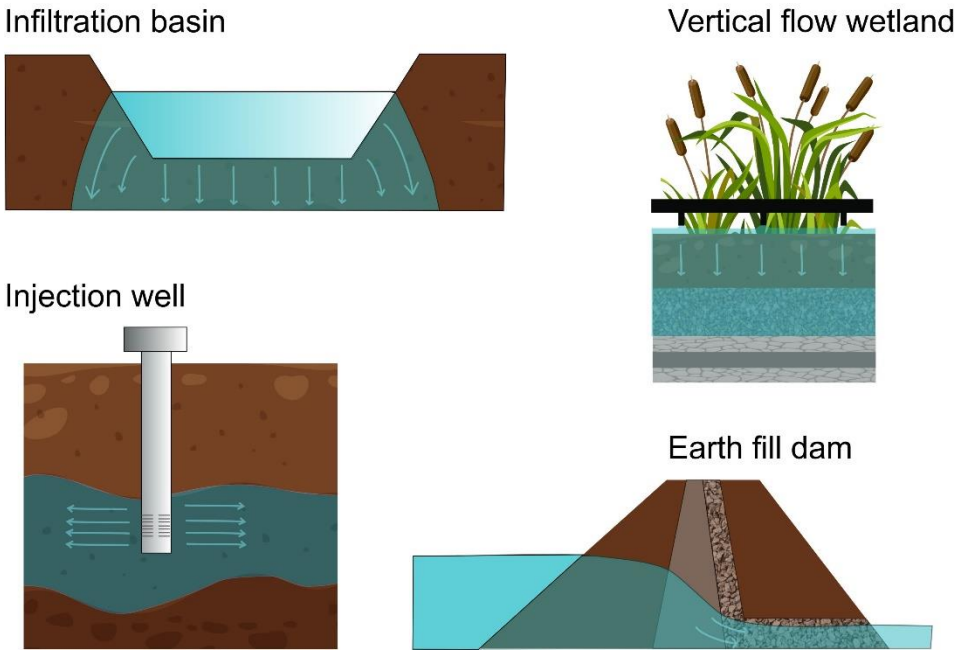

Figure 1: Examples of engineering applications in which physical clogging modelling has been studied in the literature.

2. MATERIALS AND METHOD

The first step of the literature review was the collection of studies to evaluate the developed models for physical clogging processes critically. The literature review excluded experimental and observational studies limited to cause-and-effect relationships. The review was carried out by consulting the scientific database Scopus (https://www.scopus.com), Web of Science (https://www.webofscience.com) and integrating results from Google Scholar (https://scholar.google.com). The research covered academic papers, theses and conference proceedings.

First, the research focused on physical clogging models in MAR literature to understand the state of the art within the field. The research was then extended to other engineering applications, such as petroleum engineering, subsurface flow treatment wetlands, and geotechnical applications. The research's main keywords were always “physical clogging” and “modelling”. The studies were collected and summarised within each application area, avoiding redundant studies. In addition, developed theories and relationships were highlighted by comparing and contrasting the work of later authors. The mathematical formulations representing the evolution of physical clogging were pointed out and organised in tables.

For classification and comparison, each study in the literature review was defined in terms of scope of application, model category, fines of interest and hydraulic operating conditions.

3. RESULTS

Physical clogging investigations and modelling can differ significantly in engineering studies given the respective scope of application, study contextualisation and the goal to achieve through infiltration. Operating conditions control the dynamics of the physical clogging processes. In infiltration ponds, due to the applied constant head conditions, a decrease in soil permeability results in a decrease in flow rates. On the other hand, under constant flow conditions, such as in injection wells, clogging can lead to an excessive pressure head that can damage the aquifer formation (Reddi et al., 2005). Table 1 reports the modelling studies analysed in this review, and defines their field of application, operating conditions and fines of interest with the diameter range. The range of particles considered “undesirable” for each engineering field is site and objective-specific (Gibson et al., 2009). In stormwater or vertical-flow wetland applications, suspended solids (SS) are the fines of interest. For large particles (>30 μm) , volume phenomena dominate the interstitial and deposition process according to gravity and hydrodynamic forces (Herzig et al., 1970). Depending on the particles and medium grain size distributions, straining or size exclusion can occur, leading to the formation of an “external” or “internal” filter cake in the soil (McDowell-Boyer et al., 1986). The size of the fine particles of interest affects the deposition mechanisms taking place during infiltration. For deep filtration studies applied to injection wells, the fines of interest are colloidal and intermediate particles naturally occurring in the aquifer formation. Colloidal particles have a diameter size <1 μm, and surface phenomena control the transport and particles deposition given the physical-chemical properties of the suspension (Herzig et al., 1970). Brownian motion, electrostatic interaction and London-van-der-Waals forces regulate the attachment mechanisms (McDowell-Boyer, Hunt et al. 1986, Zamani and Maini 2009). In contrast to larger suspended particles, colloidal particles have a slower sedimentation rate (Elimelech et al., 1998), and can accumulate in the pore throat, forming particles’ bridges, which can be broken at high flow rates (Kanti Sen & Khilar, 2006). A comparison of the particles size diameters range for the fines of interest in the reviewed engineering field, is reported in Fig. 2.

The operating conditions and range of fines of interest determine the choice of the numerical model to represent the physical clogging processes. The reviewed studies highlighted the following approaches to model the transport and deposition processes: (i) Macroscopic models, (ii) Probabilistic models, (iii) Analytical models and (iv) Conceptual models. The main equations and conceptualisation on the elementary volume of soil are underlined in each modelling approach. Tables 2, 3 and 4 show a transversal comparison of the mathematical expressions used by the reviewed authors in replicating individual clogging processes, namely the particles’ transport and deposition (Table 2), porosity changes (Table 3) and following hydraulic conductivity (Table 4).

Table 1: Studies of physical clogging modelling, their relative field of application, model category, characteristics of the intrusive fines in experiments and the operating hydraulic conditions. NS= not specified.

Reference	Applied field	Model category	Fines of interest	Hydraulic conditions
Pérez Paricio (2001)	Managed Aquifer Recharge	Macrosc. Model	Iron flocs (15-40 µm) Langerak case	Constant flow
Torkzaban et al. (2015)	Managed Aquifer Recharge	Macrosc. Model	Colloids (range NS)	Constant flow
Xie et al. (2020)	Managed Aquifer Recharge	Macrosc. Model	Suspended particles (2-800 µm)	Constant flow
Alem et al. (2013), Alem et al. (2014)	Filtration study	Macrosc. Model	Kaolinite (1.7 to 40µm)	Constant flow, Constant head
Wang et al. (2012)	Stormwater recharge	Conceptual	Suspended solids (38.5 – 75 µm)	Constant head
Blazejewski & Murat-Blazejewska (1997)	Vertical flow wetlands	Conceptual	Suspended solids (range NS)	Daily sewage flow
Hua et al. (2010)	Vertical flow wetlands	Conceptual	Suspended solids (range NS)	Daily sewage flow
Rege & Fogler (1988)	Chemical Engineering	Probabilistic	Kaolinite (0.02 - 0.2 µm) and emulsion droplets (2.2 – 9 µm)	Constant flow
Reddi et al. (2005)	Geotechnical engineering	Probabilistic	kaolinite particles (1.0– 12.0 µm); polymer microspheres were 1.0– 35.0 µm.	Constant flow, Constant head
Indraratna & Vafai (1997)	Geotechnical engineering	Analytical	Silica (20 - 80 µm)	Constant head
Locke et al. (2001)	Geotechnical engineering	Probabilistic and Analytical	base-soil particles (range NS)	Constant head

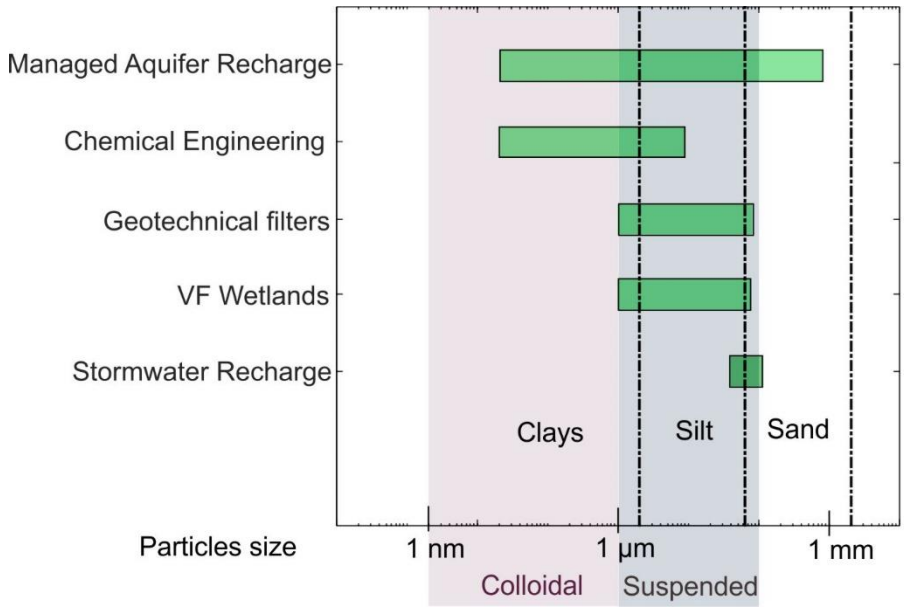

Figure 2: Particles size range (µm) for the fines of interest from the selected studies based on their field of application.

3.1 MACROSCOPIC MODELS

In macroscopic modelling, the clogging of a porous medium is described mathematically by the mass conservation and kinetic equations, describing the rate of clogging and the rate of decolmatage (Herzig et al., 1970). The porous media is considered a closed system (Fig. 3a), and starting from the mass balance under the assumption of unidirectional flow, the governing equations of granular filtration are approximated in the equation reported in Table 2(a). Iwasaki (1937) described the particle concentration profile through a filter in the form of an exponential decay function:

$$\frac{\partial C}{\partial z} = -\lambda C \tag{1}$$

With λ the filter coefficient. The filter coefficient evolves from the initial value λ_0, of the clean filter bed, at the initial stage, due to the accumulation of particles and alteration in the filtration action. This is expressed with the correcting factor $F(\sigma, \boldsymbol{\alpha})$, being $\boldsymbol{\alpha}$ a vector of unknown parameters. The filtration performance and duration are further examined through the pressure drop measurements across the porous material. The evolution in the local pressure gradient is described through the factor $G(\boldsymbol{\beta}, \sigma)$, relating the changes in permeability to the amount of deposited particles (Ives & Pienvichitr, 1965; Pendse et al., 1978; Zamani & Maini, 2009). Different expressions both for $F(\boldsymbol{\alpha}, \sigma)$ and $G(\boldsymbol{\beta}, \sigma)$ were derived fitting the observed effluent concentration profile and pressure drop changes through optimisation techniques. For a broad list of expressions from previous studies, see Bai & Tien (2000), Zamani & Maini (2009). Macroscopic models have mainly been applied in deep bed filtration to interpret the removal of colloidal particles from liquid suspensions. The physical clogging module of the model CLOG developed by Pérez Paricio (2001) for MAR applications is based on theoretical formulations

and empirical dependences of filtration theory (Pérez Paricio, 2001). A mass balance equation involving coefficients for the attachment and detachment processes has also been adopted by Xie et al. (2020) to assess the risk of physical clogging by low-density floc particles from reclaimed water in MAR, shown in Table 2(c). In the work of Torkzaban et al. (2015), for sustainable MAR operations, the effect of changes in Ionic Strength (IS) and flow velocity has been investigated in soil cores with initial clay content, with the standard advection–dispersion equation with first-order kinetic terms for colloid release and retention, shown in Table 2(b). Advection-dispersion equations in clogging appear to be a favourable method for suspended colloids or clays when studying the significance of the ionic strength (Ye et al., 2019).

A limitation to using mass balances with kinetic equations is the requirement for parameterisation for particle deposition and remobilisation rates, which cannot be determined unless observed from experimental breakthrough curves (BTCs) in soil column experiments. The macroscopic models describe the filtration process as “overall behaviour” without describing its nature or mechanism (Zamani & Maini, 2009). Since parameter values change with varying particle size distributions and pore sizes, these models are not predictive in nature (Rege & Fogler, 1988). Moreover, observations of the filtration process are required and Wennberg et al. (1995) report that further parameter adjustment is needed for more complex situations during water injection in aquifers.

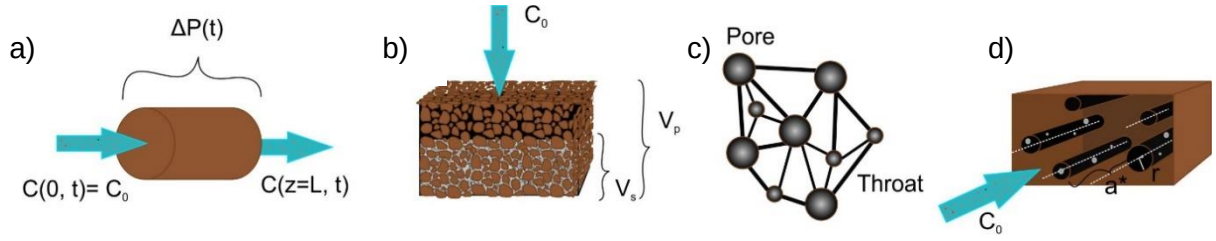

Figure 3: Different schematisation of the soil volume. Illustrated are a) soil elementary volume from (i) Macroscopic models, b) soil pore volume and volume filled with suspended solids from(iv) Conceptual models , c) pore network models from (ii) Probabilistic models, d) soil elementary volume as an ensemble of capillary tubes from (iii) Analytical models.

3.2 PROBABILISTIC MODELS

Probabilistic models in the literature represent particle transport and deposition as a combination of pore space events. A network model is generally adopted, based on a regular topology consisting of interconnected bonds intersecting at the nodes (Fatt, 1956). An example is shown in Fig. 3c. The constriction sizes of the network are derived from the packing density conditions and the particle size distribution of the porous media. Combining the probability of the presence of the suspended particle with the probability of encountering a pore space, which reflects the conditions under which the particle will deposit or pass, the filtration process can be simulated with a probability function. In the work of Silveira (1965) and Witt (1993) a

conceptual model of the pore network is used to determine the expected length of infiltration of suspended particles.

In Rege & Fogler (1988) the probability of particle capture is equivalent to the fraction of total flow in the annulus between the pore radius r_i and $r_i - \theta a_j$:

$$p(r_i, a_j) = 4\left[\left(\frac{\theta a_j}{r_i}\right)^2 - \left(\frac{\theta a_j}{r_i}\right)^3\right] + \left(\frac{\theta a_j}{r_i}\right)^4 \quad (2)$$

With θ a parameter indicating conditions favourable for deposition, r_i the radius of the pore tube , a_j the radius of the particle j..

The likelihood of particles deposition by a direct interception on the walls of the pore tubes is thus assumed under geometric and favourable conditions.

$$\theta = \theta_0 \ \exp\left[-\frac{v}{v_{cr}}\right] \quad (3)$$

With θ_0 lumped parameter depending on ionic strength and pH, v the pore fluid velocity and v_{cr} the critical velocity. Through the θ term, the model accounts for the hydrodynamic effect on the capture probability, given the critical velocity beyond which particles do not deposit. Reddi et al. (2000) adopted the same approach throughout the design of geotechnical filters, Table 2(e), using the basic principles of flow in cylindrical tubes and assuming that the elementary volume of the soil is an ensemble of capillary tubes (Fig. 3d). This simplification has been chosen by the author rather than the more rigorous network model and particle tracking approach reported by Rege & Fogler (1988). The effect of strain mechanisms is then accounted for by a pressure drop within the bond, and a new effective radius is calculated after N particles have been deposited, as shown in Table 3(c).

Probabilistic models present the advantage of accounting for the pressure drop evolution in the porous media using initially measurable parameters, such as the particle size distribution of the suspension, the sample's initial permeability, and the pore size distribution. In Rege & Fogler (1988) mercury porosimetry or photomicrographic techniques are suggested to determine the pore size distribution; in Reddi et al. (2000) the Haines method adopting increasing suction pressures is mentioned. Recent studies suggest 3D imaging techniques with X-ray micro-tomography (micro-CT) (Elrahmani et al., 2023; Xiong et al., 2016). However, in the illustrated approach, a limitation is represented by the likelihood of particles deposition, which depends on the ionic condition constant θ_0, and the critical velocity for particles wash-out v_{cr}. These parameters cannot be readily determined and their calibration would depend upon experimental data from column trials. Reddi et al. (2000) suggest adopting values from similar studies in literature, such as the θ_0 reported in Rege & Fogler (1988) for bentonite suspensions, as well as the interstitial velocities in granular soils from the experimental work of Gruesbeck & Collins (1982), at which particle deposition is unlikely. Recent computational

studies on pore-network models investigate the parameters affecting the likelihood of particle's deposition (Li et al., 2021; Lin et al., 2021).

3.3. ANALITYCAL MODEL

In the analytical model of Indraratna & Vafai (1997), the movement of noncohesive base-soil particles into granular filters is controlled by hydrodynamic effects. The soil element is represented as an ensemble of capillary tubes, defined by pores channels with a characteristic average diameter d_0, derived from the soil porosity and a mass-weighted equivalent diameter D_h (Kovács, 1981). The first geometric criteria assess the fraction of particles moving under gravitational transport for $d_i < d_0$. For particles with equal diameter size to the pore channels, an equilibrium between the external forces acting on the particle d_i is computed to determine whether the particles are transported under seepage forces. The critical hydraulic gradient acting on the particle at limit equilibrium, beyond which the hydrodynamic force overcome the frictional resistance, is:

$$i_z = \frac{4K}{\delta z \gamma_w}(\gamma_s h_s - \gamma_w h_w) tan\varphi' - \frac{2d}{3\delta z \gamma_w}(\gamma_s - \gamma_w) \quad (4)$$

With $K = tan^2[\left(\frac{\pi}{4}\right) - \frac{\varphi'}{2}]$, being φ' the effective friction angle of the material, δz is the length of the soil element, γ_s and γ_w respectively the specific weight of soil and water, h_s and h_w the height of the overlying soil and the hydraulic head.

The totality of loose particles passing through the pore channels, together with the pore water, is defined as slurry. The rate of particle transport is quantified through differential equations of conservation of mass and momentum, describing the evolution of the slurry density ρ_m and velocity *u* along the grid of soil elements. The formulations are reported in Table 2(d). A further extension of this analytical model of filtration has been carried out by Locke et al. (2001), who incorporates a deterministic equation for particle infiltration, based on a probabilistic approach derived by the filter void model of a 3D cubic network (Schuler, 1996). A similar approach for particle migration under hydromechanical effects has been followed by Federico (2017), who additionally implemented a model to derive the constriction size distribution and assess the migration length for the movable particles.

Due to their mechanistic nature, the analytical models have been developed without relying on empirical parameters from column experiments, only based on *a priori* information. Concerns for MAR application remain on the applicable boundary conditions for the model.

3.4 CONCEPTUAL MODELS

A simple conceptualisation of physical clogging processes has been undertaken by Blazejewski & Murat-Blazejewska (1997) to address clogging in vertical-flow wetlands. The model considers the soil medium's initial pore volume and the time to fill up pores with the

volumes of suspended solids (SS) daily delivered. An illustration of the filling of soil pore volume is provided in Fig. 3.b. The time for clogging is computed in the following way:

$$t_c = \frac{V_p}{V_s} = \frac{\varepsilon_{ef} h_c A}{C_s^{in} Q / \rho_s (1 - w_c)} \quad (5)$$

With C_s^{in} the mass concentration of SS in the inflowing sewage, Q the daily sewage flow, ρ_s and w_c the density and water content of SS, ε the porosity, A the area of infiltration and h_c the depth of clogging. The filled-up soil volume, and so the depth at which SS accumulate, is derived from the empirical equation from Burchak (1987), relating the effective diameter D_{10} to the depth of the heavily clogged sand layer:

$$h_c = 150 d_{10} \quad (6)$$

The relationship is valid for sands with $5 \times 10^{-5} < d_{10} < 3 \times 10^{-6}\, m$.

The reduction in soil permeability, based on the evolution of soil porosity, follows the solution of the Kozeny–Carman equation for uniform sphere particles from Bear (1988),Table 3(a).

Langergraber et al. (2003) found that the calculated theoretical clogging time is most sensitive to the density of the organic solids. The author related the clogging time to the load of suspended solids and the density of the organic solids $\rho_{\mathrm{TS,org}}$:

$$t_c = \frac{\alpha\, \rho_{\mathrm{TS,org}}}{C_s^{in} Q} \quad (7)$$

through the empirical coefficient α likely dependent upon the size distribution of particles and the bed properties (Kadlec & Wallace, 2009). However, Langergraber et al. (2003) reported a strong non-linearity between the remaining pore volume and the drop in the hydraulic conductivity in his pilot-scale constructed wetlands. This model assumes that all the larger pores are filled completely, which leads to a longer clogging time than the observed one.

The conceptual model from Hua et al. (2010) is also based on the available void space theory, developed by Blazejewski & Murat-Blazejewska (1997), additionally, it considers the fraction of washed-off SS in relation to a threshold flow rate. However, data from experimental wetlands are necessary to estimate the quantitative depth of clogging in relationship to the effective diameter D_{10}, and the evolution of the infiltration rate during the operation time. Similarly, Wang et al. (2012) developed a mathematical iteration model for clogging in urban stormwater aquifer recharge. The model is based on the accumulation of suspended solids and the formation of the clogging layer. Experimental data are necessary to quantify the clogging layer's critical thickness and hydraulic conductivity.

Table 2: Particles transport and deposition in porous media

	Paper	Equation	Parameters
(a)	Iwasaki (1937); Herzig (1970); Zamani and Maini (2009), Alem et al. (2012)	Mass balance: $u\frac{\partial C}{\partial z}+\frac{\partial \sigma}{\partial \tau}=0$ $\frac{\partial \sigma}{\partial \tau}=\lambda u C$	• C=volume fraction of particles in suspension • σ= deposited particles volume per unit of porous media volume • u= Darcy velocity • λ= filter coefficient • $\tau = \mathrm{t} - \mathrm{z}\phi/u$ • ϕ= porosity
(b)	Torkzaban et al, (2015)	Mass balance: $\frac{\partial C}{\partial t}=\frac{\mathrm{D}\partial^2 C}{\partial x^2}-\mathrm{v}\frac{\partial C}{\partial x}-\frac{r_{rel}}{n}-\frac{r_{ret}}{n}$	• r_{rel}=release rate of colloid concentration from pore walls • r_{ret}=retention rate at pore constrictions, in dependence of the ionic strength.
(c)	Xie et al. (2020)	$-\frac{\partial}{\partial t}(nC+C_s)+\frac{\partial}{\partial x}(Cv_x)=0$ $\frac{\partial C_s}{\partial t}=\alpha C-\beta C_s$	• C_s =the deposited particle mass in unit pore space (kg/m3) • α = the particle attachment coefficient (min-1) • β = the particle detachment coefficient (min-1).
(d)	Indraratna and Vafai (1997) Locke and Indraratna (2001) Federico (2017)	Mass balance: $\frac{\partial(\rho_m u)}{\partial z}=-\frac{\partial \rho_m}{\partial t}$ Momentum conservation $\sum F=\rho_m V_m(\frac{\partial u}{\partial t}+u\frac{\partial u}{\partial z})$	• $\rho_m=\frac{\rho_w V_w+\rho_s V_s}{V_w+Vs}$ density of the slurry • V_w =volume of water in each soil element • V_s =the summation of the soil particles volumes with d<d_0 • $\sum F$ = sum of forces acting on the slurry
(e)	Rege and Fogler (1988); Reddi et al. (2000)	Deposition rate: $\frac{dN(r,a)}{dt}=q(r)p(r,a)C(a)$ $p(r_i,a_j)=4\left[\left(\frac{\theta a_j}{r_i}\right)^2-\left(\frac{\theta a_j}{r_i}\right)^3\right]+\left(\frac{\theta a_j}{r_i}\right)^4$	• $N(r_i,a_j)$ =the number of particles with radius a_j deposited in the pore tube with radius • $C(a_j)$ =the concentration of particles, expressed as number per unit volume • $p(r_i,a_j)$ = probability of particles capture • $q(r)=\frac{\pi\gamma J}{8\mu}r^4$ flow rate in the tube (Poiseuille law) • a_j = the radius of the particle *j* • r_i = the radius of the pore tube *i*

Table 3: Changes in porosity ϕ

	Paper	Equation	Parameters
(a)	Blazejewski and Murat- Blazejewski (1997)	$\phi(\mathrm{t})=\phi_0-\frac{q_s \mathrm{t}}{h_c\rho_s(1-w_c)}$	• w_c= water content s.s. • q_s = daily suspended solids infiltration loads $[g/m^2 d]$
(b)	Zamani and Maini (2009), Alem et al. (2012)	$\phi(z,\mathrm{t})=\phi_0-\frac{\sigma(z,t)}{(1-\phi_d)}$ $\phi_d=1-\frac{\rho_d}{\rho_p}=1-[\frac{\rho_w}{\rho_p}+(1-\frac{\rho_w}{\rho_p})\frac{1}{a}N^{1-b}$	• ρ_d= the average deposit density; • ρ_p= the soil particles density; • N=number of particles in a deposit site • a=1, b =1.3
(c)	Rege and Fogler (1988); Reddi et al. 2000	$\frac{1}{r_{i,new}^4}=\frac{1}{r_{i,0}^4}\left\{1+3\sum_{j=1}^{M}N(r_i,a_j)\frac{a_j}{\alpha^*}\left[1-(1-\frac{a_j}{r_i})^2\right]^2 K(r_i,a_j)\right\}$	• a_j= radius of the particle *j*; • r_i= radius of the pore tube *i* • $N(r_i,a_j)$ =number of particles with radius a_j deposited in the pore tube with radius r_i

Table 4: Changes in permeability *k*

	Paper	Equation	Parameters
(a)	Blazejewski and Murat-Blazejewski (1997); Federico F. (2017); Pedretti et al. (2011)	$\mathrm{k} = \frac{1}{5}\frac{\phi^3}{(1-\phi)^2}\left(\frac{D_m}{\alpha}\right)^2$	• α = shape factor; α =6 in Bear (1972) α =10 in Blazejewski and Murat- Blazejewski (1997) • D_m can be referred to mean grain size, harmonic mean, or geometrical mean
(b)	Reddi et al. (2000)	$\mathrm{k} = C_s\phi\left(\frac{\gamma}{\mu}\right)\left[\frac{1}{4\sum_i^1 \frac{f(d_i)}{d_i}}\right]^2$	• C_s= shape factor (1/32) • $f(d_i)$= volumetric frequency of the pore group d_i
(c)	Locke and Indraratna (2001); Koenders and Williams (1992)	$\mathrm{k} = \frac{1}{\eta}D_m^2\phi\chi\left(\frac{\phi}{(1-\phi)}\right)^2$	• χ=0.0035$\pm$0.0005
(d)	Sherard et al. (1984); Indraratna et al. (1996), Indraratna and Vafai (1997)	$k = 0.35(D_{15})^2$ $k = 1.02(D_5 D_{10})^{0.93}$	• D_x particle size (mm) in filter for which *x*% by weight of particles are smaller.
(e)	Torkzaban et al. (2015); Khilar and Fogler (1998)	$\frac{K}{K_0} = \frac{1}{1+\beta\sigma}$	• β= formation damage coefficient • σ = concentration of fine particles at the pore constrictions
(f)	Pérez Paricio (2001); Xie et al. (2020)	$\frac{K}{K_0} = \frac{\phi^3}{\phi_0^3}\frac{(1-\phi)^2}{(1-\phi_0)^2}$	
(g)	Alem et al. (2012)	$\frac{K}{K_0} = \frac{\phi^3}{\phi_0^3}\frac{(1-\phi)^2}{(1-\phi_0)^2}\frac{S_0^2}{S^2}\left(\frac{T_0}{T}\right)^2$	• $S = \frac{1}{1-\phi}\left[(1-\phi_0)S_0 + (1-\phi_d)\frac{\sigma}{\rho_p}S_p\right]$ specific surface S_0 and ϕ_0 specific surface and porosity from clean bed; S_p and ϕ_d specific surface and porosity from of the deposited particles (Boller and Kavanaugh, 1995) • T=$\phi^{-\mathrm{m}}$ tortuosity, with formation factor (Archie, 1942) m=1.3 for a sandy medium.

4. DISCUSSION

The organisation of the reviewed studies allowed us to identify the main simulated processes and compare the adopted mathematical formulations in physical clogging. One of the main challenges remains the transport and deposition of suspended particles and, thus, the distribution of deposited particles along the soil profile (Table 2). The use of macroscopic models for colloid transport is recommended in the case of injection wells with highly treated water. This type of clogging can occur even in recharge wells with a low total suspended solids (TSS) concentration of 2 mg/L (Mays & Martin, 2013; Pyne, 1995). Deep-bed filtration studies from petroleum engineering can be appropriate in replicating particles' transport within the aquifer formation under constant flow injections. In this case, attachment mechanisms for colloids are influenced by surface forces, which depend on the hydrogeochemistry of the aquifer. For this purpose, parameters for attachment and detachment rates in kinetic equations

have been calibrated from the observations of the BTCs on soil column experiments, as reported in Table 2(a), 2(b), 2(c) (Alem et al., 2014; Pérez Paricio, 2001; Torkzaban et al., 2015; Xie et al., 2020). An overview of each simulation study's share of empirical and physical parameters is provided in Fig. 4. Physical parameters are intended parameters whose value can be determined from direct measurements, e.g., site characterisation.

Conversely, conceptual models developed in sub-surface wetland applications rely on an overly-simplified assumption of the pore volume, and the defined relationship for the clogging depth might be valid only on a narrow range of sands and suspended fines. Furthermore, the development of this modelling approach has required integrating empirical data from column experiments and experimental wetlands to quantify the thickness of the clogging layer and permeability variations (Hua et al., 2010; Wang et al., 2012). Probabilistic models have the advantage that they can be adapted to constant head and constant flow conditions starting from parameters that can be measured from soil samples (Reddi et al., 2005), although the pore size distribution requires specific laboratory equipment, and the simulations are performed at the pore-scale. As shown in Fig. 4, the analytical approach of Indraratna & Vafai (1997) and Locke et al. (2001) is the only model, accounting for SS transport and deposition processes, independent of empirical parameters.

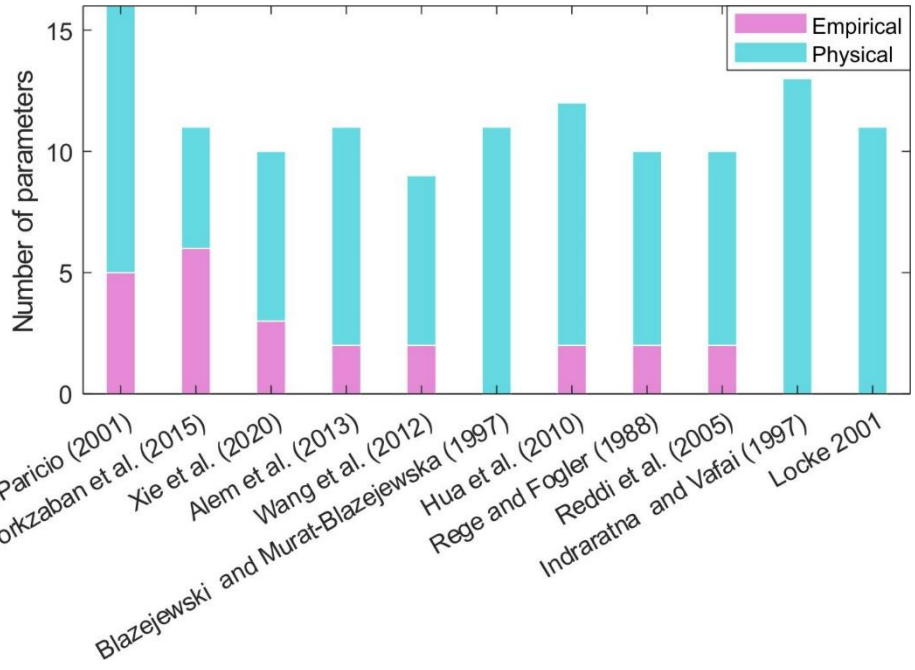

Figure 4: Number of parameters in each model for physical clogging from the reviewed studies.

In MAR surface spreading systems recharged with no pre-treated water, the incoming suspended solids mainly cause physical clogging, similar to vertical flow treatment wetlands and stormwater infiltration systems. This study revealed that numerical models based on geometric consideration for particle entrapment might be more suited to account for volume phenomena for suspended solids deposition. Surface spreading systems should incorporate

a geometric and hydraulic component to model physical clogging processes in MAR surface spreading methods. A process-based framework is presented in Fig. 5. The geometric component defines the geometric parameters for particles entrapment, as done in previous studies, based on the ratio of the diameter size of fines $d_{p,x}$ to the size of the pore constrictions $d_{0,x}$, or porous media diameter size $d_{g,x}$ (Gruesbeck & Collins, 1982; Herzig et al., 1970; Muecke, 1979). The variation in the soil porosity can be computed from the volumes of deposited particles inside the porous media, as schematised in Fig.5, similarly to most of the examined numerical models (Table 3). The morphology of the formed deposits can be included in the computation of the new porosity, considering the deposits' average density (Alem et al., 2013; Boller & Kavanaugh, 1995). This literature review also highlighted that most authors agree with using the Kozeny-Carman equation (Carman, 1937; Kozeny, 1927) in computing permeability reductions due to deposited particles (Table 4). The Kozeny-Carman model assumes the packed bed as an ensemble of capillary tubes through which the fluid flows in laminar conditions according to Poiseuille's law, under saturated conditions. The permeability *k* is in function of the two main packing material properties: the specific surface area and the packing density. As shown in Table 4, some authors prefer to use the normalised form of the Kozeny-Carman model (Alem et al., 2013; Pérez Paricio, 2001; Xie et al., 2020), while others update the soil permeability directly from the variation in soil structure (Blazejewski & Murat-Blazejewska, 1997; Indraratna & Vafai, 1997; Locke et al., 2001; Reddi et al., 2000). The normalised form of the Kozeny-Carman equation can improve predictions in the reduction of hydraulic conductivity, starting from the initial measured value and consequent reduction in porosity space and increase in surface area. Moreover, a process-based model for physical clogging should also account for the evolution of the filtration action of the porous media. Time-dependent parameters could depict the evolution of the media filtrating capability based on the already deposited particles from the previous filtration history. The self-filtration process would affect the geometric component by modifying the grain size distribution and the hydraulic component with the evolution in the soil permeability, as illustrated in Fig. 5. This effect can be replicated in process-based models for MAR application.

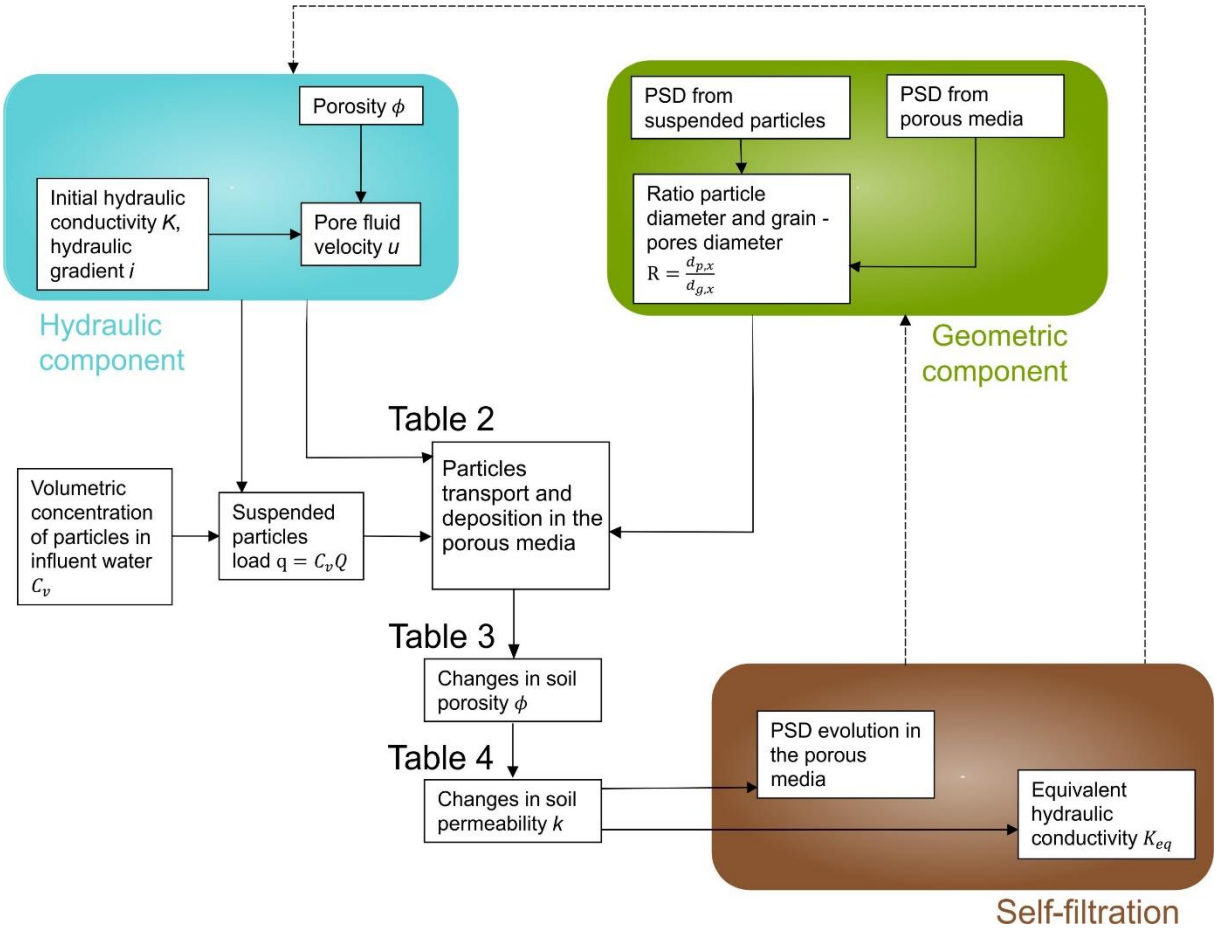

Figure 5: Process-based framework for physical clogging modelling in surface spreading methods.

The advantage of the presented framework (Fig. 5) is that it can be further developed to be parameterised with data from site characterisation. The collection of recharge water data, particularly TSS and particle size distribution (PSD), can be used to predict the effect of straining on the sediment matrix, to derive the relative reduction in hydraulic conductivity and total infiltration capacity (Lippera et al., 2023b; Lippera et al., 2023a). This framework can be transferred to multiple MAR schemes and adapted on the base of the sediments' heterogeneities, characterised by initial hydraulic conductivity, porosity and grain size distributions. The depth of the resulting clogging profile from the simulation of deposition processes can assist MAR operators in the previsions of appropriate cleaning techniques based on the expected soil depth to be treated. This methodology can also determine the expected frequency of cleaning schedules when the total infiltration capacity reaches a low threshold. In planning the MAR site, the drying and cleaning periods should be included within the definition of hydraulic loading rates (Bouwer, 2002).

5. CONCLUSION

From the wide variety of models in the literature to predict physical clogging, it is not straightforward to derive the relevant relations for applied hydrogeological purposes, which is

crucial for MAR feasibility studies. This literature review provides a modelling framework to assess the risk of physical clogging at MAR sites. It is intended to offer guidance on the use of existing models and to identify gaps that need to be closed to assess this risk with field parameters. The main physical clogging processes were identified and mathematical formulations were compared from the reviewed studies. The review showed that predicting particle transport and distribution is the main challenge in modelling physical clogging. The studies that attempt to model clogging on the overall volume of soil rely on the implementation of column experiments, for which the validity of such parameters remains constricted to the specific experimental set-up. Whereas attachment and release mechanisms are described with a probabilistic or analytical approach, these processes are computed at the pore scale and boundary conditions need to apply. To overcome this challenge, a process-based physical clogging model for surface spreading methods should possibly integrate hydraulic and geometric components to quantify fines retention in heterogeneous sediments at MAR sites. The review also proved the Kozeny-Carman model to be the most popular equation in replicating evolutions in permeability, given the variations in soil porosity from the deposition of particles. The Kozeny-Carman model can be adapted from physical parameters in soil samples' data. Thus, a compromise between a overly-sophisticated predictive model and an empirical one calibrated under a single-column experiment should be adapted to assess the risk of physical clogging for MAR sites from site characterisation data. The proposed methodology breaks down the complexity of clogging. However, in future it could be extended to include other clogging processes, e.g. biological and chemical, to provide estimates of the overall risk of clogging.

Funding Information and Conflicts of Interest: The research leading to these results has received funding from the European Union's Horizon 2020 research and innovation programme under the Marie Skłodowska-Curie grant agreement n. 814066 (Managed Aquifer Recharge Solutions Training Network - MARSoluT). On behalf of all authors, the corresponding author states that there is no conflict of interest.

Author contributions: Studies collection and data processing, Maria Chiara Lippera; writing-original draft preparation, Maria Chiara Lippera; writing-review and editing, Thomas Vienken, Ulrike Werban; supervision, Thomas Vienken, Ulrike Werban; project administration, Thomas Vienken, Ulrike Werban. All authors have read and agreed to the final version of the manuscript.

REFERENCES

Alem, A., Ahfir, N.-D., Elkawafi, A., & Wang, H. (2014). Hydraulic Operating Conditions and Particle Concentration Effects on Physical Clogging of a Porous Medium. *Transport in Porous Media, 106*(2), 303-321. https://doi.org/10.1007/s11242-014-0402-8

Alem, A., Elkawafi, A., Ahfir, N.-D., & Wang, H. (2013). Filtration of kaolinite particles in a saturated porous medium: hydrodynamic effects. *Hydrogeology Journal, 21*(3), 573-586. https://doi.org/https://doi.org/10.1007/s10040-012-0948-x

Bai, R., & Tien, C. (2000). Effect of deposition in deep-bed filtration: determination and search of rate parameters. *Journal of colloid and interface science, 231*(2), 299-311.

Bear, J. (1988). *Dynamics of fluids in porous media*. Courier Corporation.

Bedrikovetsky, P., Marchesin, D., Shecaira, F., Souza, A., Milanez, P., & Rezende, E. (2001). Characterisation of deep bed filtration system from laboratory pressure drop measurements. *journal of Petroleum Science and Engineering, 32*(2-4), 167-177.

Blazejewski, R., & Murat-Blazejewska, S. (1997). Soil clogging phenomena in constructed wetlands with subsurface flow. *Water Science and Technology, 35*(5), 183-188.

Boller, M. A., & Kavanaugh, M. C. (1995). Particle characteristics and headloss increase in granular media filtration. *Water Research, 29*(4), 1139-1149. https://doi.org/10.1016/0043-1354(94)00256-7

Bouwer, H. (2002). Artificial recharge of groundwater: hydrogeology and engineering. *Hydrogeology Journal, 10*(1), 121-142. https://doi.org/10.1007/s10040-001-0182-4

Buik, N., & Willemsen, A. (2002). Clogging rate of recharge wells in porous media. In P. J. D. (Ed.) (Ed.), *Management of Aquifer Recharge for Sustainability* (pp. 195-198). CRC Press.

Carman, P. C. (1937). Fluid flow through granular beds. *Trans. Inst. Chem. Eng., 15*, 150-166.

Conley, G., Beck, N., Riihimaki, C. A., & Tanner, M. (2020). Quantifying clogging patterns of infiltration systems to improve urban stormwater pollution reduction estimates. *Water research X, 7*, 100049.

Dillon, P., Alley, W., Zheng, Y., & Vanderzalm, J. (2022). *Managed aquifer recharge: Overview and governance. IAH Special Publication*.

Dillon, P., Stuyfzand, P., Grischek, T., Lluria, M., Pyne, R. D. G., Jain, R. C., Bear, J., Schwarz, J., Wang, W., Fernandez, E., Stefan, C., Pettenati, M., van der Gun, J., Sprenger, C., Massmann, G., Scanlon, B. R., Xanke, J., Jokela, P., Zheng, Y., Rossetto, R., Shamrukh, M., Pavelic, P., Murray,

E., Ross, A., Bonilla Valverde, J. P., Palma Nava, A., Ansems, N., Posavec, K., Ha, K., Martin, R., & Sapiano, M. (2018). Sixty years of global progress in managed aquifer recharge. *Hydrogeology Journal, 27*(1), 1-30. https://doi.org/10.1007/s10040-018-1841-z

Dillon, P. J., Hickinbotham, M. R., & Pavelic, P. (1994). Review of international experience in injecting water into aquifers for storage and reuse. In *Water Down Under 94: Groundwater Papers; Preprints of Papers: Groundwater Papers; Preprints of Papers* (pp. 13-14, 16-19). Institution of Engineers, Australia Barton, ACT.

Du, X., Ye, X., & Zhang, X. (2018). Clogging of saturated porous media by silt-sized suspended solids under varying physical conditions during managed aquifer recharge. *Hydrological Processes, 32*(14), 2254-2262. https://doi.org/10.1002/hyp.13162

Duryea, P. D. (1996). *Clogging layer development and behavior in infiltration basins used for soil aquifer treatment of wastewater* Arizona State University].

Elimelech, M., Gregory, J., & Jia, X. (1998). *Particle deposition and aggregation: measurement, modelling and simulation*. Colloid and Surface Engineering Series.

Elrahmani, A., Al-Raoush, R. I., & Seers, T. D. (2023, 2023/09/01/). Clogging and permeability reduction dynamics in porous media: A numerical simulation study. *Powder Technology, 427*, 118736. https://doi.org/https://doi.org/10.1016/j.powtec.2023.118736

Escalante, E. (2013). Practical Criteria in the Design and Maintenance of MAR Facilities in Order to Minimise Clogging Impacts Obtained from Two Different Operative Sites in Spain. In (pp. 119-154).

Fatt, I. (1956). The network model of porous media. *Transactions of the AIME, 207*(01), 144-181.

Federico, F. (2017). Particle Migration Phenomena Related to Hydromechanical Effects at Contact between Different Materials in Embankment Dams. In *Granular Materials*. https://doi.org/10.5772/67785

Fichtner, T., Barquero, F., Sallwey, J., & Stefan, C. (2019). Assessing Managed Aquifer Recharge Processes under Three Physical Model Concepts. *Water, 11*(1). https://doi.org/10.3390/w11010107

Gibson, S., Abraham, D., Heath, R., & Schoellhamer, D. (2009). Vertical gradational variability of fines deposited in a gravel framework. *Sedimentology, 56*(3), 661-676. https://doi.org/10.1111/j.1365-3091.2008.00991.x

Glass, J., Šimůnek, J., & Stefan, C. (2020). Scaling factors in HYDRUS to simulate a reduction in hydraulic conductivity during infiltration from recharge wells and infiltration basins. *Vadose Zone Journal, 19*(1), e20027.

Gruesbeck, C., & Collins, R. (1982). Entrainment and deposition of fine particles in porous media. *Society of Petroleum Engineers Journal, 22*(06), 847-856.

Herzig, J. P., Leclerc, D. M., & Goff, P. L. (1970). Flow of Suspensions through Porous Media—Application to Deep Filtration. *Industrial & Engineering Chemistry, 62*(5), 8-35. https://doi.org/10.1021/ie50725a003

Hua, G. F., Zhu, W., & Zhang, Y. H. (2010, Oct). A conceptual approach based on suspended solids to estimate clogging time in constructed wetlands. *J Environ Sci Health A Tox Hazard Subst Environ Eng, 45*(12), 1519-1525. https://doi.org/10.1080/10934529.2010.506105

Hutchison, A., Milczarek, M., & Banerjee, M. (2013). Clogging phenomena related to surface water recharge facilities. *In Martin R (ed): Clogging Issues Associated with Managed Aquifer Recharge Methods, IAH Commission on Managing Aquifer Recharge, Australia*, 106-118.

Indraratna, B., & Vafai, F. (1997). Analytical Model for Particle Migration within Base Soil-Filter System. *Journal of Geotechnical and Geoenvironmental Engineering, 123*(2), 100-109. https://doi.org/10.1061/(ASCE)1090-0241(1997)123:2(100)

Ives, K., & Pienvichitr, V. (1965). Kinetics of the filtration of dilute suspensions. *Chemical Engineering Science, 20*(11), 965-973.

Iwasaki, T. (1937). Some Notes on Sand Filtration. *Journal AWWA, 29*(10), 1591-1597. https://doi.org/10.1002/j.1551-8833.1937.tb14014.x

Kadlec, R. H., & Wallace, S. (2009). *Treatment wetlands*. CRC Press Taylor & Francis Group.

Kandra, H. S., McCarthy, D., Fletcher, T. D., & Deletic, A. (2014). Assessment of clogging phenomena in granular filter media used for stormwater treatment. *Journal of Hydrology, 512*, 518-527. https://doi.org/10.1016/j.jhydrol.2014.03.009

Kanti Sen, T., & Khilar, K. C. (2006, Feb 28). Review on subsurface colloids and colloid-associated contaminant transport in saturated porous media. *Adv Colloid Interface Sci, 119*(2-3), 71-96. https://doi.org/10.1016/j.cis.2005.09.001

Kovács, G. (1981). *Seepage Hydraulics* . Elsevier Scientific Publishers BV (North-Holland), Amsterdam, The Netherlands.

Kozeny, J. (1927). Uber kapillare leitung der wasser in boden. *Royal Academy of Science, Vienna, Proc. Class I, 136*, 271-306.

Langergraber, G., Haberl, R., Laber, J., & Pressl, A. (2003). Evaluation of substrate clogging processes in vertical flow constructed wetlands. *Water Science and Technology, 48*(5), 25-34.

Li, Z., Yang, H., Sun, Z., Espinoza, D. N., & Balhoff, M. T. (2021). A Probability-Based Pore Network Model of Particle Jamming in Porous Media. *Transport in Porous Media, 139*(2), 419-445.

Lin, D., Hu, L.-m., Bradford, S., Zhang, X., & Lo, I. (2021, 10/01). Pore-Network Modeling of Colloid Transport and Retention Considering Surface Deposition, Hydrodynamic Bridging, and Straining. *Journal of Hydrology, 603*, 127020. https://doi.org/10.1016/j.jhydrol.2021.127020

Lippera, M. C., Werban, U., Rossetto, R., & Vienken, T. (2023b). Understanding and predicting physical clogging at managed aquifer recharge systems: A field-based modeling approach. *Advances in Water Resources, 177*, 104462. https://doi.org/https://doi.org/10.1016/j.advwatres.2023.104462

Lippera, M. C., Werban, U., & Vienken, T. (2023a). Improving clogging predictions at managed aquifer recharge sites: a quantitative assessment on the vertical distribution of intrusive fines. *Hydrogeology Journal, 31*(1), 71-86. https://doi.org/10.1007/s10040-022-02581-7

Locke, M., Indraratna, B., & Adikari, G. (2001). Time-Dependent Particle Transport through Granular Filters. *Journal of Geotechnical and Geoenvironmental Engineering, 127*(6), 521-529. https://doi.org/10.1061/(ASCE)1090-0241(2001)127:6(521)

Majumdar, P. K., Sekhar, M., Sridharan, K., & Mishra, G. C. (2008). Numerical Simulation of Groundwater Flow with Gradually Increasing Heterogeneity due to Clogging. *Journal of Irrigation and Drainage Engineering, 134*(3), 400-404. https://doi.org/doi:10.1061/(ASCE)0733-9437(2008)134:3(400)

Maliva, R. G. (2020). Clogging. In R. G. Maliva (Ed.), *Anthropogenic Aquifer Recharge: WSP Methods in Water Resources Evaluation Series No. 5* (pp. 307-342). Springer International Publishing. https://doi.org/10.1007/978-3-030-11084-0_11

Martin, R. (2013). Clogging issues associated with managed aquifer recharge methods. *IAH Commission on Managing Aquifer Recharge, Australia*, 26-33.

Mays, D., & Martin, R. (2013). Clogging in managed aquifer recharge: flow, geochemistry, and clay colloids. *Clogging Issues Associated with Managed Aquifer Recharge Methods*, 14-24.

McDowell-Boyer, L. M., Hunt, J. R., & Sitar, N. (1986). Particle transport through porous media. *Water Resources Research, 22*(13), 1901-1921. https://doi.org/10.1029/WR022i013p01901

Meadows, D. L., & Rowell, S. E. (1994). Core sample test method and apparatus. *U.S. Patent No 5,325,723*.

Muecke, T. W. (1979). Formation fines and factors controlling their movement in porous media. *Journal of petroleum technology, 31*(02), 144-150.

Nivala, J., Knowles, P., Dotro, G., Garcia, J., & Wallace, S. (2012, Apr 15). Clogging in subsurface-flow treatment wetlands: measurement, modeling and management. *Water Res, 46*(6), 1625-1640. https://doi.org/10.1016/j.watres.2011.12.051

Pavelic, P., Dillon, P. J., Barry, K. E., Vanderzalm, J. L., Correll, R. L., & Rinck-Pfeiffer, S. M. (2007). Water quality effects on clogging rates during reclaimed water ASR in a carbonate aquifer. *Journal of Hydrology, 334*(1-2), 1-16.

Pavelic, P., Dillon, P. J., Mucha, M., Nakai, T., Barry, K. E., & Bestland, E. (2011, May). Laboratory assessment of factors affecting soil clogging of soil aquifer treatment systems. *Water Res, 45*(10), 3153-3163. https://doi.org/10.1016/j.watres.2011.03.027

Pendse, H., Tien, C., Rajagopalan, R., & Turian, R. (1978). Dispersion measurement in clogged filter beds: A diagnostic study on the morphology of particle deposits. *AIChE Journal, 24*(3), 473-485.

Pérez Paricio, A. (2001). *Integrated modelling of clogging processes in artificial groundwater recharge*. Universidad Politécnica de Cataluña. http://hdl.handle.net/2117/93526.

Pucher, B., & Langergraber, G. (2019). The State of the Art of Clogging in Vertical Flow Wetlands. *Water, 11*(11), 2400. https://www.mdpi.com/2073-4441/11/11/2400

Pyne, R. D. G. (1995). *Groundwater recharge and wells: a guide to aquifer storage recovery*. 1st Edition, CRC press. https://doi.org/https://doi.org/10.1201/9780203719718

Racz, A. J., Fisher, A. T., Schmidt, C. M., Lockwood, B. S., & Los Huertos, M. (2012, Jul-Aug). Spatial and temporal infiltration dynamics during managed aquifer recharge. *Groundwater, 50*, 562-570. https://doi.org/10.1111/j.1745-6584.2011.00875.x

Reddi, L. N., Ming, X., Hajra, M. G., & Lee, I. M. (2000). Permeability Reduction of Soil Filters due to Physical Clogging. *Journal of Geotechnical and Geoenvironmental Engineering, 126*(3), 236-246. https://doi.org/10.1061/(ASCE)1090-0241(2000)126:3(236)

Reddi, L. N., Xiao, M., Hajra, M. G., & Lee, I. M. (2005). Physical clogging of soil filters under constant flow rate versus constant head. *Canadian geotechnical journal, 42*(3), 804-811.

Rege, S. D., & Fogler, H. S. (1988). A network model for deep bed filtration of solid particles and emulsion drops. *AIChE Journal, 34*(11), 1761-1772. https://doi.org/10.1002/aic.690341102

Rinck-Pfeiffer, S., Ragusa, S., Sztajnbok, P., & Vandevelde, T. (2000). Interrelationships between biological, chemical, and physical processes as an analog to clogging in aquifer storage and recovery (ASR) wells. *Water Research, 34*(7), 2110-2118.

Roque, C., Chauveteau, G., Renard, M., Thibault, G., Bouteca, M., & Rochon, J. (1995). Mechanisms of formation damage by retention of particles suspended in injection water. SPE European Formation Damage Conference,

Sallwey, J., Barquero, F., Fichtner, T., & Stefan, C. (2019). Planning MAR Schemes Using Physical Models: Comparison of Laboratory and Field Experiments. *Applied Sciences, 9*(18). https://doi.org/10.3390/app9183652

Schippers, J. C., & Verdouw, J. (1980). The modified fouling index, a method of determining the fouling characteristics of water. *Desalination, 32*, 137-148. https://doi.org/10.1016/s0011-9164(00)86014-2

Schuler, U. (1996). Scattering of the composition of soils. An aspect for the stability of granular filters. Geofilters,

Silveira, A. (1965). An analysis of the problem of washing through in protective filters. Proceedings,

Terzaghi, K., Peck, R. B., & Mesri, G. (1967). Soil Mechanics in Engineering Practice, John Wiley & Sons. *Inc., New York*.

Torkzaban, S., Bradford, S. A., Vanderzalm, J. L., Patterson, B. M., Harris, B., & Prommer, H. (2015, Oct). Colloid release and clogging in porous media: Effects of solution ionic strength and flow velocity. *J Contam Hydrol, 181*, 161-171. https://doi.org/10.1016/j.jconhyd.2015.06.005

Wang, Z., Du, X., Yang, Y., & Ye, X. (2012). Surface clogging process modeling of suspended solids during urban stormwater aquifer recharge. *Journal of Environmental Sciences, 24*(8), 1418-1424. https://doi.org/10.1016/s1001-0742(11)60961-3

Wennberg, K., & Sharma, M. (1997). Determination of the filtration coefficient and the transition time for water injection wells. SPE European Formation Damage Conference,

Witt, K. (1993). Reliability study of granular filters. *Filters in geotechnical and hydraulic engineering*, 35-42.

Xie, Y., Wang, Y., Huo, M., Geng, Z., & Fan, W. (2020). Risk of physical clogging induced by low-density suspended particles during managed aquifer recharge with reclaimed water: Evidences from laboratory experiments and numerical modeling. *Environmental research, 186*, 109527.

Xiong, Q., Baychev, T. G., & Jivkov, A. P. (2016, 2016/09/01/). Review of pore network modelling of porous media: Experimental characterisations, network constructions and applications to reactive transport. *Journal of Contaminant Hydrology, 192*, 101-117. https://doi.org/https://doi.org/10.1016/j.jconhyd.2016.07.002

Ye, X., Cui, R., Du, X., Ma, S., Zhao, J., Lu, Y., & Wan, Y. (2019). Mechanism of suspended kaolinite particle clogging in porous media during managed aquifer recharge. *Groundwater, 57*(5), 764-771.

Zamani, A., & Maini, B. (2009). Flow of dispersed particles through porous media — Deep bed filtration. *Journal of Petroleum Science and Engineering, 69*(1-2), 71-88. https://doi.org/10.1016/j.petrol.2009.06.016

Zhang, H., Xu, Y., & Kanyerere, T. (2020). A review of the managed aquifer recharge: Historical development, current situation and perspectives. *Physics and Chemistry of the Earth, Parts A/B/C*, 102887.

Zou, Z., Shu, L., Min, X., & Chifuniro Mabedi, E. (2019). Clogging of Infiltration Basin and Its Impact on Suspended Particles Transport in Unconfined Sand Aquifer: Insights from a Laboratory Study. *Water, 11*(5). https://doi.org/10.3390/w11051083

Hydrogeology Journal
https://doi.org/10.1007/s10040-022-02581-7

PAPER

Improving clogging predictions at managed aquifer recharge sites: a quantitative assessment on the vertical distribution of intrusive fines

Maria Chiara Lippera[1,3] · **Ulrike Werban**[3] · **Thomas Vienken**[2,3]

Received: 13 April 2022 / Accepted: 5 December 2022

Abstract
Managed aquifer recharge (MAR) is an emerging approach to enhancing water storage capacity, improving water supply security and countering groundwater overexploitation. However, physical clogging, i.e. accumulation of suspended organic and inorganic solids within a sediment matrix, can lead to a significant reduction of infiltration rates and present difficulties in the functioning of MAR infrastructure. Clogging and subsequent reduction in infiltration capacity are often quantified based on monitoring data or field investigations, rather than on forecasts. Existing predictive models require specific parameterisation, making an application to heterogeneous sites, or under changing conditions, difficult. Hence, a generalised understanding of how intrusive fine particles distribute over depth during water recharge cycles for typical MAR infiltration basin sediments is needed to predict clogging susceptibility and clogging patterns already in the planning phase and before operation of MAR schemes. The study will contribute to operational reliability, deduce optimised management practices, and, ideally, reduce maintenance efforts. To achieve this goal, data from different soil-column clogging experiments are reviewed and complemented with experiments to establish a generally valid relationship for the vertical distribution of intrusive fines under consideration of the primary porous media's and intruding particles' characteristics. Obtained results allow for quantification of the amount of particles retained at the surface of the porous media, i.e. formation of a filter cake, a description of the distribution of fines over depth, and total clogging depth. Finally, the findings are applied to a real MAR case study site to showcase the quantification of clogging effects on recharge rates.

Keywords Managed aquifer recharge (MAR) · Clogging · Soil processes · Hydraulic properties

Introduction

Managed aquifer recharge (MAR) techniques are increasingly needed to enhance water storage capacity, improve water supply security and reduce impacts associated with fresh groundwater overexploitation (Dillon et al. 2018; Sprenger et al. 2017). The reduction in recharge rate due to clogging is one of the main concerns in the functioning of MAR systems (Bouwer 2002). Clogging originates from the accumulation of organic and inorganic suspended solids at the infiltration surface and in the migration of interstitial fines within the sediment matrix (Bennion et al. 1998; Goss et al. 1973; Wang et al. 2012). The particle size distribution of the infiltrating particles in relation to the pore bodies of the passed-through soil controls the shape of the clogging profile. Suspended particles with a larger particle size than the porous-media grain size accumulate on the surface of the granular material, forming the surface or external filter cake. Smaller suspended particles enter the interstitial space of the bed and deposit according to the mechanism of straining, leading to the occurrence of internal clogging. Straining is the blockage by fine particles at down-gradient pore constrictions that do not allow their passage (Bradford et al. 2003; Herzig et al. 1970). When fines intrude into the soil matrix, they increase the media surface area to volume ratio and reduce the media porosity (McDowell-Boyer et al. 1986). MAR sites can experience a decrease in infiltration

✉ Maria Chiara Lippera
maria-chiara.lippera@tum.de

[1] Technical University of Munich, TUM Campus Straubing for Biotechnology and Sustainability, Straubing, Germany

[2] Weihenstephan-Triesdorf University of Applied Sciences, TUM Campus Straubing for Biotechnology and Sustainability, Straubing, Germany

[3] UFZ - Helmholtz Centre for Environmental Research, Leipzig, Germany

Published online: 29 December 2022

capacity by orders of magnitude due to physical clogging (Racz et al. 2012). Often, sedimentation ponds reduce the concentration of suspended fines in the infiltration water; however, infiltration sites can accumulate fine particles transported from weathering reactions or from the rearrangement of deposits (Hutchison et al. 2013). The loss in performance can cause an increase in operation and maintenance costs (Dillon et al. 2016), the restoration of infiltration basins and boreholes (Martin 2013), and in extreme cases, the abandonment of the site (Hutchison et al. 2013). Ross and Hasnain (2018) report, for infiltration-basin recharged with untreated water, average MAR scheme costs of 0.77 USD capital cost per metre cubed recharged and a 0.13 USD operation and maintenance cost per metre cubed recharged. Despite these MAR schemes being relatively inexpensive to install, the costs for basin maintenance can be high, including the shut-down period for the cleaning and drying of passages (Ross and Hasnain 2018).

In the current state of the art of MAR clogging surveillance, instantaneous profile measurement systems of water content have been developed to accurately monitor reductions in infiltration capacity in the field (Barquero et al. 2019). Geophysical monitoring in MAR sites can track infiltration pathways by time-lapse electrical resistivity tomography (De Carlo et al. 2020; Nenna et al. 2014; Ulusoy et al. 2015). Thermal loggers and fiber-optic distributed temperature sensing assist in detecting spatial and temporal variations in infiltration rates (Becker et al. 2013; Mawer et al. 2016; Racz et al. 2012). Martin (2013) suggests observing the hydraulic responses in nearby observation wells during recharge to detect the presence of clogging (Pyne 1995). In MAR numerical simulations, the variation in hydraulic conductivity can be integrated through a time-variable scaling factor calibrated via an experimental setup (Glass et al. 2020). Although the up-to-date research improves basin management and clogging detection after development, there is still the necessity to design modelling tools to predict potential reductions in MAR infiltration capacity during the conceptual phase. So far, the basic water quality parameters used for MAR design have been total suspended solids (TSS), turbidity level for smaller particles (nephelometric turbidity units, NTU), and dissolved organic carbon (DOC) (Bouwer 2002; Dillon 2002; Okubo and Matsumoto 1983). However, the limit values of these parameters in reference to clogging can vary widely from site to site (Bouwer 2002).

Similarly, existing mathematical models for physical clogging and MAR design have been developed by fitting the breakthrough concentrations to the mass balance solution from a specific sand column setup (Torkzaban et al. 2015; Xie et al. 2020). The parametrisation derived from the column's breakthrough curves for a specific MAR site is not transferable to a different MAR context. The growing interest in MAR and its implementation worldwide requires further thorough studies into systematic clogging mechanisms and prevention (Zhang et al. 2020); hence, there exists a need to derive a general model for predicting physical clogging that can be adapted to multiple sites through site characterisation. Different factors determine the reductions in infiltration rates in the field—effluent water quality, basin soil texture, ponding depth, hydraulic loading rate and recharge cycles. However, the rate and degree of clogging are controlled mainly by the rate of suspended solids deposition, the size distribution of the fines and the size distribution of the receiving sediments (Hutchison et al. 2013).

One of the main obstacles in clogging research is predicting the characteristic depth of the particles' intrusion and deposition (Locke et al. 2001), thus the vertical distribution of fines within the porous media. Clogging profiles have already been expressed through an exponential decay function for sediment transport studies in hydraulically turbulent open channel flow (Cui et al. 2008; Huston and Fox 2015). Understanding how particles distribute along the porous media profile is essential in determining how fast and up to which depth the porous media will be severely clogged. The assessment of the site's susceptibility to clogging before construction prevents high unexpected costs and leads to evaluating the optimal design and operational options.

This study aims to improve physical clogging predictions by quantitatively assessing the distribution and volumes of deposited particles over soil depth during water recharge. The final scope is to determine the reduction in infiltration rates over the operational period of the infrastructure and the depth of the damage. To overcome the challenge of determining the characteristic depth of the particles' intrusion and deposition, the porous medium is hypothesised as a multilayer mesh in which a certain depth-varying percentage of particles are trapped, based on their diameter size, following an exponential decay. The novelty of this study is to propose an overall model to predict physical clogging, transferable to multiple MAR sites, while not relying on a specific set of parameters determined over a single-column experiment.

Therefore, results from existing column experiments in literature applicable to MAR conditions were reviewed and complemented with additional experiments to investigate whether a general relationship can be established between the vertical distribution of the fines and the porous-media and particle characteristics. The relevance of this work is highlighted by its application to the case study of a floodwater infiltration basin in Italy, assessing the risk of clogging and potential reductions in infiltration rates.

Methods

Literature review

To examine how intrusive fines distribute in porous media, available profiles of deposited fines were selected from

multiple-sand-column experiments. The experimental setup of these studies had to reflect MAR conditions, i.e., employing a porous media in the grain size range of coarse-medium sand (0.25–1 mm) and a low concentration of fine particles in suspension. In column experiments, constant head conditions best reflect the operating conditions for infiltration basins; however, in contrast, remobilisation of particles caused by the increase in injection pressure to overcome the resistance of the already declined hydraulic conductivity can be observed for column experiments under a constant flow rate. This behaviour is recognisable in the breakthrough curves from the increase of the relative concentrations of fines at the column effluent over time; hence, column experiments under a constant flow rate are less suitable for the analysis. In order to avoid high-water-pressure effects, the data derived from the sand column experiments under constant-head conditions described in Alem et al. (2014) were collected. The study under constant head conditions for 83 pore volumes (NVp) showed stable clay concentrations at the effluent; thus, the filtration action of the porous media did not change during the run of the column experiment. The experiments of Ahfir et al. (2017), for three sandy porous media in constant flow rate conditions, were also selected. Their study observed retention profiles for the duration of 3 NVp; thus, the clogged state of the porous media does not affect the vertical distribution of the fines yet, and the exerted water pressures are not further increased. Lastly, four-column experiments were run with artificial and natural material of defined grain-size ranges at the Helmholtz Centre for Environmental Research, Department of Monitoring and Exploration Technologies in Germany (Tippelt 2015). The experiments' scope was to observe the impact of fines input on the long-term infiltration capacity of a specific infiltration basin. In all three studies, the clay content was wet-sieved and weighed at the column sections, and the mass of fines deposited per unit of porous media mass was expressed as the retention profile.

In order to compare the datasets from the selected studies, the relative mass of deposited particles to the total mass of infiltrated particles was computed for each section. An averaged value over the section length was assumed at the central point to attribute the relative mass of deposited clay to a specific depth. Table 1 provides an overview of the setups of the column experiments from the selected studies. The number of datasets is limited by the availability of retention profiles in the literature. Filtration studies often lack this information since particle concentrations are conventionally automatically measured at the effluent. The lack of retention profile data in studies is indeed a limitation in understanding the straining and deposition processes occurring within the porous media. Retention profile data from experiments in gravel substrates were omitted, e.g. Gibson et al. (2009) and Tang et al. (2020). Due to the different experimental setups, the silt profiles in chromatography columns from Du et al. (2018) were also excluded. The latter case of silt particles depositing superficially in fine sand is indeed a case of interest for MAR site applications.

Experiments

Four experiments were additionally performed to increase the number of datasets and extend the analysis to the case of silt particles blocked at the porous media surface. A particle suspension was infiltrated in constant head conditions in sandy porous media in four grain-size ranges. The column of 4.8 cm in diameter and 50 cm in height had a constant head of 20 cm above the sand material for a total hydraulic gradient of 1.44 cm/cm. The experimental setup schematic is shown in Fig. 1a. The column was saturated from the bottom to avoid air trapping. After the outflow from the column reached stable conditions, the suspension was let to infiltrate at the concentration of 1 g/L. Differently from the other selected studies in Table 1, the experiments were performed with silt material, with a median diameter $d_{50} = 31.01$ (± 0.20) µm (Fig. 1b). The silt was previously obtained by dry-sieving a silty soil, and the particle size distribution was measured with laser diffraction (Cilas Particle Size 920). The suspension was allowed to infiltrate quartz sands in the grain-size ranges 0.5–1.0, 0.4–0.8, 0.2–0.7, and 0.1–0.4 mm (Euroquarz GmbH). An overview of the setup of the four experiments is reported in Table 1 under 'This study (2022)' followed by the experiment identifier number. The outflow of the column was measured with a precision balance scale (KERN PCB) and recorded via a USB to RS232 serial port. Turbidity values (NTU) for the column effluent were measured with a turbidimeter (HACH 2100P) to check the mass balance within the porous media. Previously a calibration was made between the known a priori suspended particles (SP) concentrations and the measured NTU values. At the end of the experiment, samples were taken at the column sections and at the porous media surface. The samples were dried and weighed, and the difference in weight was annotated after wet-sieving and drying.

Results

This section describes the analysis, modelling steps and results that contribute to assessing clogging profiles in porous media. The subsections are organized with the following contents:

Table 1 Experimental setups of the selected studies. The experiment identifier number distinguishes the single column experiments for the reference study. For each column experiment, the length and diameter of the column are indicated along with the number of sections in the column, the concentration of particles in the influent water, the number of pore volumes infiltrated, the diameter size range of the suspended particles, the diameter size range of the porous media, median particles size of the suspension (d_{50}), and median diameter size of the porous media (D_{50})

Study reference and experiment ID	Column length (cm)	Column diameter (cm)	No. of sections	Concentration (mg/L)	No. of pore volumes (NVp)	Size range (µm) and material -SP	Size range (µm) and material -PM	d50 (µm) -SP	D50 (µm) -PM
Ahfir et al. (2017) -1	62	4.4	15	500	3	2–30 kaolinite	315–630 sand	10	440
Ahfir et al. (2017) -2	62	4.4	15	500	3	2–30 kaolinite	315–800 sand	10	570
Ahfir et al. (2017) -3	62	4.4	15	500	3	2–30 kaolinite	630–800 sand	10	715
Alem et al. (2014)	40	4.5	9	250	83	1.7– 40 kaolinite	315–630 sand	15	410
Tippelt (2015) -1	50	30	5	102	30.78	0.36–103 bentonite	400–700 glass beads	7.68	530
Tippelt (2015) -2	50	30	5	102	30.78	0.36–103 bentonite	400–700 glass beads	7.68	530
Tippelt (2015) -3	50	30	5	102	30.31	0.36–103 bentonite	1,500 glass beads	7.68	1,500
Tippelt (2015) -4	50	30	5	102	23.44	0.36–103 bentonite	500–1,000 sand	7.68	710
This study (2022) -1	50	4.8	7	1,000	39.07	1–90 silt	500–1,000 sand	31	760
This study (2022) -2	50	4.8	7	1,000	40.43	1–90 silt	400–800 sand	31	590
This study (2022) -3	50	4.8	7	1,000	41.82	1–90 silt	200–700 sand	31	420
This study (2022) -4	50	4.8	7	1,000	32.51	1–90 silt	100–400 sand	31	230

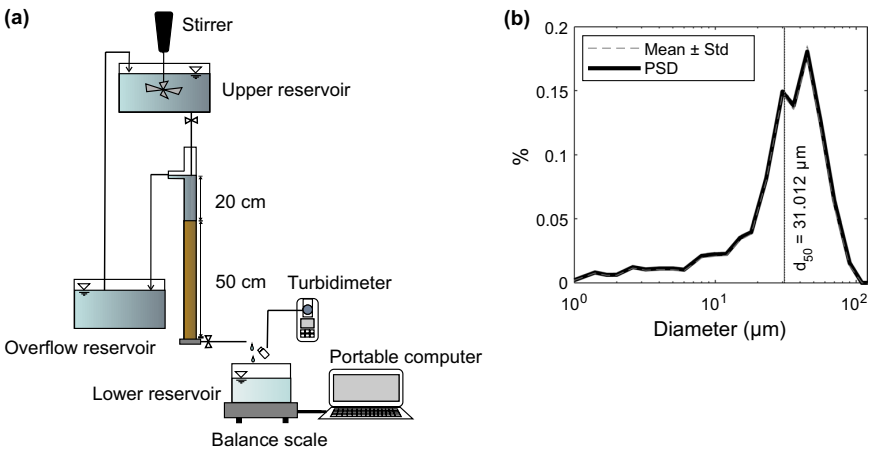

Fig. 1 Information on the four performed experiments. **a** The column experimental setup, **b** particle size distribution (PSD) of the silt material used for the suspension

- Data analysis: retention profiles are expressed in relative masses of deposited fines over depth, and the vertical profiles are parametrized as exponential decay functions.
- A relationship is established between the relative mass of fines at the water–sediment interface and the geometric ratio d_{50}/D_{50} of the experimental setup.

- A mathematical solution defines the decay rate of fines deposition over depth. The expected depth of clogging and the clogging vertical profile are thus determined from the previously established relationship.
- For the experiments in superficial clogging conditions, the process leading to the external cake formation is formulated through a retention limit at the surface.
- The use of the Kozeny-Carman equation in computing reductions in soil permeability is tested for the observed outflow rates from the performed experiments.

An extensive discussion of the results is reported in section 'Discussion'.

Data analysis

From the literature review, three studies consisting of eight-column experiments reflecting MAR conditions were analysed, and four additional experiments were performed to extend the range of validity of the analysis. The profiles of deposited fines are expressed as the relative mass with respect to the total infiltrated mass of particles. The vertical distribution of the fines is outlined by an exponential decay function over the depth z (cm):

$$f(z) = f_{z=0} e^{-\alpha z} \tag{1}$$

with $f_{z=0}$ being the mass fraction of particles at the water–sediment interface and α being the decay rate, accounting for the reduction in the particles' retention per unit of depth:

$$\frac{df}{dz} = -\alpha f(z) \tag{2}$$

The fitting of the exponential decay curves to each clogging profile from the column experiments leads to the parameters describing the relative mass at the surface ($f_{z=0}$) and the decay rate of deposition (α). This formulation is valid for profiles not exceeding a saturation limit at the water–sediment interface, which corresponds to the maximum retention of fines. After this limit, the external cake starts forming. Therefore, only the experiments under internal clogging conditions are used to calibrate the parameters describing the clogging profiles. In Fig. 2, it can be observed that for greater deposition at the top of the column, a stronger fit to the exponential decay function is observed (Fig. 2a, e–g, i with respectively $R^2 = 0.97$, $R^2 = 0.93$ and $R^2 = 0.96$), in comparison to the other clogging profiles (Fig. 2b,c,h with $R^2 = 0.89$, $R^2 = 0.87$ and $R^2 = 0.70$). In contrast, the profile presenting the limit case for internal clogging, thus very

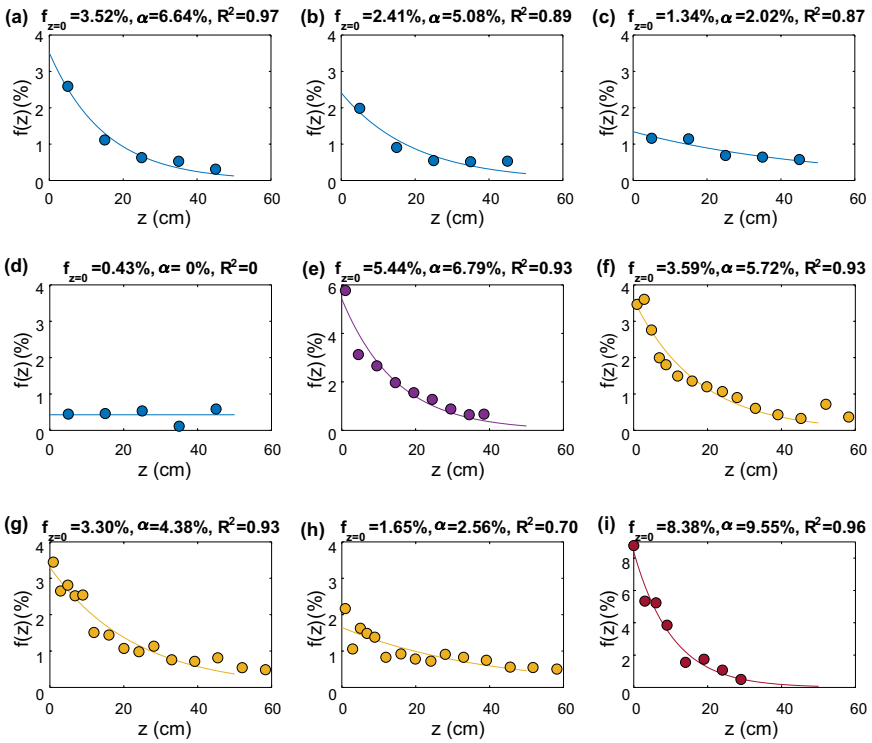

Fig. 2 Fitting of the exponential decay functions for the column experiment data from Tippelt (2015); **a**–**b** glass spheres 400–700 µm; **c** sand 500–1,000 µm, and **d** glass spheres 1,500 µm. Also, the condition used by Alem et al. (2014) and Ahfir et al. (2017); **e**–**f** sand 315–630 µm; **g** sand 315–800 µm, **h** sand 630–800 µm, and **i** This study (2022) sand 500–1,000 µm. The relative mass of fines $f(z)$ is the deposited mass (%) to the total mass of infiltrated particles per unit depth z. Above each graph are reported the values for $f_{z=0}$ (%) and α (%) from the exponential fit, and the coefficient of determination (R^2)

low deposition at the surface, does not show a variability around the mean value that can be explained by the exponential decay (Fig. 2d, $R^2 = 0$). The deposited fines are thus assumed to be distributed homogeneously through the soil with a decay rate α equal to zero. In the following sections, the exponential decay parameters are related to a geometric clogging predictor to explore the dependency of the clogging profile on the primary porous media and particle characteristics.

Clogging predictor

The parameters $f_{z=0}$ and α are related to the straining factors controlling the shaping of the retention profile; thus, predictors should summarise the primary porous-media and particle characteristics. Clogging predictors based on the system geometry account for the diameter of the suspended particles (d_p) relative to that of the porous media (d_g), i.e., d_p/d_g (see Gruesbeck and Collins 1982; Herzig et al. 1970; Khilar and Fogler 1998; Muecke 1979; Sakthivadivel 1969). In Bradford et al. (2003), the straining coefficient is a function of the ratio of the suspended solids' median particles size (d_{50}) to the porous media median grain size (D_{50}). Based on Bradford et al. (2003) the median diameter is assumed representative of the porous media and particles distribution. The median diameter is an immediate statistic to describe the particle size distribution, and it can be interpreted as a proxy for the average pore body size of the porous media (Mahmoodlu et al. 2016). The median diameters' values for the porous media grain distribution and suspended particles of each column experiment are reported in Table 1. For the retention profiles of the nine column experiments on internal clogging conditions, the relative mass of particles deposited at $z = 0$ cm is related to the geometric ratio d_{50}/D_{50}. The fraction of fines at the water–sediment interface follows a linear trend with increasing values of the geometric ratio d_{50}/D_{50} (Fig. 3).

The linear relationship verifies that fines retained superficially are close to zero for small median particle sizes to larger matrix grain diameters. The suspended particles with small size ranges intrude deeper into the soil formation, crossing a larger void space. Particles with larger median sizes instead lead to superficial clogging when intruding into a matrix with smaller grain diameters. Setting the boundary point at the origin ($f_{z=0} = 0, d_{50}/D_{50} = 0$), the following linear relationship for surface deposition at the water–porous media interface is established:

$$f_{z=0} = 1.76\frac{d_{50}}{D_{50}} \tag{3}$$

with $R^2 = 0.90$.

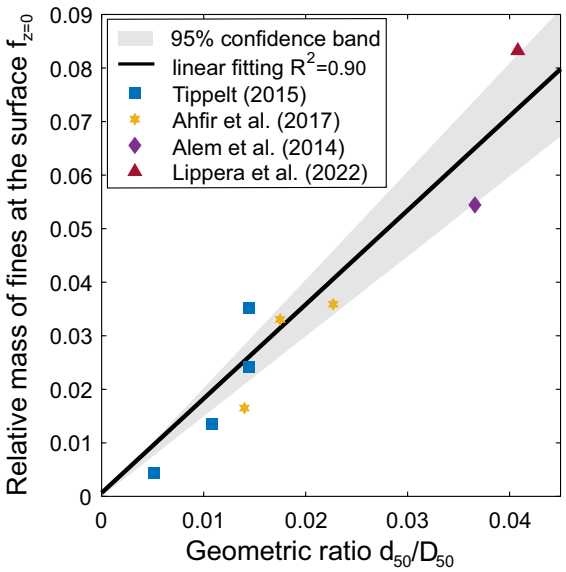

Fig. 3 Relationship between the relative mass of fines at the porous media's surface and the geometric ratio for the selected studies and one additional experiment under internal clogging conditions

The geometric ratio d_{50}/D_{50} provides systematic information on the relative mass of fines captured at the surface. The random error term is independent of the predictor d_{50}/D_{50} and has a mean value of zero, as proved by the one-sample t-test performed on the residuals ($p = 0.68$, H0: data are from a normal distribution with a mean equal to zero). Thus, the simple model with only the geometric ratio explains the variations in $f_{z=0}$. In order to assess whether Eq. (3) approximates the population regression line given the limited datasets, the model is tested with the leave-one-out cross-validation. Nine training data sets were generated, leaving out the data from one single-column experiment on which the model prediction is tested.

The unbiased estimates for the nine test errors in Table 2 provide an average MSE of 9.06e-05. The slope coefficients for the eight linear regressions fall within the 95% confidence interval of the full dataset relationship [1.49, 2.02]. Figure 3 reports the 95% confidence interval for the fitted linear regression with the full dataset.

Clogging depth and profile

In addition to the parameter $f_{z=0}$, the clogging profile is also defined by the decrease in relative mass over depth. The decay rate α expresses the exponential decay of captured particles over depth. Integrating from zero to infinite depth, for the function defining the fractions of retained fines up to the sum of 1, the following solution is obtained:

Table 2 Slope coefficients calibrated for the 9 datasets generated with the leave-one-out cross-validation method and mean square error (MSE) of the prediction on the excluded dataset

Parameter	Data set 1	Data set 2	Data set 3	Data set 4	Data set 5	Data set 6	Data set 7	Data set 8	Data set 9
Slope	1.78	1.75	1.78	1.73	1.76	1.76	1.77	1.87	1.59
MSE	2.06E-05	5.83E-06	7.20E-05	1.03 E-04	2.04E-06	2.24E-05	3.29E-05	1.97E-04	3.60E-04

$$\int_0^\infty f_{z=0} e^{-\alpha z} dz = 1 \tag{4}$$

$$\left[\frac{f_{z=0} e^{-\alpha z}}{-\alpha}\right]_0^\infty = 1 \tag{5}$$

$$\alpha = f_{z=0} \tag{6}$$

Equation (6) shows that the reduction factor per unit of depth α is directly correlated to the fraction of retained fines at the surface $f_{z=0}$, and the data from the eight retention profiles in Fig. 2 confirm this relationship with an $R^2 = 0.59$ and RMSE = 0.0169. Part of the error might be attributed to the fact that the entire mass of intrusive fines is not recovered in all the experiments. It is preferable to adopt the mathematical solution for the calibration of α, to guarantee that the defined fractions of fines amount to one over the total porous media depth. Equation (6) verifies that for an extreme condition in *surface* clogging, the retention decreases steeply with depth ($\alpha = f_{z=0} \approx 1$), and the soil exhibits a short clogging profile. By contrast, the soil exhibits a deep clogging profile for an extreme condition in *internal* clogging ($f_{z=0} = \alpha \approx 0$), and a constant fraction of suspended particles is retained with depth. The clogging depth can also be assessed for intermediate conditions of the clogging profile. Assuming 0.5% retained fines as an arbitrary threshold for ending the clogging profile, the depth of clogging z_{clog} (cm) is:

$$z_{clog} = -\ln\left(\frac{0.005}{f_{z=0}}\right)\frac{1}{\alpha} \tag{7}$$

with $f(z_{clog}) = 0.005$ being the relative mass at the bottom of the clogging profile.

Thus, the fines-fraction profile through the sediment matrix can be estimated only from the ratio of the median particle diameter size to the median grain diameter size. Substituting in Eq. (1) the parameters $f_{z=0}$ and α from the linear regressions reported in Eqs. (3) and (6), the final equation describing the clogging profile is:

$$f(z) = \left(1.76\frac{d_{50}}{D_{50}}\right)\exp\left(-1.76\frac{d_{50}}{D_{50}}z\right) \tag{8}$$

This formulation expresses the fractions of particles captured along the porous media's depth, as long as the saturation limit at the water–sediment interface is not reached and particles intrude internally.

External cake formation

The relationship for the clogging profile (Eq. 8) can be adopted for internal clogging only since it does not account for the formation of the external cake. In surface clogging conditions, after exceeding a saturation limit for the fines' retention at the surface, the porous media would start accumulating the fines at the top. The overall amount of fines depositing externally of the porous media would diverge from the retention profiles expressed in relative mass. The fines in excess at $z = 0$ are dependent on the total amount of infiltration fines after the retention limit at the water–sediment interface has been reached. In this regard, the three performed experiments in surface clogging conditions are used for validation. It is assumed that the particles would start distributing internally during infiltration, according to Eq. (8), up to a total mass of infiltrated particles, after which the formation of the external cake begins. The mass retained at the porous media surface, after which particles stop intruding internally, can be defined as $M_{z=0,limit}$:

$$M_{z=0,limit} = f_{z=0} M_{tot,limit} \tag{9}$$

with $M_{tot,limit}$ (g) the total mass of infiltrated particles up to the limit of the external cake formation. The retention limit at the porous media surface can be approximated by the volume of voids V_v (cm). This volume at the water–sediment interface, is defined for the infiltration area A (cm) with the radius of the median grain (cm):

$$V_v = An\frac{D_{50}}{2} \tag{10}$$

with the porosity n of the porous media. The void space is filled with particles having bulk density ρ_s (g/cm^3); thus, the maximum retained mass at the water–sediment interface is:

$$M_{z=0,limit} = V_v \rho_s \frac{d_0}{d_{50}} \tag{11}$$

the parameters D_{50} (cm) and d_{50} (cm) account for the straining effect given by the proportion of the median particle diameters to the average pore diameter $d_0 = 0.235\ D_{50}$ (Mahmoodlu et al. 2016). Combining Eqs. (9) and (11), the

input of fines after which the external cake would start forming is the following:

$$M_{\text{tot,limit}} = \frac{An\rho_s 0.117{D_{50}}^2}{d_{50} f_{z=0}} \tag{12}$$

with $f_{z=0}$ from Eq. (3).

The particles' profile in superficial clogging conditions is thus corrected to account for the formation of the external cake:

$$f(z) = \left(1.76\frac{d_{50}}{D_{50}}\right)\exp\left(-1.76\frac{d_{50}}{D_{50}}z\right)\frac{M_{\text{tot,limit}}}{M_{\text{tot}}} + \frac{M_{\text{tot}} - M_{\text{tot,limit}}}{M_{\text{tot}}}(z=0) \tag{13}$$

with M_{tot} (g) the total infiltrating mass of particles. The equation is applied to the observed clogging profiles from the three experiments exhibiting superficial clogging, as shown in Fig. 4. The model predicts the observed relative masses of fines at the column sections with RMSE values of 0.0119, 0.0152 and 0.00902. This formulation closes the gap in predicting soil permeability reductions at discrete depths and the overall decrease in infiltration capacity.

Permeability reductions

The previous section described the formulation for the quantitative assessment of the vertical distribution of fines. Estimating the volume of intruded and deposited particles at discrete depths improves models that predict the evolution of soil infiltration capacity. When particles intrude into the soil matrix, the media surface area to volume ratio is increased, and the soil porosity is reduced, leading to a decrease in soil permeability. Most clogging studies conducted for engineering purposes (Alem et al. 2013; Blazejewski and Murat-Blazejewska 1997; Federico 2017; Herzig et al. 1970; Locke et al. 2001; Reddi et al. 2000) rely on the Kozeny-Carman equation (Carman 1937; Kozeny 1927) to compute the reduction in soil permeability. The model that provided a greater fit to the flow decrease observed from the column experiments is the one proposed by Alem et al. (2013):

$$\frac{k(z,t)}{k_0} = \frac{n(z,t)^3}{n_0^3}\frac{\left(1+n_0\right)^2}{\left(1+n(z,t)\right)^2}\frac{S_0^2}{S(z,t)^2}\left(\frac{T_0}{T(z,t)}\right)^2 \tag{14}$$

with n the porosity, S the specific surface area per unit volume of particles (1/cm) and T the tortuosity (cm/cm). For more details on Eq. 14, please refer to Alem et al. (2013).

The physical characteristics of the porous media evolve along with the volume of particles intruded, expressed per unit of porous media volume, as:

$$\sigma(z,t) = \frac{M_{\text{tot}}(t)}{Al\rho_s} f(z) \tag{15}$$

with $M_{\text{tot}}(t)$ the total infiltrated particles up to time t, $f(z)$ from Eqs. (8) and (13), ρ_s the particles' specific density (g/cm^3), A the infiltrating area (cm) and l the unit depth (cm). The decrease in porosity of the porous media follows the formulation from Herzig et al. (1970):

$$\frac{n(z,t)}{n_0} = 1 - \frac{\beta\sigma(z,t)}{n_0} \tag{16}$$

with β the inverse of the compaction factor of retained particles $\beta = 1/(1-n_d)$. The porosity of the retained fines n_d is derived from the average densities of deposited particles (Alem et al. 2013; Boller and Kavanaugh 1995).

For the total infiltrated suspension with a concentration of 1 g/L of suspended particles, the recorded outflow rates at the column were converted into total permeability reduction given the constant gradient. The decrease in soil permeability modelled according to the Kozeny-Carman equation (Eq. 14) explains the observed total variation in permeability at the column, as shown in Fig. 5.

The decrease in soil permeability shown in Fig. 5 has been modelled from the estimated vertical distribution of fines based on the geometric ratios d_{50}/D_{50} (Eqs. 8 and 13). The limit at which particles start accumulating superficially, forming the external cake, is computed from Eq. (12). For the reduction in permeability at discrete depths (Eq. 14), the total reduction in permeability in the internal clogging conditions (Fig. 5a) is:

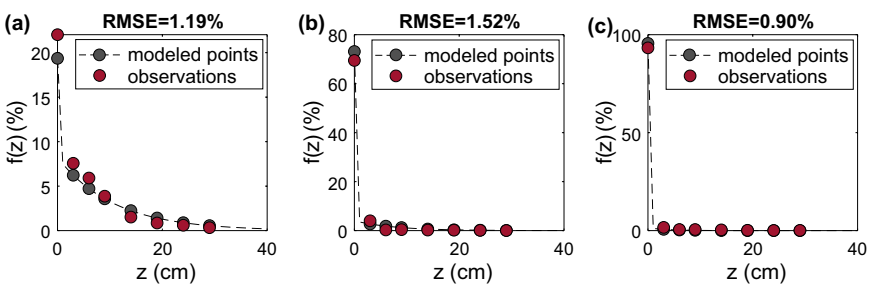

Fig. 4 The clogging profiles from Eq. (13) under superficial clogging conditions are tested for the observed relative mass of fines (%) deposited over depth for the experiments of This study (2022) **a** sand 0.4-0.8 mm, **b** sand 0.2-0.7 mm and **c** sand 0.1-0.4 mm

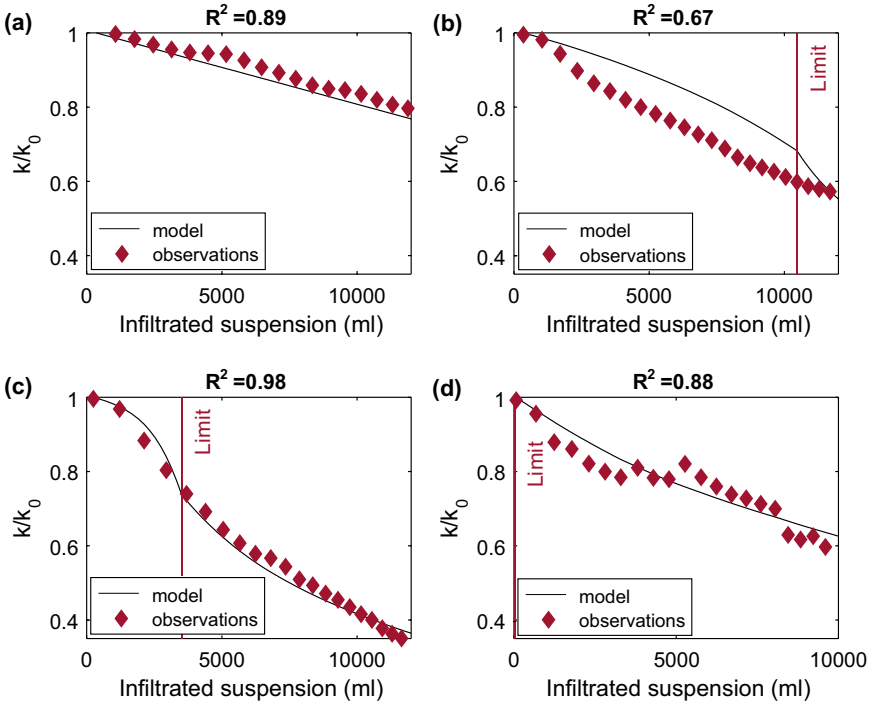

Fig. 5 The model prediction from the Kozeny-Carman equation for permeability decrease k/k_0 compared with the observed reduction in permeability from the column outflow during the experiments of This study (2022): **a** sand 0.5–1 mm, **b** sand 0.4–0.8 mm and **c** sand 0.2–0.7 mm, **d** sand 0.1–0.4 mm. The red vertical line indicates the retention limit at which the external cake starts forming

$$\frac{k_{\text{tot}}(t)}{k_0} = \frac{L}{\sum_{z=0}^{L} \frac{l}{\frac{k(z,t)}{k_0}}} \tag{17}$$

with L the total length of the porous media and $k(z,t)/k_0$ the permeability's reduction per unit depth l.

In superficial clogging conditions (Fig. 5b,c,d), the total decrease in permeability is computed by accounting for external cake layering:

$$\frac{k_{\text{tot}}(t)}{k_0} = \frac{L + L_{\text{cake}}(t)}{\sum_{z=0}^{L} \frac{l}{\frac{k(z,t)}{k_0}} + \frac{L_{\text{cake}}(t)}{\frac{k_{\text{cake}}}{k_{z=0,\text{limit}}}}} \tag{18}$$

with $L_{\text{cake}}(t)$ being the thickness of the external cake, $k_{z=0,\text{limit}}$ the permeability of the porous media at the surface when $M_{z=0,\text{limit}}$ is met, and k_{cake} a calibrated parameter associated with the permeability of the fines depositing superficially. For all three experiments under surface clogging conditions (Fig. 5b,c,d) one unique calibrated value was set: $k_{\text{cake}} = 0.0003$ (cm/s).

The previously shown equations can be implemented to develop a model for physical clogging at MAR sites. The profile of the damage and the time for the facility to be clogged can be estimated from parameters collected in the field. The application of these findings is illustrated in the next section, in order to estimate the evolution in infiltration rates due to the input of fines at a MAR field site.

MAR application

This section showcases how MAR operators can implement the findings in section 'Results' in order to assess the site's vulnerability to clogging. The clogging depth and the evolution over time in infiltration rates can be deduced from the hydraulic loading of several flooding events. In this scenario analysis, no maintenance is performed at the MAR site. The Loria infiltration test site is presented with the sole intention of highlighting the applicability of the results. The site is situated approximately 15 km north of Cittadella in the Province of Padua, Italy, within the catchment area of the river Brenta, and the source for infiltration is flood water of the Lugana stream. The long-term infiltration capacity of the site is susceptible to physical clogging due to eroded clays reaching the pond during flood events. This MAR scheme does not comprise a sedimentation pond; thus, the transported clay is deposited as a soil overlay. For further information on the site, see P.A.T.I. (2013), Fontana et al. (2014) and Tippelt (2015). For the Tippelt (2015) study, four representative soil samples were collected from the basin and analysed, observing the thickness of the clayey overlay, soil humidity, vegetation, and coarse gravels in the overlay. The respective sampling locations are shown in Fig. 6. The provided information is used in this study to assess the risk of clogging in the MAR basin.

The grain size distribution of the four soil/sediment samples is reported in Fig. 7. The samples were collected from the basin's top layer, up to a depth of 30 cm. The particle size distribution of the finer material is plotted as a separate curve, and the median diameter of 12.33 µm is indicated with a *vertical line*. The finer fraction is differentiated from the sediment matrix, considering the suspended load comprising mainly clay and silt particles. It is here assumed that the analysed fines from the soil samples have likely close origins to the material transported by the river, given the similar granulometric curves in all the finer fractions of the soil samples. The same finer-particle size distribution is thus assumed for the incoming fines from the flood events.

The grain distributions (see Fig. 7) for the sampled sediments allow for quantification of the geometric ratios (d_{50}/D_{50}). For the depositing fines of flood origin, the gradation of the fines is determined by the input of sediments reaching the basin and the expected vertical distribution $f(z)$ from Eqs. (8) and (13). Time series of inflows to the basin are not available for the site, as the pond is filled at irregular intervals during flood events through an adjustable inlet. Assuming the basin reaches its total capacity of 40,000 m^3 for each flood event, and given the concentration of suspended solids C (mg/L), $M_{tot} = V_{basin}\ C$ is the total mass of fines (g) in input to the basin for each flood event. Therefore, from a new input of fines, the expected retained mass with depth per unit volume of porous media (g/cm^3) is expressed for each sediment type as in Eq. (15):

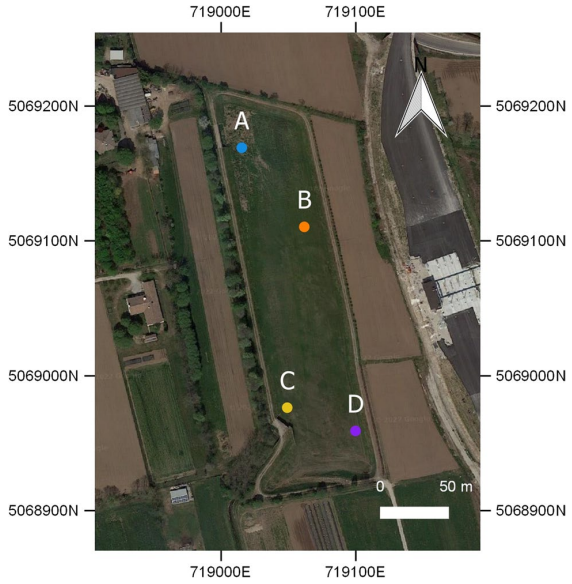

Fig. 6 Sampling spots in the Loria infiltration basin (Italy). The external grid shows the easting and northing UTM-coordinates (WGS 84) in meters

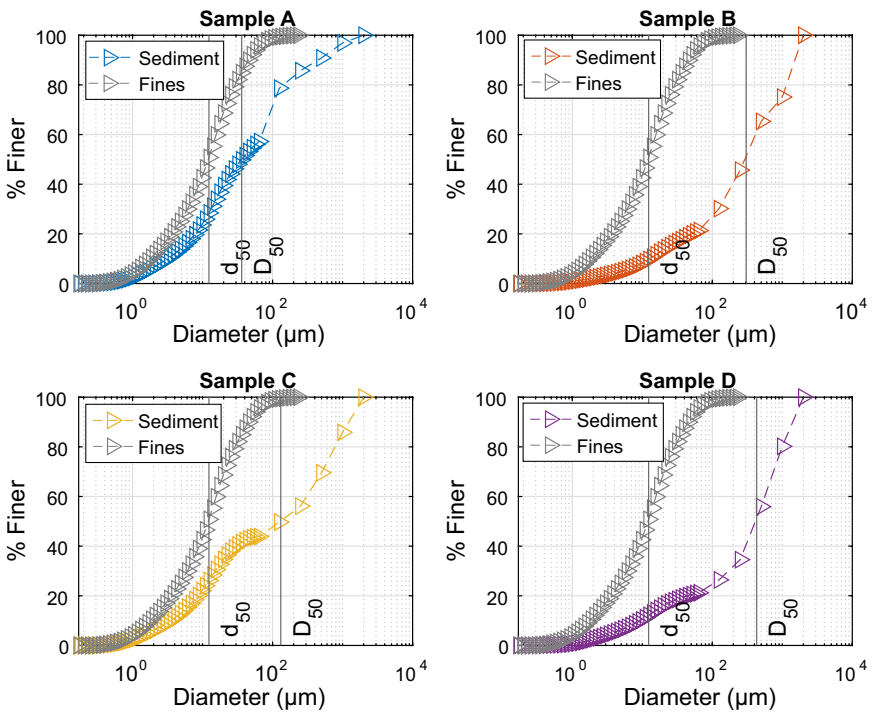

Fig. 7 Comparison of fines size distribution and total grain size distributions from the sampled spots A, B, C, D. Median values of the fines size (d_{50}) and the total grain size (D_{50}) are marked with the vertical lines

$$\sigma(z,t) = \frac{M_{tot}(t)}{A_{basin} l \rho_s} f(z) \quad (19)$$

with A_{basin} the area of the infiltrating basin (cm^2) and l the 1-cm unit depth. Tippelt (2015) reported a peak concentration of 102 mg/L of suspended solids in the river water. For the vulnerability analysis, it is assumed that the peak concentration of fines reaches the basin at each flood event and there is a homogenous infiltration along the basin. For every input of fines following the flooding event, the porous media's initial conditions are updated, namely the porosity, the surface area and tortuosity, according to Eq. (14). The initial porosity, in the absence of field measurements, is here estimated from the coefficient of uniformity (U) through an empirical relationship (Vukovic and Soro 1992):

$$n = 0.255\left(1 + 0.83^{U}\right) \quad (20)$$

The initial soil permeability for the native sediments at the sampling locations is derived from the grain size distribution with the Hazen (1893) formula, and a value of permeability of 10^{-8} (cm/s) is considered for the k_{cake} of the clayey material, according to Fitts (2002).

The reductions in soil permeability for the fines material input are expressed in terms of the ratio k/k_0. Figure 8 shows the permeability reductions with soil depth over an accumulation of fines for 50 flooding events.

Applying the Darcy law and a unitary gradient for the downward flow controlled by gravity, the infiltration rate is directly coupled to the decline in soil permeability. The expected reductions in infiltration rate considering the 50 flood events are shown for the four sampling locations in Fig. 9.

Sample A, collected in the proximity of the basin inlet, presents conditions for superficial clogging due to the high presence of fines already in the soil matrix. It is estimated that 95% of new incoming particles are retained superficially from the vertical distribution function. The soil would reach an 83% reduction of the initial infiltration rates after 50 flood events. Similarly, location C, close to the outlet, would exhibit a reduction of 86%. In the north area close to the inlet and along the shortest path to the outlet, soil treatment techniques should be applied to the first upper 5 cm, with frequent scraping schedules to remove the external cake. In location B, in the central part of the basin, the clogging superficial layer would start forming after 37 flooding

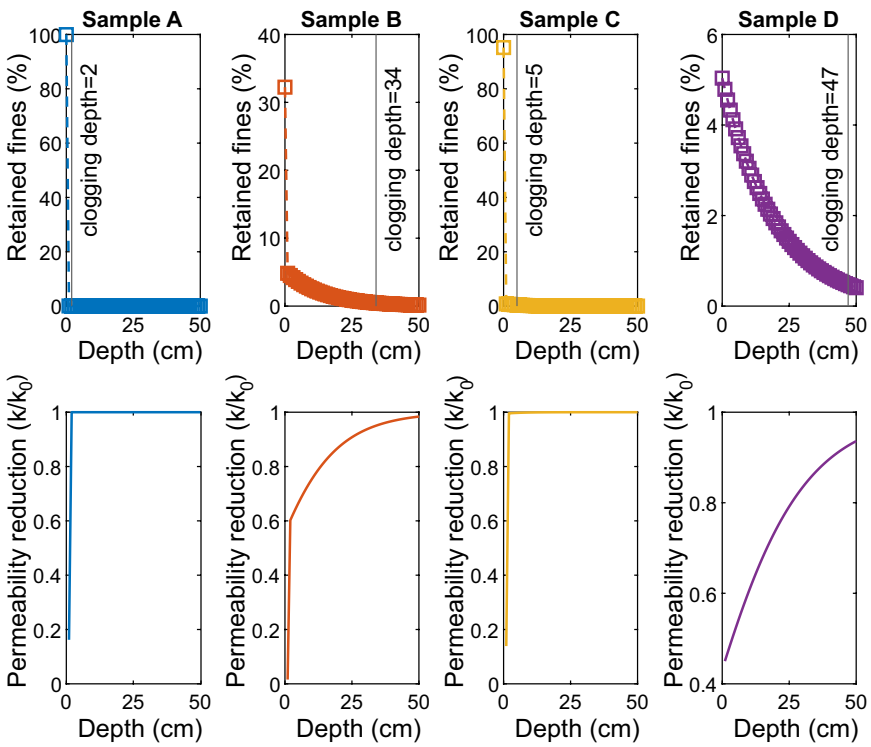

Fig. 8 Vertical profiles for the retained fines and reduction in soil permeability after 50 flood events. The vertical line is the clogging depth in cm (Eq. 7). Please note the different scales on the y-axes

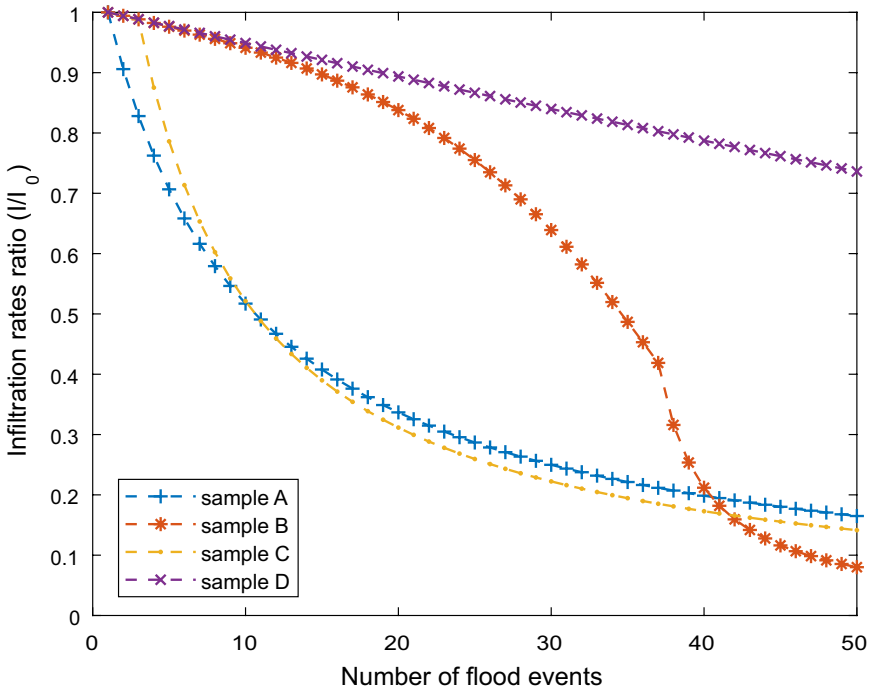

Fig. 9 Predictions in performance of the total infiltration rates, for several potential flood events, at the four sampling locations

events, drastically reducing the infiltration rates. On the other side, sample D, located in the southeast part of the basin, exhibits internal clogging conditions. With 5% of the fines retained superficially, after 50 flooding events, the soil would reach a 26% reduction in infiltration rates; however, further MAR operations could require treating a portion of soil up to a depth of 47 cm. Through the use of site characterisation, soil treatment techniques can be scheduled and programmed in basin zones based on the different lithological characteristics.

Discussion

Predictions of the decline of infiltration rates for MAR sites due to physical clogging are improved by the computation of changes in the soil granulometry and porosity at discretised depths. The main challenge was the quantitative assessment of fines over depth during water recharge. Establishing a generally valid model for the vertical distribution of intrusive fines based on the primary sediment matrix and particles' characteristics leads to a solution suitable for applied hydrogeology purposes. Comparison of experimental results conducted on different column experiments, applicable to MAR conditions, was possible assuming the relative mass of particles to follow an exponential decay with depth. The resulting parameterisation showed that under internal clogging conditions, the percentage of particles retained at the surface increases linearly with increasing ratio of infiltrated particles of median diameter to grains of median diameter. The exponential decay rate correlates to the amount of fines captured superficially, indicating data from the multiple column experiments to be consistent. Despite the existence of several column experiments for deep bed filtration, the empirical models developed for filter design do not reflect the infiltration basins' operating conditions. Most of these studies provide the residual concentrations in the effluent for colloid transport (diameter size <1 μm) in constant flow rate conditions. Filtration studies often lack information on the retention profile within the porous media. This is indeed a limitation in understanding the straining and deposition processes occurring within the porous media. In recharge basin construction, sandy soils are preferred due to typical infiltration rates being in the range of 0.3–3 m/day (Bouwer 1999; Dillon and Arshad 2016). The interval of interest for this analysis was within a geometric ratio d_{50}/D_{50} of 0.001–0.25. These two reference values correspond to the extreme cases of clay (lower size range 0.98 μm) infiltrating into coarse sand (upper size range 1,000 μm), and to the case of silt (upper size range 62.5 μm) infiltrating into medium sand (lower size range 250 μm), according to the Wentworth scale. In comparison to the profiles under internal clogging conditions from the literature, the additional performed experiments verified that the external cake formation leads to a discrepancy in the relative amount of particles accumulating at the surface. The vertical distribution of fines was

corrected in superficial clogging conditions introducing a retention mass limit at the surface, after which particles accumulate at the top. This solution follows considerations on pore structure concerning median grain diameters and is an approximation for sandy porous media; therefore, there might be limitations for soils with different sediment mixing and compaction. In this regard, the column experiments were performed with porosity values similar to the ones from the literature studies for the same grain size ranges. Although the porous media's compaction likely affects the vertical distribution of fines, the data from the literature provided a negative correlation coefficient ($\rho = -0.0314$) between the porosity and the relative mass at the water–sediment interface. In contrast, this work confirms that straining mechanisms are strongly controlled by the ratio of the diameter size of the suspended particles to the grain diameter size of the porous media. The illustrated findings agree with the qualitative categorisation of Khilar and Fogler (1998) for plugging behaviour due to blocking, bridging and piping, based on previous clogging analysis (Gruesbeck and Collins 1982; Herzig et al. 1970; Muecke 1979). The categorisation is based on ratios determined by the size of fines d_p to the size of the pore constriction d_0. Considering $d_p = d_{50}$ and the average pore diameter (μm) as $d_0 = 0.235\ D_{50}$ valid for sands (Mahmoodlu et al. 2016), the results are consistent with the formation of the external cake for $\frac{d_p}{d_0} > 1$, the occurrence of multiparticle blocking between 0.1–0.01, and piping below 0.01 (Kanti Sen and Khilar 2006). Other authors employ the ratio of the size of the suspended particles to the media size as critical factors in particle straining and reduction in permeability. The results are in good agreement with the threshold of $d_{50}/D_{50} = 0.005$ for initial straining of particles (Bradford et al. 2003; Zaidi et al. 2020) and with $d_{50}/D_{50} = 0.05$ for significant straining (Bradford et al. 2002; Sakthivadivel 1969). It is important to point out that all the selected studies for the analysis measured the d_{50} via laser diffraction. For comparison, the fines' median particle diameter should not be measured with sedimentation methods (Buurman et al. 2001; Di Stefano et al. 2010; Fisher et al. 2017); further discussion is needed to relate the effect of the hydrodynamic conditions in shaping the fines fraction profiles. At lower flow rates, particles would tend to form bridges at pore constrictions, while higher drag forces would break apart these bridges, and particles would be transported deeper into the porous media (Khilar and Fogler 1998). Since this study does not address filtration under high water flow injection, the analysis focuses on comparing the porous media's ability in particle capture, given only the information on the particles' and porous media's median size characteristics. Nevertheless, in constant head conditions, it should be verified whether the median grain diameter D_{50} controls the effect of the hydraulic conductivity and flow rates on the clogging profiles, confirming the geometric ratio to be the primary predictor. Another point of discussion is whether the particles' concentration in the suspension affects the plugging phenomena, thus altering the retention profile itself. The column experiments of Alem et al. (2014) under constant head conditions were performed for four different concentrations of fines within a range of 0.25–1.5 g/L. By using the same data analysis methods as in section Data analysis', the datasets returned a standard deviation for the $f_{z=0}$ parameter of 0.13%. Considering the concentrations of the experiments summarised in Table 1, the validity of the model reported here is limited to the investigated range of 0.1–1 g/L, which already represents a TSS range of concern in MAR site design. Thus, the results of this work in assessing the vertical distribution of intrusive fines appear to be valid for a broad range of MAR applications. Finally, the field application should not be regarded as a field validation. The sole intention is to clearly show the relevance of the work in evaluating the vulnerability to physical clogging from data commonly collected during site characterizations. In the field application described in section 'MAR application', data are from a site characterization performed in 2015. Additional field measurements of initial soil porosity and hydraulic conductivity should be integrated when possible. Especially, the value of the k_{cake} parameter has a certain relevance in reducing the total permeability of the native sediment, in relation to the original k_0. The model is meant to be applied to determine, in a quick and cost-effective manner, areas of concern to deduce maintenance schemes.

Conclusion

In summary, this work contributes to the research on predicting physical clogging behaviour through an overall model transferable to multiple MAR sites. The novelty of this approach is to not rely on a specific set of parameters determined over a single column experiment, but rather on data easily collectable at the MAR field site. During site characterisation, representative soil samples should be collected, annotating the presence of vertical lithologic discontinuities. The fines are expected to accumulate differently in correspondence with these heterogeneities with distinct retention profiles. A linear relationship defines the expected maximum fraction of fines at the infiltration medium surface and the decrease in particle deposition with depth as a function of the ratio of the infiltrating particle size to the median grain size. When the mass of intruding fines exceeds the retention limit at the surface, this accounts for external cake formation. This mathematical formula can be integrated into clogging models jointly with data on influent suspended solids concentration, frequency of recharge cycles and hydraulic loads, overcoming the gap in estimating

the reductions in infiltration rate. The results for the single soil samples could be extended to the basin area and integrated within an infiltration model, not excluding the fact that more fines would be transported in areas with higher permeability during the infiltration process. Unlike previous studies, the depth-based prediction facilitates the estimation of the maximum operation duration and maintenance costs to remove the soil-clogged layer. Providing information on the expected thickness of the clogged layer makes it possible to address operations of soil replacement and the necessary equipment to restore the infiltration rates for the basin over time. During preliminary analysis, MAR practitioners can use this study's findings to address the risks of physical clogging in multiple infiltration sites.

Acknowledgements The authors express their gratitude to the associate editors and reviewers for their constructive comments contributing to the improvement of the manuscript.

Funding Open Access funding enabled and organized by Projekt DEAL. The research leading to these results has received funding from the European Union's Horizon 2020 research and innovation programme under the Marie Skłodowska-Curie grant agreement No. 814066 (Managed Aquifer Recharge Solutions Training Network - MARSoluT).

Declarations

Conflicts of interest On behalf of all authors, the corresponding author states that there is no conflict of interest.

References

Ahfir ND, Hammadi A, Alem A, Wang H, Le Bras G, Ouahbi T (2017) Porous media grain size distribution and hydrodynamic forces effects on transport and deposition of suspended particles. J Environ Sci (China) 53:161–172. https://doi.org/10.1016/j.jes.2016.01.032

Alem A, Ahfir N-D, Elkawafi A, Wang H (2014) Hydraulic operating conditions and particle concentration effects on physical clogging of a porous medium. Transp Porous Media 106(2):303–321. https://doi.org/10.1007/s11242-014-0402-8

Alem A, Elkawafi A, Ahfir N-D, Wang H (2013) Filtration of kaolinite particles in a saturated porous medium: hydrodynamic effects. Hydrogeol J 21(3):573–586. https://doi.org/10.1007/s10040-012-0948-x

Barquero F, Fichtner T, Stefan C (2019) Methods of in situ assessment of infiltration rate reduction in groundwater recharge basins. Water 11(4). https://doi.org/10.3390/w11040784

Becker MW, Bauer B, Hutchinson A (2013) Measuring Artificial Recharge with Fiber Optic Distributed Temperature Sensing. Groundwater 51(5):670–678. https://doi.org/10.1111/j.1745-6584.2012.01006.x

Bennion DB, Bennion DW, Thomas FB, and Bietz RF (1998) Injection water quality: a key factor to successful waterflooding. 37(6). https://doi.org/10.2118/98-06-06

Blazejewski R, Murat-Blazejewska S (1997) Soil clogging phenomena in constructed wetlands with subsurface flow. Water Sci Technol 35(5):183–188. https://doi.org/10.1016/S0273-1223(97)00067-X

Boller MA, Kavanaugh MC (1995) Particle characteristics and headloss increase in granular media filtration. Water Res 29(4):1139–1149. https://doi.org/10.1016/0043-1354(94)00256-7

Bouwer H (1999) Artificial recharge of groundwater: systems, design, and management, chap 24. In: Hydraulic design handbook. Engineering 360, Albany, NY, 44 pp

Bouwer H (2002) Artificial recharge of groundwater: hydrogeology and engineering. Hydrogeol J 10(1):121–142. https://doi.org/10.1007/s10040-001-0182-4

Bradford SA, Simunek J, Bettahar M, Van Genuchten MT, Yates SR (2003) Modeling colloid attachment, straining, and exclusion in saturated porous media. Environ Sci Technol 37(10):2242. https://doi.org/10.1021/es025899u

Bradford SA, Yates SR, Bettahar M, Simunek J (2002) Physical factors affecting the transport and fate of colloids in saturated porous media. Water Resour Res 38(12):63–1–63–12. https://doi.org/10.1029/2002WR001340

Buurman P, Pape T, Reijneveld JA, De Jong F, Van Gelder E (2001) Laser-diffraction and pipette-method grain sizing of Dutch sediments: correlations for fine fractions of marine, fluvial, and loess samples. Neth J Geosci 80(2):49–57. http://www.njgonline.nl/publish/articles/000035/article.pdf

Carman PC (1937) Fluid flow through granular beds. Trans Inst Chem Eng 15:150–166

Cui Y, Wooster JK, Baker PF, Dusterhoff SR, Sklar LS, Dietrich WE (2008) Theory of fine sediment infiltration into immobile gravel bed. J Hydraul Eng 134(10):1421–1429. https://doi.org/10.1061/(ASCE)0733-9429(2008)134:10(1421)

De Carlo L, Caputo MC, Masciale R, Vurro M, Portoghese I (2020) Monitoring the drainage efficiency of infiltration trenches in fractured and karstified limestone via time-lapse hydrogeophysical approach. Water 12(7):2009. https://doi.org/10.3390/w12072009

Di Stefano C, Ferro V, Mirabile S (2010) Comparison between grain-size analyses using laser diffraction and sedimentation methods. Biosyst Eng 106(2):205–215. https://doi.org/10.1016/j.biosystemseng.2010.03.013

Dillon P (2002) Banking of stormwater, reclaimed water and potable water in aquifers. In: Proc. of the International Groundwater Conference on Sustainable Development and Management of Groundwater Resources in Semi-Arid Region with Special Reference to Hard Rocks: IGC-2002, Dindigul, Tamil Nadu, India, 20–22 February 2002 (pp. 71–80). AA Balkema Publishers.

Dillon P, Arshad M (2016) Managed aquifer recharge in integrated water resource management. In: Jakeman AJ, Barreteau O, Hunt RJ, Rinaudo J-D, Ross A (eds) Integrated groundwater management: concepts, approaches and challenges. Springer, Cham, Switzerland, pp 435–452

Dillon P, Stuyfzand P, Grischek T, Lluria M, Pyne RDG, Jain RC, Bear J, Schwarz J, Wang W, Fernandez E, Stefan C, Pettenati M, van der Gun J, Sprenger C, Massmann G, Scanlon BR, Xanke J, Jokela P, Zheng Y et al (2018) Sixty years of global progress in

managed aquifer recharge. Hydrogeol J 27(1):1–30. https://doi.org/10.1007/s10040-018-1841-z
Dillon P, Vanderzalm J, Page D, Barry K, Gonzalez D, Muthukaruppan M, Hudson M (2016) Analysis of ASR clogging investigations at three Australian ASR sites in a Bayesian context. Water 8(10):442 https://www.mdpi.com/2073-4441/8/10/442
Du X, Ye X, Zhang X (2018) Clogging of saturated porous media by silt-sized suspended solids under varying physical conditions during managed aquifer recharge. Hydrol Process 32(14):2254–2262. https://doi.org/10.1002/hyp.13162
Federico F (2017) Particle migration phenomena related to hydromechanical effects at contact between different materials in embankment dams. In: Sakellariou M (ed.) Granular Materials. IntechOpen. https://doi.org/10.5772/67785
Fisher P, Aumann C, Chia K, O'Halloran N, Chandra S (2017) Adequacy of laser diffraction for soil particle size analysis. PLoS One 12(5):e0176510. https://doi.org/10.1371/journal.pone.0176510
Fitts CR (2002) Groundwater science. Elsevier Science Ltd., Academic Press, 450 pp.
Fontana A, Mozzi P, Marchetti M (2014) Alluvial fans and megafans along the southern side of the Alps. Sediment Geol 301:150–171. https://doi.org/10.1016/j.sedgeo.2013.09.003
Gibson S, Abraham D, Heath R, Schoellhamer D (2009) Vertical gradational variability of fines deposited in a gravel framework. Sedimentology 56(3):661–676. https://doi.org/10.1111/j.1365-3091.2008.00991.x
Glass J, Šimůnek J, Stefan C (2020) Scaling factors in HYDRUS to simulate a reduction in hydraulic conductivity during infiltration from recharge wells and infiltration basins. Vadose Zone J 19(1):e20027. https://doi.org/10.1002/vzj2.20027
Goss D, Smith S, Stewart B, Jones O (1973) Fate of suspended sediment during basin recharge. Water Resour Res 9(3):668–675. https://doi.org/10.1029/WR009i003p00668
Gruesbeck C, Collins R (1982) Entrainment and deposition of fine particles in porous media. SPE J 22(06):847–856. https://doi.org/10.2118/8430-PA
Hazen A (1893) Some physical properties of sands and gravels, with special reference to their use in filtration. In: 24th Annual Rep., Massachusetts State Board of Health, Pub. Doc. No. 34: 539–556. Boston, MA
Herzig JP, Leclerc DM, Goff PL (1970) Flow of suspensions through porous media: application to deep filtration. Ind Eng Chem 62(5):8–35. https://doi.org/10.1021/ie50725a003
Huston DL, Fox JF (2015) Clogging of fine sediment within gravel substrates: dimensional analysis and macroanalysis of experiments in hydraulic flumes. J Hydraul Eng 141(8). https://doi.org/10.1061/(asce)hy.1943-7900.0001015
Hutchison A, Milczarek M, Banerjee M (2013) Clogging phenomena related to surface water recharge facilities. In: Martin R (ed.) Clogging issues associated with managed aquifer recharge methods. IAH Commission on Managing Aquifer Recharge. 95–106. https://recharge.iah.org/files/2015/03/Clogging_Monograph.pdf
Kanti Sen T, Khilar KC (2006) Review on subsurface colloids and colloid-associated contaminant transport in saturated porous media. Adv Colloid Interf Sci 119(2–3):71–96. https://doi.org/10.1016/j.cis.2005.09.001
Khilar KC, Fogler HS (1998) Migration of fines in porous media. Kluwer Academic Publishers, Dordrecht, The Netherlands
Kozeny J (1927) Uber kapillare Leitung der Wasser in Boden [About capillary conduction of water in soil]. Royal Academy of Science, Vienna Proc Class I 136:271–306
Locke M, Indraratna B, Adikari G (2001) Time-dependent particle transport through granular filters. J Geotech Geoenviron 127(6):521–529. https://doi.org/10.1061/(ASCE)1090-0241(2001)127:6(521)
Mahmoodlu MG, Raoof A, Sweijen T, Van Genuchten M (2016) Effects of sand compaction and mixing on pore structure and the unsaturated soil hydraulic properties. Vadose Zone J 15. https://doi.org/10.2136/vzj2015.10.0136
Martin R (ed.) (2013) Clogging issues associated with managed aquifer recharge methods. IAH Commission on Managing Aquifer Recharge. https://recharge.iah.org/files/2015/03/Clogging_Monograph.pdf
Mawer C, Parsekian A, Pidlisecky A, Knight R (2016) Characterizing heterogeneity in infiltration rates during managed aquifer recharge. Ground Water 54(6):818–829. https://doi.org/10.1111/gwat.12423
McDowell-Boyer LM, Hunt JR, Sitar N (1986) Particle transport through porous media. Water Resour Res 22(13):1901–1921. https://doi.org/10.1029/WR022i013p01901
Muecke TW (1979) Formation fines and factors controlling their movement in porous media. J Petrol Technol 31(02):144–150. https://doi.org/10.2118/7007-PA
Nenna V, Pidlisecky A, Knight R (2014) Monitoring managed aquifer recharge with electrical resistivity probes. Interpretation 2(4):T155–T166. https://doi.org/10.1190/INT-2013-0192.1
Okubo T, Matsumoto J (1983) Biological clogging of sand and changes of organic constituents during artificial recharge. Water Res 17(7):813–821. https://doi.org/10.1016/0043-1354(83)90077-5
P.A.T.I. (2013) Relazione geologica ed idrogeologica PATI Loria e Castello di Godego [Geological and hydrogeological relationship of PATI Loria and Castello di Godego]. http://www.prc.loria.geonweb.com/documents/elaborati_QC/Relazione%20geologica%20ed%20idrogeologica.pdf. Accessed December 2022
Pyne RDG (1995) Groundwater Recharge and Wells: A Guide to Aquifer Storage Recovery (1st ed.). CRC Press. https://doi.org/10.1201/9780203719718
Racz AJ, Fisher AT, Schmidt CM, Lockwood BS, Los HM (2012) Spatial and temporal infiltration dynamics during managed aquifer recharge. Ground Water 50(4):562–570. https://doi.org/10.1111/j.1745-6584.2011.00875.x
Reddi LN, Ming X, Hajra MG, Lee IM (2000) Permeability reduction of soil filters due to physical clogging. J Geotech Geoenviron 126(3):236–246. https://doi.org/10.1061/(ASCE)1090-0241(2000)126:3(236)
Ross A, Hasnain S (2018) Factors affecting the cost of managed aquifer recharge (MAR) schemes. Sustain Water Resources Manag 4(2):179–190. https://doi.org/10.1007/s40899-017-0210-8
Sakthivadivel R (1969) Clogging of a granular porous medium by sediment. Rep. HEL 15–7, 106 pp., Hydraul. Eng. Lab., Univ. of Calif.,Berkeley, CA
Sprenger C, Hartog N, Hernández M, Vilanova E, Grützmacher G, Scheibler F, Hannappel S (2017) Inventory of managed aquifer recharge sites in Europe: historical development, current situation and perspectives. Hydrogeol J 25(6):1909–1922. https://doi.org/10.1007/s10040-017-1554-8
Tang Y, Yao X, Chen Y, Zhou Y, Zhu DZ, Zhang Y, Zhang T, Peng Y (2020) Experiment research on physical clogging mechanism in the porous media and its impact on permeability. Granul Matter 22(2). https://doi.org/10.1007/s10035-020-1001-8
Tippelt T (2015) Investigation of the influence of fine sediment input during flooding events on the long-term infiltration capacity of the Loria infiltration basin (Italy). MSc Thesis, Institute of Geophysics and Geology, Leipzig University, Leipzig, Germany
Torkzaban S, Bradford SA, Vanderzalm JL, Patterson BM, Harris B, Prommer H (2015) Colloid release and clogging in porous media: effects of solution ionic strength and flow velocity. J Contam Hydrol 181:161–171. https://doi.org/10.1016/j.jconhyd.2015.06.005
Ulusoy İ, Dahlin T, Bergman B (2015) Time-lapse electrical resistivity tomography of a water infiltration test on Johannishus Esker, Sweden. Hydrogeol J 23(3):551–566. https://doi.org/10.1007/s10040-014-1221-2

Vukovic M, Soro A (1992) Determination of hydraulic conductivity of porous media from grain-size composition. Water Resources Publications, Littleton, CO

Wang Z, Du X, Yang Y, Ye X (2012) Surface clogging process modeling of suspended solids during urban stormwater aquifer recharge. J Environ Sci 24(8):1418–1424. https://doi.org/10.1016/s1001-0742(11)60961-3

Xie Y, Wang Y, Huo M, Geng Z, Fan W (2020) Risk of physical clogging induced by low-density suspended particles during managed aquifer recharge with reclaimed water: evidences from laboratory experiments and numerical modeling. Environ Res 186:109527. https://doi.org/10.1016/j.envres.2020.109527

Zaidi M, Ahfir N-D, Alem A, El Mansouri B, Wang H, Taibi S, Duchemin B, Merzouk A (2020) Assessment of clogging of managed aquifer recharge in a semi-arid region. Sci Total Environ 730:139107. https://doi.org/10.1016/j.scitotenv.2020.139107

Zhang H, Xu Y, Kanyerere T (2020) A review of the managed aquifer recharge: historical development, current situation and perspectives. Phys Chem Earth, parts A/B/C, 118–119:102887. https://doi.org/10.1016/j.pce.2020.102887

Advances in Water Resources 177 (2023) 104462

Contents lists available at ScienceDirect

Advances in Water Resources

journal homepage: www.elsevier.com/locate/advwatres

Understanding and predicting physical clogging at managed aquifer recharge systems: A field-based modeling approach

Maria Chiara Lippera [a,d,*], Ulrike Werban [d], Rudy Rossetto [c], Thomas Vienken [b,d]

[a] Technical University of Munich, TUM Campus Straubing for Biotechnology and Sustainability, Straubing, Germany
[b] Weihenstephan-Triesdorf University of Applied Sciences, TUM Campus Straubing for Biotechnology and Sustainability, Straubing, Germany
[c] Scuola Superiore Sant'Anna, Crop Science Research Center, Pisa, Italy
[d] UFZ - Helmholtz Centre for Environmental Research, Leipzig, Germany

ARTICLE INFO

Keywords:
Managed aquifer recharge
Infiltration basin
Hydraulic conductivity
Physical clogging
Erosion

ABSTRACT

Managed aquifer recharge (MAR) techniques are in demand to cope with water scarcity challenges posed by climate change and groundwater overexploitation. One of the long-lasting technical issues associated with MAR systems is physical clogging. The intrusion and deposition of external fines during water recharge reduce the infiltration capacity of the site over time. Operation and maintenance (O&M) costs are experienced directly at the site to restore the original efficiency of infiltration rates. Thus, investors need reliable estimations of the risk of clogging during the planning of the site. As a rule, in MAR design, the main parameter of concern for physical clogging is the total suspended solids (TSS), and most clogging models rely on experiment calibrations in 1D sand columns. However, secondary processes can control the development and spatial distribution of physical clogging in field conditions. The proposed work aims to detect key clogging factors directly in the field and to model these processes for reproducibility at other sites. The fieldwork is conducted at the two-stage infiltration basin in Suvereto (Tuscany, Italy). Spatial factors are included in the analysis (i.e. basin topography) to explain clogging patterns in the field altered by erosion processes. The observed clogging profiles at two sampled locations exhibiting clogging are replicated by a mathematical model. Based on the computation of annual erosion rates in the pond and fines' redistribution, the exceeding fines' contents over depth are validated with an RMSE of 2.53% and 12.53%. The infiltration capacity of the site is estimated to reach a stable value of 90% of the initial infiltration capacity over 20 years, given the Suvereto basin features. The model's parameterisation from field measurements represents a great advantage over existing clogging models due to its transferability to other MAR sites. The assessment of the risk of clogging supported by field characterization and numerical modelling is cost-effective and assists the deduction of O&M schemes for MAR sites.

1. Introduction

Climate change and increasing groundwater withdrawals compromise the sustainability of aquifer systems (Treidel et al., 2011; Wu et al., 2020), intended as the groundwater availability for future beneficial use avoiding environmental or socio-economic implications (Alley et al., 1999). In this context, managed aquifer recharge (MAR) techniques are promising in combating groundwater depletion and increasing groundwater availability (Dillon et al., 2018; Sprenger et al., 2017; Zhang et al., 2020). MAR sites' design and management aim to increase these technologies' operational efficiency. In this regard, clogging, the reduction of recharge rates in space and time during MAR operations, is typically the key constraint in MAR facility performance (Bouwer, 2002; Dillon and Arshad, 2016; Pyne, 2005). The processes responsible for clogging are mainly physical, biological, chemical, and mechanical (Bouwer, 1996; Jeong et al., 2018; Pyne, 2005; Rinck-Pfeiffer et al., 2000). Physical clogging results in the accumulation of organic and inorganic suspended solids and the migration of interstitial fines (Bennion et al., 1998; Goss et al., 1973; Wang et al., 2012). The growth of microorganisms and bio-flocs accumulation cause biological clogging (Baveye et al., 1998; Kim et al., 2010). Precipitation of minerals, such as calcium carbonate, irons, and manganese oxide hydrates, is responsible for chemical clogging, while mechanical clogging results in the clogging layer's compression and air binding (Bouwer, 1996; Pyne, 2005).

* Corresponding author.
E-mail address: maria-chiara.lippera@tum.de (M.C. Lippera).

https://doi.org/10.1016/j.advwatres.2023.104462
Received 2 December 2022; Received in revised form 6 May 2023; Accepted 15 May 2023
Available online 16 May 2023

Although these are interrelated processes, numerous studies appointed physical clogging as the most critical process affecting the reduction in hydraulic conductivity (Pavelic et al., 2011; Rinck-Pfeiffer et al., 2000). Clogging occurs at the basin's bottom in spreading methods (Duryea, 1996; Schuh, 1990), at the well-aquifer interface in recharge wells (Dillon et al., 2016; Pavelic et al., 2007), at the bottom and walls of trenches (Bergman et al., 2011; Conley et al., 2020), and in the riverbed in riverbank filtration (Grischek and Bartak, 2016). From observations of whole-pond infiltration rates and point measurements, Racz et al. (2012) reported a decline of one to two orders of magnitude for a 3-ha MAR infiltration pond. Recharge water high in total suspended solids (TSS) concentrations can primarily affect the clogging layer's formation in MAR's basins. When TSS concentrations are low, biological processes are mainly responsible for declines in recharge rates, and physical clogging processes are controlled by other transports and deposition mechanisms, such as erosion, wave action, and windborne dust (Hutchinson et al., 2013a). In MAR literature, the effect of clogging on infiltration dynamics has been integrated into numerical simulations by the increase in the filter cake thickness around the well screen in MODFLOW (Majumdar et al., 2008), and by a time-varying scaling factor for the hydraulic conductivity at the infiltration interface in HYDRUS (Glass et al., 2020). Adjusting parameters for clogging effects requires calibration from laboratory experiments or observations of water levels to replicate the overall behaviour. Furthermore, these models do not account for different clogging rates in the spatial domain and are not a function of both the soil type and water quality (Glass et al., 2020). Clogging processes have been simulated with the numerical model CLOG, applied in various laboratory experiments and one field study case (Pérez Paricio, 2001). However, mathematical models for physical clogging in MAR based on the mass balances of suspended particles, are calibrated on the breakthrough concentrations of a specific column set-up (Torkzaban et al., 2015; Xie et al., 2020). Besides the limited parameter transferability to other hydrogeological contexts, there could be gaps from the 1D processes to the field scale representation (Wennberg et al., 1995). Spatial development and distribution of physical clogging on the field should be included in physical clogging predictions at MAR sites.

Few studies have been undertaken to understand clogging development directly in the field. Gette-Bouvarot et al. (2014) collected and analysed soil samples from two basins to relate the influence of accumulated fines and biofilm growth to the decline in hydraulic properties. Gonzalez-Merchan et al. (2012) continuously monitored water inflow, depth, and temperature for seven years in a stormwater infiltration pond and found vegetation to control clogging by creating macropores. Detecting spatial patterns of clogging in the field can provide further information on key clogging factors that cannot be reproduced in column experiments. Cannavo et al. (2018) observed a heterogeneous spatial distribution of sediment layer thickness and organic matter content (OM) mainly driven by the water flow and sediment granulometry from the inlet to the outlet. Zaidi et al. (2020) and Fetzer et al. (2017) buried sand-filled columns in the field to observe vertical clogging gradation at different locations. By implanting pickets, higher deposit thickness was observed in topographical depressions due to water stagnation and in the bank not covered by vegetation due to surface erosion (Zaidi et al., 2020). Escalante (2013) mapped the distribution of clogging processes and observed physical clogging in topographical depressions due to clay and silt deposition and subsequent compression. The same consideration for the bottom geometry can be applied to furrows design, as fine silts accumulate on the valleys compared to the crests (Escalante, 2013). Further work is thus necessary to assess the risk of physical clogging at MAR sites, including understanding spatial clogging patterns in the field. Potential locations for sediment accumulation and penetration or biofouling play a role in this regard (Racz et al., 2012). Existing mathematical models for physical clogging have not been applied to explain local observations of physical clogging at the field and predict the overall evolutions in infiltration capacity. Our work aims at assessing the risk of physical clogging in MAR systems by means of site characterization techniques and mathematical modelling. To achieve this aim, we integrate secondary factors controlling clogging at the field. Spatial patterns for fines remobilisation and accumulation are detected to incorporate the controlling factors in the analysis, e.g. the basin topography. To achieve this aim, we conducted a field characterization at the EU LIFE REWAT two-stage infiltration basin in Suvereto (Italy). The site is distinguished by recharge water with low turbidity crossing a sedimentation pond before infiltration. The presence and degree of clogging can thus be related to the remobilization of fines inside the basin. Section 2 'Materials and methods' reports the description of the site, the methods involved in the characterization of the site and the laboratory analysis. Section 3 'Modelling framework' reports the modelling steps to reproduce the input of fines, in this case from erosion processes, the retention profiles formation and effect of fines on the hydraulic conductivity. The modelling outcomes are validated against field observations, illustrated and discussed in Section 4 'Results and Discussion'. Section 5 'Conclusion' highlights these findings' relevance in designing new MAR sites and developing operation and maintenance (O & M) strategies. The approach we propose can be transferred to other MAR sites, collecting data from site characterization and modelling the impact on the infiltration capacity of the site.

2. Material and methods

In order to collect field parameters to assess the formation and distribution of clogging, we conducted a field campaign in October 2021 at the EU LIFE REWAT infiltration site in Suvereto (Tuscany, Italy)(Caligaris et al., 2022). The MAR site and its operations are described in Section 2.1, followed by the methodology for the site characterization in Section 2.2 and the laboratory analysis in Section 2.3.

2.1. Study area

The MAR site is located in the alluvial plain of the Cornia River. The area is characterized by Holocene alluvial deposits presenting alternated sandy-gravel layers and silty-clay deposits up to 40 m in depth (Barazzuoli et al., 1999). The recharge scheme consists of a two-stage infiltration basin infiltrating harvested water from the Cornia River during high-flow periods (Caligaris et al., 2022). The basin is seated in a former gravel quarry and it is divided into a settling pond (700 m^2) and an infiltration pond (1600 m^2)(Benucci et al., 2017). The soil, consisting of sandy/silty gravel, is hydraulically connected with the phreatic aquifer. The drilling of a piezometer inside the basin displayed a 3 m soil core of coarse gravels in a silty matrix (GM in USCS). Recharge operations follow two steps. First, the water is diverted from the River Cornia through a conveyance channel and pumped at a rate of 80 L/s. Second, the water enters the settling pond, where the suspended solids are deposited, and then moves to the adjacent pond by three outlets. A supervisory control and data acquisition (SCADA) system regulates the pump switching on/off only based on the monitored water quality and the river's minimum environmental flow set thresholds. E.g., during river peak discharge periods, if the turbidity value exceeds 100 NTU, the water is not pumped. As the pump diverts water at 80 L/s and the basin infiltration rate is lower than that, a level sensor (at 1.70 m depth at the centre of the basin) checks that the water level is below a set level to avoid basin overflow. When the threshold is exceeded, the pump stops, and only infiltration takes place. Once the level is restored to a set minimum threshold, pumping starts again. Fig. 1 presents the MAR scheme. Upstream and downstream of the recharge plant, a network of instrumented piezometers monitor the groundwater head and quality parameters in compliance with the current Italian regulation for managed aquifer recharge (DM 100/2016). Recharge operations usually expand from December to June of the following year. Fig. 2 shows the ponding depths and daily infiltration rates from the seasonal operations recorded at the Suvereto infiltration basin, Italy. Maintenance

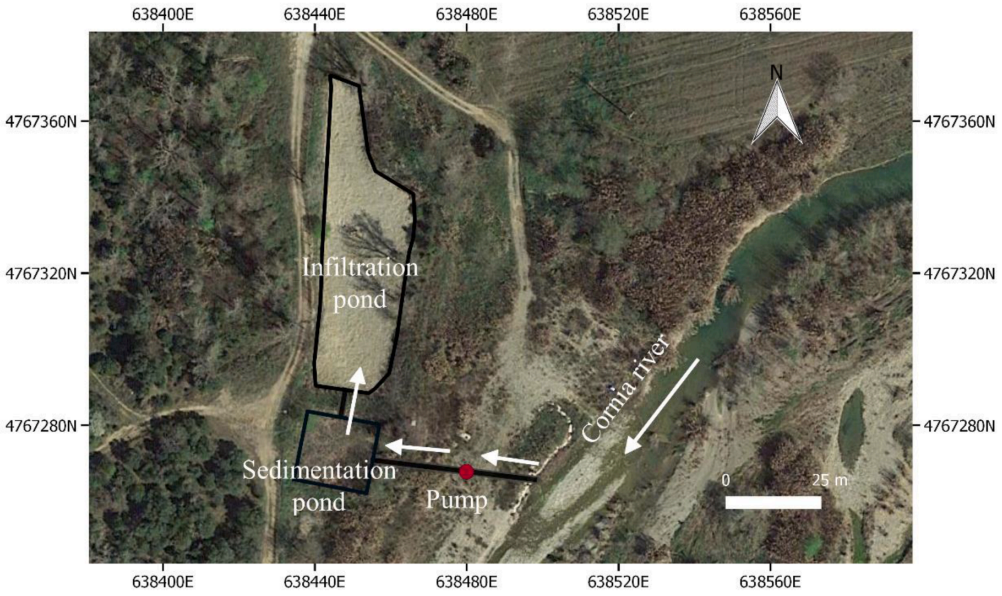

Fig. 1. MAR scheme in Suvereto, Italy. The external grid shows the Easting and Northing UTM-Coordinates (WGS 84) in meters.

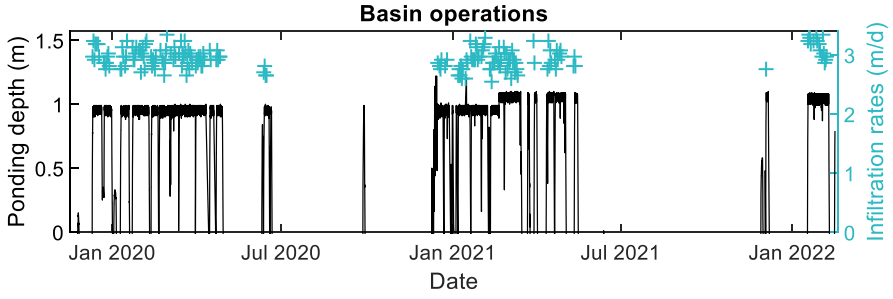

Fig. 2. Operating season at the MAR scheme in Suvereto, Italy, from November 2019 to February 2022. With the *black line* are shown the ponding depths from the recorded water levels at the centre of the basin. In *blue* with the *symbol* "+" are the daily infiltration rates from the pump activation time during full operation.

operations are related to the SCADA and monitoring system maintenance (sensors maintenance, software update, etc.), vegetation clearance around the site, and yearly basin ploughing. The basin floor is ploughed once a year before the start of the recharge season, usually in November.

2.2. Site characterization

The scope of the fieldwork at the EU LIFE REWAT infiltration site is to detect the physical and hydraulic parameters affecting clogging inside the basin at the end of the recharge season 2020/2021. An Electromagnetic Induction (EMI) survey was performed with the CMD Mini Explorer (GF Instruments, Brno, CZ) electromagnetic conductivity metre operated in horizontal dipole orientation. EMI surveys are employed to map the variability of soil properties, such as the soil texture and clay content (Doolittle and Brevik, 2014). The surveyed effective penetration depths were up to 0.25 m, 0.5 m, and 0.9 m, respectively. Apparent Electrical Conductivity (ECa) values were recorded in continuous mode with the DGPS (Leica TPS1200+, Leica Geosystems, Heerbrugg, CH) at 0.2 s frequency. The data were post-processed in RStudio to remove outliers, and maps were computed via Ordinary Kriging interpolation in SAGA GIS software, fitting the variograms with a power model.

Six locations were selected for soil sampling, covering the infiltration pond's inlet, centre, and opposite side. In each location, soil samples were collected within an area of 20 × 20 cm at depth intervals of 0–1 cm, 1–3 cm, 3–8 cm, 8–13 cm, 18–23 cm. Coarse gravels did not always allow the augers to collect the necessary soil material for the deepest sampling depth and nor to perform soil porosity measurements by core sampling. The surface crust, detectable at the top with a thickness <1 mm, was collected for analysis. A Turbidity/TSS correlation could not be established from the river water samples due to concentrations of suspended solids <1 mg/L at the time of investigations.

In the proximity of the sampled locations, the hydraulic characterization was performed via double-ring infiltrometer tests (Eijkelkamp Soil & Water, Giesbeek, NL; ASTM D33 85–03 standard test method). The measurement points were selected in flat areas located between ridges. The infiltration curve obtained from the course of infiltration capacity in time was interpreted with the Philip (1957) model. We set a robust regression with bisquare weights to reduce the effect of the extreme initial infiltration rates in initially dry soils. The full weights were given to the bulk data reaching the saturated hydraulic conductivity asymptotically.

Finally, the map of the slopes of the basin was computed from the DGPS elevation measurements in QGIS 2.18.24. A filter was applied to reclassify the values in three slope classes and reduce noise based on the predominant value in a neighbourhood of 3 × 3 cells.

2.3. Laboratory analysis

The soil samples collected at the field were dried and split in the laboratory for particle size and total carbon analysis. First, the grain size analysis was performed by wet-sieving up to the 63 μm diameter grain size. No chemical pre-treatment was deemed necessary for the analysis. Laser diffraction determined the volumetric grain size proportions for the fine material 63–0.7 μm (Cilas Particle Size 920). In wet dispersion mode, the suspension was stirred and underwent ultrasound treatment before the measuring cycle. Each measurement was repeated three times, and the particle's size distribution statistics were computed. The complete particle's size curve in the range 0.7–4000 μm was then reconstructed for each sample. Weight Loss-on-Ignition (LOI) test was performed to measure the organic matter content in samples. The residual water content was initially removed at 105 °C, and then samples were placed at 360 °C in the muffle furnace for two hours, annotating the% loss in ignition.

3. Modelling framework

The modelling framework illustrated here has been developed based on the results of the site characterization at the Suvereto infiltration site and the transferable mathematical model for physical clogging developed by Lippera et al. (2023). The modelling steps are reported and the workflow is illustrated in Fig. 3 to provide a comprehensive data analysis framework. The objective of the modelling study is to validate whether the parameters collected in the field sufficiently explain the observed clogging for reproducibility at other sites. First, a module for soil erosion computes the eroded fines at the basin slopes, providing the input of remobilized fines material. The mass of remobilized fines is then assumed to be evenly distributed at the basin bottom. The clogging module reproduced the vertical retention profile of fines over the sediment matrix and, thus, the resulting type of clogging at the locations. Finally, reductions in infiltration rates at clogged locations are computed through the infiltration rate module and the resulting evolutions in the infiltration capacity of the basin.

3.1. Fines input

The Suvereto infiltration site presents extended banks and low concentrations of suspended solids in the recharge water. Thus, erosion processes are included in the analysis to quantify the remobilized and redistributed fines contributing to physical clogging. Wind erosion from surrounding agricultural areas was excluded due to the basin location at a topographical low depression. The embankments are fully covered by vegetation and a fence surrounds the area. Wind can still contribute in internally redistributing the fines inside a MAR basin, however the applicability of wind erosion models is questioned (Jarrah et al., 2020). During recharge operations, the water level fluctuates at a very slow rate, wave-induced shear stress is excluded given the absences of turbulences inside the basin. Furthermore, turbidity measurements from water samples collected at the pond during operations didn't provide evidence of resuspension of sediments. Erosion processes pertaining to the Suvereto infiltration can be attributed mainly to sheet and rill erosion during the pond's initial filling and drainage. Besides the soil textures, other factors govern soil erodibility, such as the soil structure, organic matter content and permeability. Sheet and rill erosion models are widely used in soil and water conservation programs, and can assist the assessment of sediment loads and sediment control planning (Flanagan et al., 2001; Ketema and Dwarakish, 2021; Nearing, 2013; Renard et al., 1997). The Universal Soil Loss Equation - USLE (Wischmeier and Smith, 1960; Wischmeier and Smith, 1978) was chosen for its simplicity and ease of use in quantifying the annual erosion rate (ton/ha/year) by water in fields. (Eq. (1)):

$$Annual\ soil\ loss\ =\ R\ K\ LS\ C\ P \tag{1}$$

with R the rainfall erosivity factor (MJ mm/h/ha/year), K the soil erodibility factor (ton h/MJ/mm), LS the slope length and gradient factor, C the cover management factor and P the erosion control practice factor.

Modified USLE (MUSLE) models are applied to individual runoff

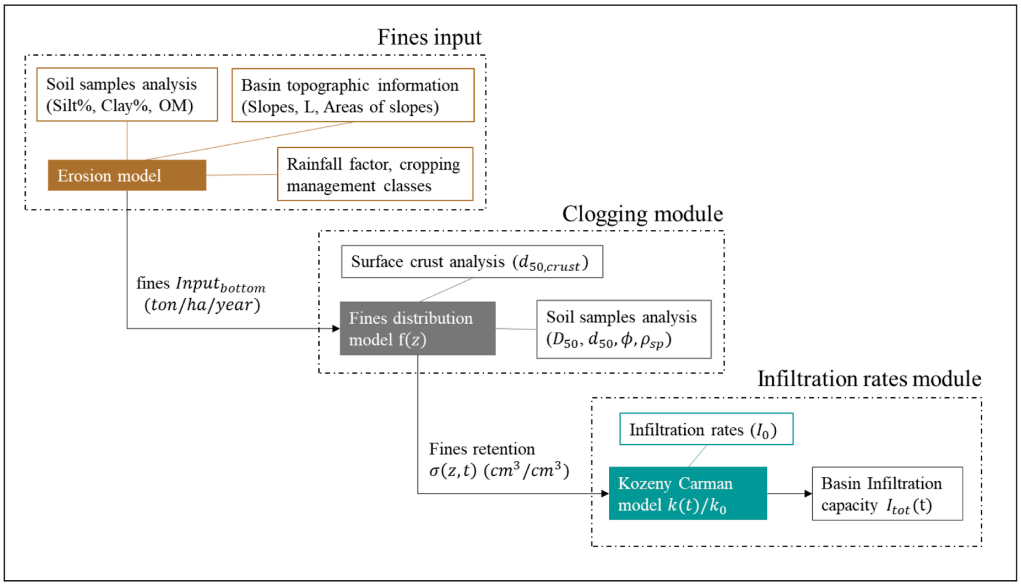

Fig. 3. Modelling workflow validating the clogging risk assessment at MAR sites.

events by means of a runoff energy factor (Williams, 1974). For this type of model, the R factor should be calibrated with sediment yield observations to provide good estimates (Sadeghi et al., 2014). The replacement of the USLE's rainfall erosivity factor allows the model to predict sediment yield from channel erosion, gully erosion and floodplain scour (Ketema and Dwarakish, 2021). When adapting USLE sub-factors to particular study sites, special attention must always be paid to unit consistency (Benavidez et al., 2018). The R factor was calibrated from the observed superficial erosion at the sampled locations with slopes > 3%. In order to reflect the annual impact energy on the ground from the filling and draining cycles, an R factor = α *N* was defined, with $\alpha = \frac{R}{N} =$ 680.34 MJ mm/h/ha and N $year^{-1}$ the number of filling and draining cycles at the basin over the year.

The *K* soil erodibility factor includes five soil parameters in the algebraic approximation by Wischmeier and Smith (1965) adapted by Renard et al. (1997) (Eq. (2)):

$$K = \left[\left(2.1(Silt\ (100 - Clay))^{1.14}10^{-4}(12 - OM) + 3.25(b-2) + 2.5(c-3)\right) / 100\right]0.131 \quad (2)$$

With *Silt* (%) the soil textural percentage comprehensive of fine sands (0.1–0.002 mm) and *Clay* (%), the percentage <0.002 mm from the grain size distribution curves. *OM* is the organic matter content (%). The average OM content from the analysed soil samples is 4.34%. The parameters *b* and *c* are values dependant on the soil structure and profile permeability class. The slope and the length of the slope (*LS*) control the surface flow and the speed of flow over the field (Eq. (3)):

$$LS = \left[0.065 + 0.0456\,(slope) + 0.006541\,(slope)^2\right](slope\,length \div 22.1)^{NN} \quad (3)$$

The slope (%) and slope length (m) are calculated from the site map using Geographic Information System. *NN* is a tabulated factor dependant on the slope (Soil Loss Equation Federal Register Notice, Natural Resources Conservation Service, USDA).

The annual soil loss is calculated from the basin areas with a slope >3%, classified into the gentle slope ($Loss_{gs}$) with slopes 3–8%, and basin banks ($Loss_{banks}$) with slopes 8–30%. The input of fines to the bottom of the basin per unit area is estimated (Eq. (4)):

$$Input_{bottom} = \frac{Loss_{gs}\ Area_{gs} + Loss_{banks}\ Area_{banks}}{Area_{bottom}} \quad (4)$$

and the yearly mass redistribution is then converted into g/cm^2/year.

3.2. Clogging profiles

The clogging profiles from the redistribution and intrusion of fines at the clogged locations are computed through the formulation presented in Lippera et al. (2023). The equation describes the distribution of intrusive fines over the soil depth *z* (cm) dependent on the sediment-particles size setting expressed with the geometric ratio d_{50}/D_{50}:

$$\left(1.76\frac{d_{50}}{D_{50}}\right)\exp\left(-1.76\frac{d_{50}}{D_{50}}z\right)\ if\ M_{tot} < M_{tot,\ limit} \quad (5a)$$

$$f(z) = \left\{\left(1.76\frac{d_{50}}{D_{50}}\right)exp\left(-1.76\frac{d_{50}}{D_{50}}z\right)\frac{M_{tot,\ limit}}{M_{tot}} + \frac{M_{tot} - M_{tot,\ limit}}{M_{tot}}(z=0)\ if\ M_{tot} > M_{tot,\ limit}\right. \quad (5b)$$

M_{tot} is the total infiltrating mass of fines (g) and $M_{tot,limit}$ is the mass of infiltrating fines (g) after which the external cake would start forming in superficial clogging conditions.M_{tot} and $M_{tot,limit}$ are defined over an infiltration area *A* (cm^2) with known sediment matrix, being M_{tot}=$Input_{bottom}A$. For more information on the determination of $M_{tot,\ limit}$ see Lippera et al. (2023).

The median diameter $D_{50}$of the sediment matrix is computed, from the soil samples at the Suvereto site, from the median values of the curves analysed at 8–13 cm depths. Due to the low variation in fines content in the deeper layers, the sediment distribution at depth 8–13 cm is assumed for initial conditions to be the undisturbed matrix since the last cleaning operations in November 2020. With the site ploughing, a uniform sediment matrix is recreated at the top 15 cm by mixing the sediments at the start of the recharge season. Under this assumption for the initial conditions, however, deep clogging profiles cannot be discerned over the observed depth. Since the remobilized and deposited fines exhibited a bimodal distribution, one median diameter $d_{50,silt}$ is computed for the peak of the finer material ($d_{50} = 8.03 \pm 0.87\ \mu m$) and one median diameter $d_{50,sand}$ is computed for the fine-sand peak detected from the surface crust analysis ($d_{50,crust} = 104.40 \pm 0.39 \mu m$). The combined effect of the two groups of fines on the native soil matrix is analysed and validated for the locations where clogging was observed.

3.3. Infiltration rates

Coupling the mass of redistributed fines over one year at the basin bottom from the erosion model and the expected vertical distribution of fines *f*(*z*) given the fine particles-sediment matrix characteristics, the intruded particles' volumes are expressed per unit of porous media volume (Eq. 6), at the time step *t* and depth *z*, in the form of a retention profile:

$$\sigma(z,t) = \frac{Input_{bottom}(t)}{\rho_s\ l} f(z) \quad (6)$$

with $Input_{bottom}$ the mass of fines per unit area (g/cm^2/year) from Eq. (4), *f*(*z*) the expected vertical distribution of fines from Eq. 5a and 5b, ρ_s the particles' specific density (g/cm^3), *l* the sediment unit depth (cm).

The decrease in porosity of the porous media follows the formulation from Herzig et al. (1970) (Eq. 7):

$$\frac{n(z,t)}{n_0} = 1 - \frac{\beta\sigma(z,t)}{n_0} \quad (7)$$

with β the inverse of the compaction factor of retained particles $\beta = 1/(1 - n_d)$. The porosity of the retained fines n_d is derived from the average densities of deposited particles (Alem et al., 2013; Boller and Kavanaugh, 1995).

The Kozeny-Carman equation (Carman, 1937; Kozeny, 1927) estimates variations in soil permeability from the volume of intruded fines in the interstitial space. The formulation from Alem et al. (2013) adequately depicted the observations from previous laboratory experiments in Lippera et al. (2023) (Eq. 8):

$$\frac{k(z,t)}{k_0} = \frac{n(z,t)^3}{n_0^3}\frac{(1+n_0)^2}{(1+n(z,t))^2}\frac{S_0^2}{S(z,t)^2}\left(\frac{T_0}{T(z,t)}\right)^2 \quad (8)$$

with *k* the permeability (cm/s), *n* the porosity, *S* the specific surface area per particles' unit volume (1/cm) and T the tortuosity. Please refer to Alem et al. (2013) for a detailed explanation of the single terms in Eq. (8).

The estimated reductions in soil permeability at discrete depths over time provide the following total reduction in soil permeability for the vertical flow direction:

$$\frac{k_{tot}(t)}{k_0} = \frac{L + L_{cake}(t)}{\sum_{z=0}^{L} \frac{1}{\frac{k(z,t)}{k_0}} + \frac{L_{cake}(t)}{k_{z=0,\ limit}}} \tag{9}$$

With $L_{cake}(t)$ (cm) the thickness of the external clogged layer, estimated from the volumes of fines depositing superficially. The term $k_{z=0,\ limit}$ (cm/s) is the estimated permeability of the porous media at the surface when the limit retention of fines is met, and k_{cake} (cm/s) is the permeability of the fines depositing superficially.

The computation of soil permeability reductions at the clogged location points is extended to the whole basin. Equally probable stochastic maps of soil texture classes, conditioned at the sampled locations, are computed by Sequential Gaussian Simulations (SGS) (Dietrich and Newsam, 1993). The spatial distribution of the %Silt attribute in the basin, given the constant%Clay from the soil samples, reflects the uncertainty in the spatial distribution of soil texture classes inside the basin. The physical and hydraulic parameters measured at the single locations are transferred to the areas with the same classified soil texture, and an aggregated value for I_{bottom} is computed.

For each realization, at the start of the simulation, the lateral infiltration component $I_{sides} = I_{gs} + I_{banks}$, is derived from a balance with the initial infiltration rates of the whole basin I_{tot}:

$$I_{sides} = \frac{I_{tot}Area_{tot} - I_{bottom}Area_{bottom}}{Area_{tot} - Area_{bottom}} \tag{10}$$

The reduction in soil permeability is then computed for the bottom area $Area_{bottom}$having slopes <3%, based on the spatial distribution of the soil texture classes, the corresponding physical and hydraulic properties, and the input of fines. Through the use of the Darcy's law with a unitary gradient for the downward flow controlled by gravity, the decline in permeability at the basin bottom is converted to a decline in the bottom infiltration component I_{bottom}, and the total infiltration rate I_{tot} is iteratively computed. The initial total infiltration rate I_{tot}, taken as the model input, is the median measured value at the Suvereto infiltration basin for the recharge season 2020–2021, concluded before the site characterization.

The decline in total infiltration rates is thus computed exclusively from the decline in hydraulic properties at the basin bottom, replicating the accumulation of sediments from the banks' erosion. The process accounts for the cleaning operations with the mixing the sediment matrix every year. Thus, the overall effect of the redistribution of the sediment budget from the sides of the pond to the bottom is simulated, allowing forecasting the evolution in infiltration capacity at MAR sites.

4. Results and discussion

The site characterization led to the detection of clogging patterns and the collection of clogging key parameters affecting the remobilization and redistribution of fines. The maps in Fig. 4a show the interpolated ECa values at effective penetration depths up to 0.25 m and up to 0.9 m respectively. The basin appears homogenous in soil properties at both investigation depths. The presence of gravel inside the basin likely contributed to obtaining uniform readings. The low range of electrical conductivity values, respectively 3.65 - 5 mS/m and 3.35 - 4.7 mS/m, indicate sand and gravel sediments (von Suchodoletz et al., 2022). The EMI data confirm that mixed sediments are evenly distributed over the basin up to 1 m depth. Fig. 4b shows the soil texture classes for the six locations at the sampled depth of 0–1 cm, 1–3 cm, 3–8 cm, and 8–13 cm. The soil classification is according to the USDA soil textural triangle. The sampled soils fall into the classes: very gravelly sandy loam, gravelly sandy loam, very gravelly loam, gravelly loam, very gravelly silt loam and gravelly silt loam (USDA-NRCS classification). The maximum clay content for the fine-earth fraction (≤2 mm) is 12.87%. In this regard, the EMI investigation cannot provide information on fine-grained material presence at the very top, because clay minerals are only present to a minor extent and effective penetration depths differ from sampling depth. From the textural triangle in Fig. 4b, locations 1 and 6, at the extremes of the pond length, show clustered soil classes over depth. In other sampling locations, the most superficial layers exhibit a different class than the deeper layers. By visual inspection, the presence of clay material deposited was partially noticeable on the field. However, the measurements conducted by laser diffraction might have underestimated the clay content in the soil samples. Laser diffraction was employed for the sediment analysis for comparison with other field clogging investigations (Gette-Bouvarot et al. 2014; Zaidi et al., 2020).

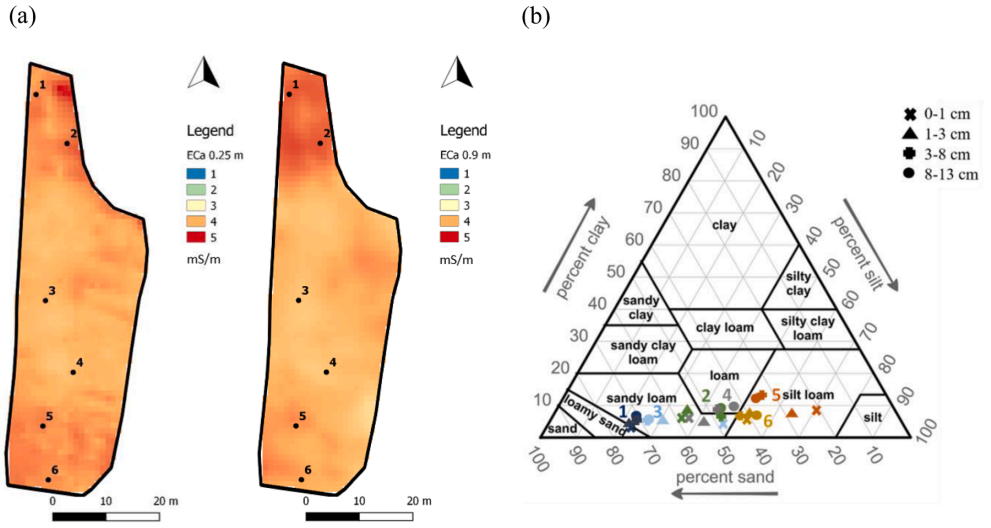

Fig. 4. (a) EMI maps at effective depths up to 0.25 m and up to 0.90 m. B*lack dots* indicate the sampling locations. (b) Soil classification of the sampled soils according to the USDA soil textural triangle (Soil Survey Division Staff 1993). *Different colours* indicate the sampling location, and *different shapes* report the depth at which the soil was collected.

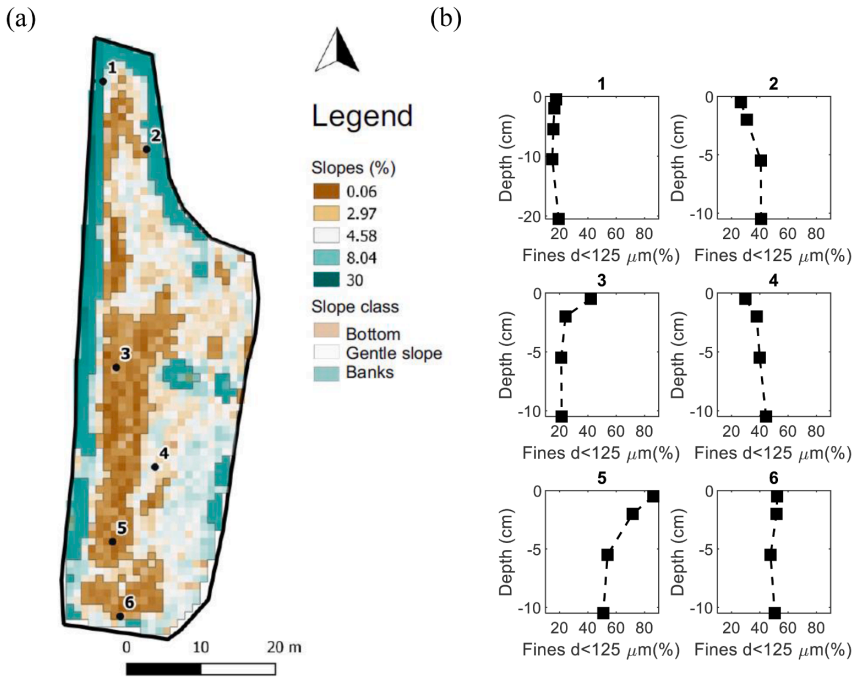

Fig. 5. (a) Map with the slopes (%) of the basin and sampling locations. (b) Fines content with diameter $d < 125$ μm for the depths 0–1 cm, 1–3 cm, 3–8 cm, 8–13 cm at the six sampling locations. The number associated with each soil profile corresponds to the location indicated in the map (a).

4.1. Erosion rates

The information from the soil samples, collected at different depths, can be related to the spatial features of the basin. In Fig. 5a, the area with slopes in the range of 0–3% is assigned to the basin bottom, 3–8% slope is the area with gentle slope, and 8–30% slopes outline the basin banks. On the other side, Fig. 5b shows the observed profiles of fines content in mass percentages for the size diameter $d < 125$ μm. Locations 3 and 5 present increasing fines content at the surface, indicating superficial clogging. The other locations inside the basin do not show clear signs of clogging. In contrast, locations 2 and 4 show depletion of fines at the surface, which might be explained by lateral erosion. Loamy soils with a large amount of fine sand and silt particles are susceptible to erosion since they are non-cohesive sediments. Especially the fine-sand particles could not have been transported as suspended particles, from the recharge water and overcome the sedimentation pond, unless redistributed internally by erosion. The turbidity measurements revealed a mean value of 1.07 NTU with a standard deviation (SD) of 0.72 NTU for the river. While concomitant turbidity measurements taken inside the recharged pond had a mean value 1.08 NTU and 0.98 NTU SD. Given the clear water conditions and absence of turbulences during the recharge operations, the changes over the sediment matrix in Locations 3 and 5 can thus be attributed to the erosion processes observed at the other locations. From the locations of the analysed samples and the basin's topography in Fig. 5, it can be inferred that fines material is accumulated at the basin bottom from the remobilization of fines at the basin slopes. This process might be enhanced during flushes at the initial time of recharge. Also, at the start of the recharge season, the fall ploughing operation might contribute to the re-siting of fine particles

From the erosion module described in Section 3.1, an input of 54.29 kg/m^2/year of soil in the fine sand–silt range is estimated from the basin areas with a slope >3% and redistributed over the bottom.

4.2. Clogging profiles

For the clogged locations 3 and 5 at the bottom of the basin, the observed complete grain-sized distribution curves are illustrated in detail in Fig. 6a and 6b. The grain size distribution curves are shown for the sediments collected at the four sampled depths. For comparison, the particle size distributions of eroded fines in the fine-sand and silt range are displayed. These two groups of eroded fine material were obtained from the laser diffraction analysis of the surface crust and the finer accumulated material from the samples.

The clogging module described in Section 3.2 is used to explain the vertical distribution of fines for these two locations. From Eq. 5, the model estimates that 99.74% of the eroded fine-sand is accumulated superficially in location 3, while the fines in the silt range deposit internally with an average deposition of 0.89% over depth. At location 5, the model exhibits superficial clogging by the deposition of both eroded fine-sand and finer material (100% retention in $z = 0$) for a total thickness of the external cake of 2.05 cm. The expected vertical distributions of fines computed by Eq. 5 are in agreement with the soil grain distributions observed at the sampled locations. In location 3 (Fig. 6a) at the very superficial layer 0–1 cm, mostly particles in the fine-sand range are clearly accumulated superficially. The matrix's deeper layers are not disturbed by intrusive sediments in the silt fraction. For location 5, the estimated superficial accumulation of the total eroded sediments and the formation of a 2.05 cm thick cake layer is in agreement with the observed sediments in Fig. 6b. The superficial layer 0–1 cm consists only of eroded fine material, and the layer at 1–3 cm depth is composed partly of gravels and partly of accumulated fines material. Thus, the sampled top 2.05 cm sediments might be solely eroded fines, as explained by the model.

In addition, in Location 5 at depth 3–8 cm (Fig. 6b), the coarse fraction in the gravel range approaches the one at 8−13 cm depth, being the undisturbed matrix. Differently from the other sampled locations,

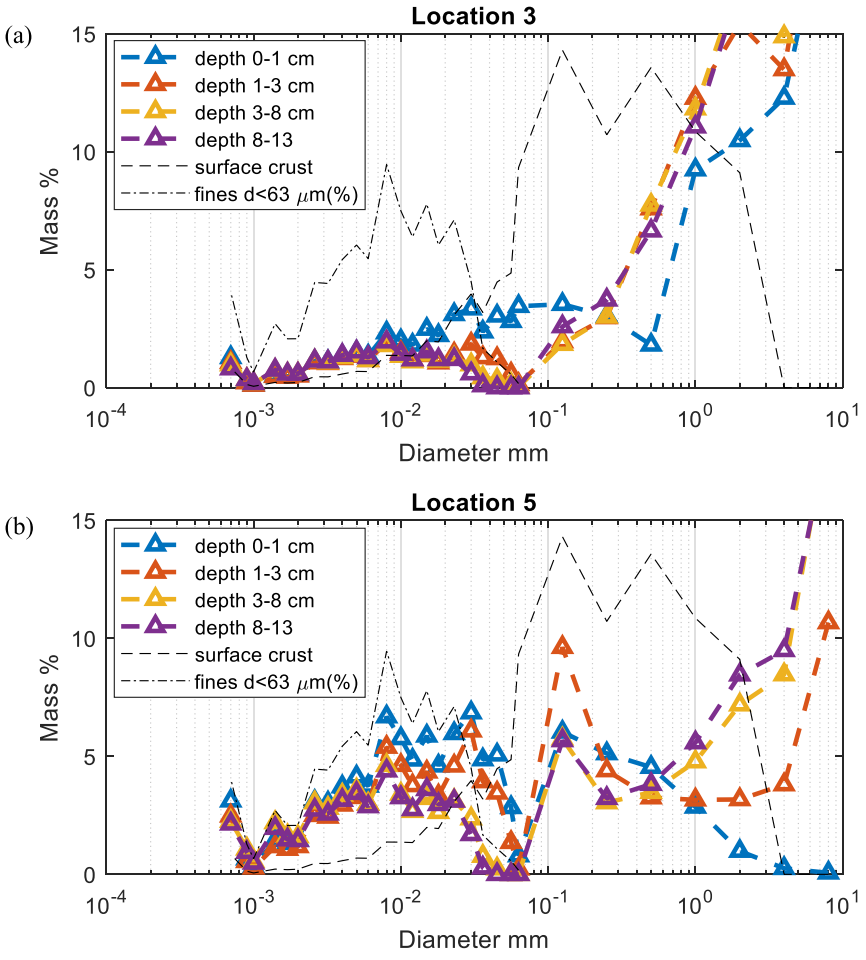

Fig. 6. Observed grain sizes distributions of the samples collected at depth 0–1, 1–3, 3–8 and 8–13 cm in (a) Location 3 and (b) Location 5. *Dashed lines* report the particles size distributions of the surface crust and the average fines size distribution for the fines <63 μm. The fines distribution is obtained by averaging the particles sizes distributions $d < 63$ μm at the samples top layers.

the deepest layer shows higher content of particles in the fine-sand range. The erosion and surface accumulation processes likely heightened the bottom of the basin, confirming the initial hypothesis that a uniform sediment matrix at the top 15 cm is recreated at every year cleaning operation by ploughing the site.

The quantification of the input of fines from the lateral erosion, according to the modified USLE model, and the consequent retention profiles, expressed as fines volume over porous media volume, are validated with the observed content of fines material in the samples (Fig. 5b), here reported in detail for the clogged locations 3 and 5 (Fig. 7a and 7b).

The yearly eroded mass intruded in the sediment matrix is summed to the pre-existing fines content in layer 8–13 cm, considered the undisturbed matrix.

The estimated contents of fines are compared with the observed ones from the sieving analysis for the fraction $d < 125$ μm in Fig. 7. The modified USLE model coupled with the model for the clogging profiles explains the surplus of fines depositing over depth with a root mean square error (RMSE) of 2.53% for Location 3 and 12.53% for Location 5. The parameter uncertainty in the model output is reported for ranges of total porosity values from literature according to their soil textural classes (Rawls et al., 1983).

4.3. Infiltration rates

The infiltration tests performed at the field during the site characterization (Section 2.2) indicated clogging at the basin bottom in agreement with the information from the soil samples. Higher hydraulic conductivity values were measured close to the basin banks where potentially erosion occurred. Table 1 shows that location 1, with gravelly sandy loam, has an infiltration rate one order of magnitude higher than the rest of the basin, with 223.56 mm/h. Infiltration rates are lower in the two locations at the bottom of the basin, presenting accumulated fines. Location 3 exhibits a K-value near saturation of 6.67 mm/h, drastically lower compared to location 1, having same textural class (Fig. 4b). Location 5 also exhibits a K-value near saturation of 2.34 mm/h, a lower infiltration rate compared to location 6, also having a silt loam texture (Fig. 4b).

It should be noted that, according to Bouwer (1986), double-ring measurements can still be affected by lateral spreading of flow and edge effects. This method is robust in case of an impending layer on the surface, minimizing the effect of the leakage along the inner cylinder wall. However, the greater accuracy of the single-ring with the divergence correction method has been proved by Rice et al. (2014), and it is recommended for the design of infiltration sites. This method requires

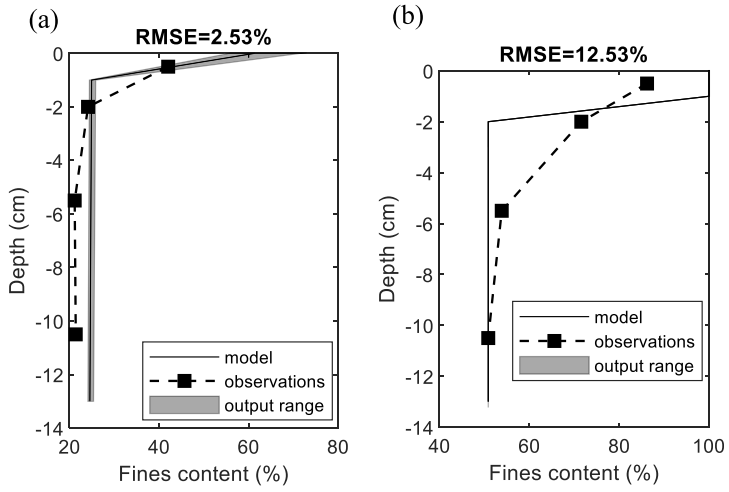

Fig. 7. Modelled and observed fines content over depth from the input of fines by the USLE model in (a) Location 3 and (b) Location 5. The output range is associated to the parameter uncertainty of the porosity value.

Table 1
Hydraulic conductivity values near saturation from the infiltrometer tests (mm/h).

Location 1	Location 2	Location 3	Location 4	Location 5	Location 6
223.56 mm/h	22.07 mm/h	6.67 mm/h	15.44 mm/h	2.34 mm/h	11.64 mm/h

the determination of the wetting depth and distance (x) of lateral divergence by partially digging out the wetted soil at the conclusion of the test.

From the infiltration rates module presented in Section 3.3, reductions in hydraulic properties (Eq. 8), can be estimated starting from the modelled erosion of fine material over one year and deposition at the basin bottom, as illustrated in the overall workflow (Fig. 3).

The accumulation of fines in Location 3 and estimated reduction in soil permeability would explain an original K-value of 50.17 mm/h from the last cleaning operations, while for Location 5, the K-value would have been 9.15 mm/h. Despite Location 5 presenting a higher accumulation of sediments at the surface, compared to Location 3, the sediment matrix is composed already of fine material at the deeper layers; thus, a further accumulation at the top would not lead to a drastic reduction in infiltration rates. In Location 3, the fine-sand material on the top would have a higher impact on the native coarser matrix instead. Overall, the estimated reductions in hydraulic conductivity can explain an initial value in the range of the deeper layer's textural classes.

The same analysis can be extended to the entire basin and for the next operating years. Other factors typically implicated in field clogging are the precipitation of calcium carbonate or biofilm formation. The dilute hydrochloric acid (HCl) solution test revealed a violent effervescence for the surface crust, thus a high content of carbonates. Also the higher content of soil organic carbon (7.80%) in the surface crust indicated potential for biological clogging, e.g. biofilm formation on the substrate. The modelling of chemical and biological activities interconnected with the fines mobilization goes beyond the purposes of this study. Although the surface crust might have had a role in superficially retaining fines, and a crust of <1 mm thickness can reduce infiltration rates during the wetting period forming an impermeable layer. Measuring the hydraulic conductivity in dry conditions, the crust layer was already cracked during the infiltration tests, hence having a low impact on the infiltration rates, which were controlled by the thicker deposits of fine material. The infiltration basin undergoes a long drying period typically from June to November, favouring the decomposition and shrinking of the biological and chemical clogging materials. The recharge operations taking place mostly in winter and spring time (due to the recharge source availability) considerably reduce the hydraulic loading and the associated biological-chemical clogging compared to other MAR schemes. The analysis is extended to the entire basin based on the already described physical processes to assess the impact of the redistribution and accumulation of sediments.

Due to the limited number of sampling points inside the basin, the uncertainty in the local variability of soil texture classes within the basin was incorporated by performing multiple equally probable stochastic realizations by Sequential Gaussian Simulations (SGS), see Dietrich and Newsam (1993). The modelling procedure is described in Section 3.3. Fig. 8 shows the decrease in infiltration capacity following 20 years of operations, with a highlight on the median estimation. The overall model assumes that the soil is mixed by the cleaning operation at the start of each operation year, thus recreating a uniform sediment matrix in the upper 15 cm.

Due to the remobilization and redistribution of fines from the basin slopes to the bottom, the total infiltration capacity might decrease to a stable value of 90% of the original infiltration capacity. Mixing operations for the upper 15 cm of sediments at the start of the operating season are included in the analysis. When the total infiltration capacity reaches a stable value, the bottom is clogged and the basin's infiltration mainly occurs at the sides.

As shown in Fig.8, the decrease in infiltration rates would be negligible over the years. The extensive slopes of the basin undergoing erosion would not be impacted by clogging. Despite the fines' colmation at the bottom, the investigated MAR site maintained high stable infiltration rates over the past four years of operations, in agreement with our simulation. The median value measured in the operation year 2019–2020 is 2.97 m/d, while in the operation year 2020–2021 is 2.91 m/d. In comparison to the year before it is a 98% ratio. Given the low suspended solids in the recharge water, the low content of clays, the presence of gravels and vegetation at the banks contributing to slope stability, the Suvereto infiltration basin has proved to be an excellent example for MAR design.

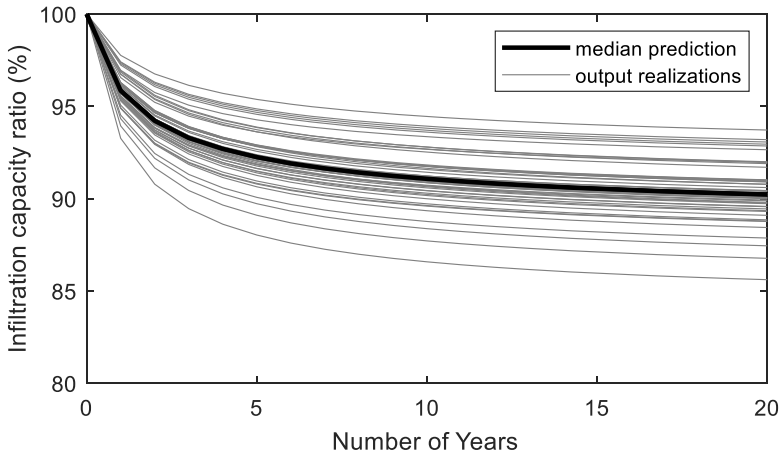

Fig. 8. Decline in infiltration capacity (%) of the basin given the accumulation of fines at the basin bottom from erosion processes.

5. Conclusions

Our work contributes to understanding secondary factors controlling physical clogging in MAR systems with low input of suspended solids. Despite the excellent quality of the recharged water and the sediment matrix's apparent homogeneity, physical clogging was detected at the bottom of the investigated basin. This study highlights the role of basin topography in the formation of clogging patterns. We found in the field that particles ranging from fine sand to silt were eroded superficially starting from a $>$ 3% slope. These fines are likely transported in topographic depressions during rainfall events and the washing of slopes caused by the complete drainage and following filling of the MAR site during recharge operations. The Universal Soil Loss Equation (USLE) present limitations in incorporating soil losses from other types of erosion than rainfall processes, accounting for seasonal effects or suiting specific site conditions (Benavidez et al., 2018). The modified USLE could approximate the quantity of remobilized fines and redistribution over the bottom through the observation of lateral erosion at sampled locations. Concepts for process-based erosion models to predict lateral erosion of infiltration basins should be developed due to the lack in literature. Given the fines input to the bottom, the developed model for clogging was validated with a RMSE of 2.53% and 12.53% compared to the fines content variations observed at discrete depths from the two clogged locations. Under the current maintenance procedures, the consequent analysis of the reduction in hydraulic properties was extended to the whole basin for the next 20 years of operations. For the Suvereto infiltration basin, the remobilization of fines, constituted mainly by silt particles, leads to a median stable value of infiltration capacity at 90% of the initial infiltration capacity. Our analysis shows that the basin's topographical features can contribute to sustaining high infiltration rates. Prior one-dimensional analysis of clogging from the literature in sand columns cannot depict soil heterogeneity and spatial factors contributing to fines remobilization and accumulation. Field studies on surface spreading facilities also observed higher permeability at the sidewalls of the basins due to the redistribution of fines. In infiltration systems, Conley et al. (2020) noted that the bottom clogged rapidly and very little material accumulated on the side infiltration surfaces. Although it might appear convenient to design a deep basin to maintain lateral infiltration, it is not recommended in shallow aquifer systems to avoid groundwater mounding. Moreover, maximum side slopes of 1:3 (V:H) are recommended by Hutchinson et al. (2013a) for infiltration practices design to avoid instability. Basin banks should also be protected from erosion and wave action as a design strategy, and it is warned of the inability to clean deeper basins on banks with a 1:3 slope (Hutchinson et al., 2013b). To conclude, in basins with extended banks, the assessment of the risk of clogging should account not only for the input in suspended particles from the recharge water, but also for the potential erosion at the sides given the specific basin features. Design consideration can be derived to reduce clogging at MAR sites during the planning phase. Our work based on site characterization combined with modelling is a cost-effective method to assess the risk of physical clogging and can be replicated at multiple sites, improving estimations of O&M costs.

Funding

The research leading to these results has received funding from the European Union's Horizon 2020 research and innovation programme under the Marie Skłodowska-Curie grant agreement no 814066 (Managed Aquifer Recharge Solutions Training Network - MARSoluT). The EU LIFE REWAT infiltration basin was built within the LIFE REWAT project, receiving funding from the European Union's Life Programme LIFE 14 ENV/IT/001290. On behalf of all authors, the corresponding author states that there is no conflict of interest.

CRediT authorship contribution statement

Maria Chiara Lippera: Conceptualization, Methodology, Software, Validation, Formal analysis, Investigation, Writing – original draft, Visualization. **Ulrike Werban:** Supervision, Writing – review & editing, Investigation, Resources, Project administration, Funding acquisition. **Rudy Rossetto:** Writing – review & editing, Investigation, Resources, Project administration, Funding acquisition. **Thomas Vienken:** Supervision, Writing – review & editing, Conceptualization, Project administration, Funding acquisition.

Declaration of Competing Interest

The authors declare that they have no known competing financial interests or personal relationships that could have appeared to influence the work reported in this paper.

Data availability

Data will be made available on request.

Acknowledgments

The authors wish to thank ASA spa (Mirko Brilli, Claudio Benucci and Patrizio Lainà) and Consorzio di Bonifica 5 Toscana Costa (Alessandro Fabbrizzi, Roberto Benvenuto and Giancarlo Vallesi) for technical support at the MAR scheme. Maria Chiara Lippera performed the research as ESR9 PhD student within the framework of the MARSOLUT ITN project. Our gratitude also goes to the Department of Applied Geology, MLU Halle-Wittenberg, Halle, for giving the availability of their soil lab and laser-diffraction equipment for the soil samples analysis, especially we thank Juri Buchantschenko for the support. Finally, we also thank the reviewers for their constructive and insightful comments.

References

Alem, A., Elkawafi, A., Ahfir, N.-D., Wang, H, 2013. Filtration of kaolinite particles in a saturated porous medium: hydrodynamic effects. Hydrogeol. J. 21 (3), 573–586. https://doi.org/10.1007/s10040-012-0948-x.

Alley, W., Reilly, T., Franke, O, 1999. Sustainability of Ground-Water Resources. USGS Circular 1186. US Geological Survey, Denver, CO.

Barazzuoli, P., Bouzelboudjen, M., Cucini, S., Király, L., Menicori, P., Salleolini, M., 1999. Olocenic alluvial aquifer of the River Cornia coastal plain (southern Tuscany, Italy): database design for groundwater management. Environ. Geol. 39 (2), 123–143.

Baveye, P., Vandevivere, P., Hoyle, B.L., DeLeo, P.C., de Lozada, D.S., 1998. Environmental impact and mechanisms of the biological clogging of saturated soils and aquifer materials. Crit. Rev. Environ. Sci. Technol. 28 (2), 123–191. https://doi.org/10.1080/10643389891254197.

Benavidez, R., Jackson, B., Maxwell, D., Norton, K., 2018. A review of the (Revised) Universal Soil Loss Equation ((R)USLE): with a view to increasing its global applicability and improving soil loss estimates. Hydrol. Earth Syst. Sci. 22 (11), 6059–6086. https://doi.org/10.5194/hess-22-6059-2018.

Bennion D.B., Bennion D.W., Thomas F.B., and Bietz R.F. (1998). Injection water quality-a key factor to successful waterflooding. 37(6). doi:10.2118/98-06-06.

Benucci C., Ruggiero M., Manetti E., Maggiorelli R., Leoni R., Lazzaroni F., Manzella F., Fabbrizzi A., Rossetto R., de Filippis G., Sabbatini T., Rinaldi S., Ciccolini V., Ercoli L., Matani E., and Piacentini S.M. (2017). Progetto Definitivo per Impianto Pilota Dimostrativo di Ricarica della falda in condizioni controllate in località Forni (Suvereto) ai sensi del DM 100/2016. *REWAT PROJECT (LIFE14 ENV/IT/001290),* http://www.cbtoscanacosta.it/images/Conferenze_dei_Servizi/Ricarica_Falda_19_12_2017/progetto_definitivo_14_12_2017_v6.0_per_caric_sito.pdf.

Bergman, M., Hedegaard, M.R., Petersen, M.F., Binning, P., Mark, O., Mikkelsen, P.S., 2011. Evaluation of two stormwater infiltration trenches in central Copenhagen after 15 years of operation. Water Sci. Technol. 63 (10), 2279–2286.

Boller, M.A., Kavanaugh, M.C., 1995. Particle characteristics and headloss increase in granular media filtration. Water Res. 29 (4), 1139–1149. https://doi.org/10.1016/0043-1354(94)00256-7.

Bouwer, H., 1986. Intake rate: cylinder infiltrometer. Methods of Soil Analysis, pp. 825–844.

Bouwer, H., 1996. Issues in artificial recharge. Water Sci. Technol. 33 (10–11), 381–390. https://doi.org/10.1016/0273-1223(96)00441-6.

Bouwer, H., 2002. Artificial recharge of groundwater: hydrogeology and engineering. Hydrogeol. J. 10 (1), 121–142. https://doi.org/10.1007/s10040-001-0182-4.

Caligaris, E., Agostini, M., Rossetto, R, 2022. Using heat as a tracer to detect the development of the recharge bulb in managed aquifer recharge schemes. Hydrology 9 (1), 14. https://doi.org/10.3390/hydrology9010014.

Cannavo, P., Coulon, A., Charpentier, S., Béchet, B., Vidal-Beaudet, L., 2018. Water balance prediction in stormwater infiltration basins using 2-D modeling: an application to evaluate the clogging process. Int. J. Sediment Res. 33 (4), 371–384.

Carman, P.C., 1937. Fluid flow through granular beds. Trans. Inst. Chem. Eng. 15, 150–166.

Conley, G., Beck, N., Riihimaki, C.A., Tanner, M, 2020. Quantifying clogging patterns of infiltration systems to improve urban stormwater pollution reduction estimates. Water Res X 7, 100049.

Dietrich, C.R., Newsam, G.N., 1993. A fast and exact method for multidimensional Gaussian stochastic simulations. Water Resour. Res. 29 (8), 2861–2869.

Dillon, P., Arshad, M, 2016. Managed aquifer recharge in integrated water resource management. In: Jakeman, AJ, Barreteau, O, Hunt, RJ, Rinaudo, J-D, Ross, A (Eds.), Integrated Groundwater Management: Concepts, Approaches and Challenges. Springer International Publishing, Cham, pp. 435–452.

Dillon, P., Stuyfzand, P., Grischek, T., Lluria, M., Pyne, R.D.G., Jain, R.C., Bear, J., Schwarz, J., Wang, W., Fernandez, E., Stefan, C., Pettenati, M., van der Gun, J., Sprenger, C., Massmann, G., Scanlon, B.R., Xanke, J., Jokela, P., Zheng, Y., Rossetto, R., Shamrukh, M., Pavelic, P., Murray, E., Ross, A., Bonilla Valverde, J.P., Palma Nava, A., Ansems, N., Posavec, K., Ha, K., Martin, R., Sapiano, M, 2018. Sixty years of global progress in managed aquifer recharge. Hydrogeol. J. 27 (1), 1–30. https://doi.org/10.1007/s10040-018-1841-z.

Dillon, P., Vanderzalm, J., Page, D., Barry, K., Gonzalez, D., Muthukaruppan, M., Hudson, M, 2016. Analysis of ASR clogging investigations at three Australian ASR sites in a bayesian context. Water (Basel) 8 (10), 442. Retrieved from. https://www.mdpi.com/2073-4441/8/10/442.

Doolittle, J.A., Brevik, E.C., 2014. The use of electromagnetic induction techniques in soils studies. Geoderma 223, 33–45.

Duryea, P.D., 1996. Clogging Layer Development and Behavior in Infiltration Basins Used For Soil Aquifer Treatment of Wastewater. Arizona State University.

Escalante E. (2013). Practical Criteria in the Design and Maintenance of MAR Facilities in Order to Minimise Clogging Impacts Obtained from Two Different Operative Sites in Spain. In (pp. 119–154).

Fetzer, J., Holzner, M., Plötze, M., Furrer, G, 2017. Clogging of an Alpine streambed by silt-sized particles – Insights from laboratory and field experiments. Water Res. 126, 60–69. https://doi.org/10.1016/j.watres.2017.09.015.

Flanagan, D.C., Ascough, J.C., Nearing, M.A., Laflen, J.M., 2001. The water erosion prediction project (WEPP) model. Landsc. Eros. Evol. Model. 145–199.

Gette-Bouvarot, M., Mermillod-Blondin, F., Angulo-Jaramillo, R., Delolme, C., Lemoine, D., Lassabatere, L., Loizeau, S., Volatier, L., 2014. Coupling hydraulic and biological measurements highlights the key influence of algal biofilm on infiltration basin performance. Ecohydrology 7 (3), 950–964.

Glass, J., Šimůnek, J., Stefan, C, 2020. Scaling factors in HYDRUS to simulate a reduction in hydraulic conductivity during infiltration from recharge wells and infiltration basins. Vadose Zone J. 19 (1), e20027.

Gonzalez-Merchan, C., Barraud, S., Le Coustumer, S., Fletcher, T, 2012. Monitoring of clogging evolution in the stormwater infiltration system and determinant factors. Eur. J. Environ. Civil Eng. 16 (sup1), s34–s47. https://doi.org/10.1080/19648189.2012.682457.

Goss, D., Smith, S., Stewart, B., Jones, O., 1973. Fate of suspended sediment during basin recharge. Water Resour. Res. 9 (3), 668–675.

Grischek, T., Bartak, R., 2016. Riverbed clogging and sustainability of riverbank filtration. Water (Basel) 8 (12), 604. https://doi.org/10.3390/w8120604.

Herzig, J.P., Leclerc, D.M., Goff, P.L., 1970. Flow of suspensions through porous media—Application to deep filtration. Ind. Eng. Chem. 62 (5), 8–35. https://doi.org/10.1021/ie50725a003.

Hutchinson, A., Milczarek, M., Banerjee, M., 2013a. Clogging phenomena related to surface water recharge facilities. IAH Commission on Managing Aquifer Recharge). Australia.

Hutchinson, A., Phipps, D., Rodriguez, G., Woodside, G., Milczarek, M, 2013b. Surface Spreading Recharge Facility Clogging-The Orange County Water District Experience. Australia.

Jarrah, M., Mayel, S., Tatarko, J., Funk, R., Kuka, K, 2020. A review of wind erosion models: data requirements, processes, and validity. Catena 187, 104388.

Jeong, H.Y., Jun, S.-C., Cheon, J.-Y., Park, M, 2018. A review on clogging mechanisms and managements in aquifer storage and recovery (ASR) applications. Geosci. J. 22 (4), 667–679. https://doi.org/10.1007/s12303-017-0073-x.

Ketema, A., Dwarakish, G, 2021. Water erosion assessment methods: a review. ISH J. Hydraul. Eng. 27 (4), 434–441.

Kim, J.W., Choi, H., Pachepsky, Y.A., 2010. Biofilm morphology as related to the porous media clogging. Water Res. 44 (4), 1193–1201. https://doi.org/10.1016/j.watres.2009.05.049.

Kozeny, J., 1927. Uber kapillare leitung der wasser in boden. R. Acad. Sci., Vienna Proc. Class I 136, 271–306.

Lippera, M.C., Werban, U., Vienken, T., 2023. Improving clogging predictions at managed aquifer recharge sites: a quantitative assessment on the vertical distribution of intrusive fines. Hydrogeol. J. 31 (1), 71–86. https://doi.org/10.1007/s10040-022-02581-7.

Majumdar, P.K., Sekhar, M., Sridharan, K., Mishra, G.C., 2008. Numerical Simulation of Groundwater Flow with Gradually Increasing Heterogeneity due to Clogging. J. Irrig. Drain. Eng. 134 (3), 400–404. https://doi.org/10.1061/(ASCE)0733-9437(2008)134:3(400.

Nearing, M.A., 2013. Soil Erosion and Conservation. Dev. Environ. Modell. 365–378.

Pavelic, P., Dillon, P.J., Barry, K.E., Vanderzalm, J.L., Correll, R.L., Rinck-Pfeiffer, S.M., 2007. Water quality effects on clogging rates during reclaimed water ASR in a carbonate aquifer. J. Hydrol. (Amst.) 334 (1–2), 1–16.

Pavelic, P., Dillon, P.J., Mucha, M., Nakai, T., Barry, K.E., Bestland, E, 2011. Laboratory assessment of factors affecting soil clogging of soil aquifer treatment systems. Water Res. 45 (10), 3153–3163. https://doi.org/10.1016/j.watres.2011.03.027.

Philip, J., 1957. The theory of infiltration. Soil Sci. 83, 345–357.

Pyne R.D.G. (2005). *Aquifer storage recovery: a guide to groundwater recharge through wells:* ASR systems.

Racz, A.J., Fisher, A.T., Schmidt, C.M., Lockwood, B.S., Los Huertos, M., 2012. Spatial and temporal infiltration dynamics during managed aquifer recharge. GroundWater 50, 562–570. https://doi.org/10.1111/j.1745-6584.2011.00875.x.

Rawls, W.J., Brakensiek, D.L., Miller, N., 1983. Green-Ampt infiltration parameters from soils data. J. Hydraul. Eng. 109 (1), 62–70.

Renard K.G., Foster G.R., Weesies G.A., Mccool D.K., and Yoder D.C. (1997). *Predicting soil erosion by water : a guide to conservation planning with the Revised Universal Soil Loss Equation (RUSLE).*

Rice R.C., Milczarek M.A., and Keller J.K. (2014). *A Critical Review of Single Ring Cylinder Infiltrometers with Lateral Flow Compensation.*

Rinck-Pfeiffer, S., Ragusa, S., Sztajnbok, P., Vandevelde, T., 2000. Interrelationships between biological, chemical, and physical processes as an analog to clogging in aquifer storage and recovery (ASR) wells. Water Res. 34 (7), 2110–2118.

Sadeghi, S.H.R., Gholami, L., Khaledi Darvishan, A., Saeidi, P, 2014. A review of the application of the MUSLE model worldwide. Hydrol. Sci. J. 59 (2), 365–375. https://doi.org/10.1080/02626667.2013.866239.

Schuh, W.M., 1990. Seasonal variation of clogging of an artificial recharge basin in a northern climate. J. Hydrol. (Amst.) 121 (1–4), 193–215.

Sprenger, C., Hartog, N., Hernández, M., Vilanova, E., Grützmacher, G., Scheibler, F., Hannappel, S, 2017. Inventory of managed aquifer recharge sites in Europe:

historical development, current situation and perspectives. Hydrogeol. J. 25 (6), 1909–1922. https://doi.org/10.1007/s10040-017-1554-8.

Torkzaban, S., Bradford, S.A., Vanderzalm, J.L., Patterson, B.M., Harris, B., Prommer, H., 2015. Colloid release and clogging in porous media: effects of solution ionic strength and flow velocity. J. Contam. Hydrol. 181, 161–171. https://doi.org/10.1016/j.jconhyd.2015.06.005.

Treidel, H., Martin-Bordes, J.L., Gurdak, J.J., 2011. Climate Change Effects On Groundwater Resources: a Global Synthesis of Findings and Recommendations. CRC Press.

von Suchodoletz, H., Pohle, M., Khosravichenar, A., Ulrich, M., Hein, M., Tinapp, C., Schultz, J., Ballasus, H., Veit, U., Ettel, P., Werther, L., Zielhofer, C., Werban, U, 2022. The fluvial architecture of buried floodplain sediments of the Weiße Elster River (Germany) revealed by a novel method combination of drill cores with two-dimensional and spatially resolved geophysical measurements. Earth Surf. Process. Landf. 47 (4), 955–976. https://doi.org/10.1002/esp.5296.

Wang, Z., Du, X., Yang, Y., Ye, X, 2012. Surface clogging process modeling of suspended solids during urban stormwater aquifer recharge. J. Environ. Sci. 24 (8), 1418–1424. https://doi.org/10.1016/s1001-0742(11)60961-3.

Wennberg K., Batrouni G., and Hansen A. (1995). Modelling Fines Mobilization, Migration and Clogging. In.

Williams, J.R., 1974. Sediment-yield prediction with universal equation using runoff energy factor[1]. ARS-S (40–49), 244.

Wischmeier, W.H., Smith, D.D., 1960. A universal soil-loss equation to guide conservation farm planning. Trans. 7th Int. Congr. Soil Sci. 1, 418–425.

Wischmeier W.H., and Smith D.D. (1965). Predicting rainfall-erosion losses from cropland east of the Rocky Mountains.

Wischmeier, W.H., Smith, D.D., 1978. Predicting Rainfall Erosion Losses: a Guide to Conservation Planning. Department of Agriculture, Science and Education Administration.

Wu, W.-.Y., Lo, M.-.H., Wada, Y., Famiglietti, J.S., Reager, J.T., Yeh, P.J.F., Ducharne, A., Yang, Z.-.L., 2020. Divergent effects of climate change on future groundwater availability in key mid-latitude aquifers. Nat. Commun. 11 (1), 3710. https://doi.org/10.1038/s41467-020-17581-y.

Xie, Y., Wang, Y., Huo, M., Geng, Z., Fan, W, 2020. Risk of physical clogging induced by low-density suspended particles during managed aquifer recharge with reclaimed water: evidences from laboratory experiments and numerical modeling. Environ. Res. 186, 109527.

Zaidi, M., Ahfir, N.-.D., Alem, A., El Mansouri, B., Wang, H., Taibi, S., Duchemin, B., Merzouk, A, 2020. Assessment of clogging of managed aquifer recharge in a semi-arid region. Sci. Total Environ. 730, 139107.

Zhang, H., Xu, Y., Kanyerere, T, 2020. A review of the managed aquifer recharge: historical development, current situation and perspectives. Phys. Chem. Earth, 102887.

Pérez Paricio, A., 2001. Integrated modelling of clogging processes in artificial groundwater recharge. Doctoral thesis. UPC, Departament d'Enginyeria del Terreny, Cartogràfica i Geofísica. ISBN 8469955217. Available at: http://hdl.handle.net/2117/93526.